Author version of: ChemPhysChem 2018, doi:10.1002/cphc.201701090

Supramolecular organization and confined nanospaces

Gloria Tabacchi

Abstract: Empty spaces are abhorred by nature, that immediately rushes in to fill the void. Humans have learnt pretty well how to make ordered empty nanocontainers, and to get useful products out of them. When such an order is imparted to molecules, new properties may appear,often yielding advanced applications. This review illustrates how the organized void space inherently present in various materials – zeolites, mesoporous silica/organosilica, and metal organic frameworks (MOF), for example, can be exploited to create confined, organized, and self-assembled supramolecular structures of low-dimensionality. Features of the confining matrices relevant to organization are presented with special focus on molecular-level aspects. Selected examples of confined supramolecular assemblies- from small molecules to quantum dots or luminescent species- are aimed to show the complexity and potential of this approach. Natural confinement (minerals) and hyperconfinement (high pressure) provide further opportunities to understand and master the atomistic-level-interactions governing supramolecular organization under nanospace restrictions.

1. Introduction

Supramolecular organization[1,2] is a central idea in chemistry,[3–7] and a driving force in technology.[8,9] It refers to the formation of correlated domains of molecules or nanoscale objects, often accompanied by the appearance of collective properties or new functionalities. Molecular machines[5,9–11] or photonic antennas,[12] are classic examples of supramolecular structures. The assembly process may occur via spontaneous phenomena - like ferroelectricity or ferromagnetism, by molecular recognition between specifically designed species, or with the help of an external agent:[13] for example light, electric/magnetic fields or space confinement. In the latter case, matrices with regular porous networks are particularly effective, because their voids can be exploited as nanosized receptors for matter to create confined, supramolecular structures of low-dimensionality.[14] Empty space architectures are a distinctive feature of various materials: zeolites, crystalline mesoporous silicas, or metal organic frameworks, among others. Because of the regular distribution of nanosized empty space, such frameworks may be ideally considered as the negative image of highly structured nanomaterials, constitued by arrays of molecules, quantum dots, or molecular wires.[15] When confined in those matrices, guest species not only are subjected to the geometrical constraints of the cavities, but are in principle prone to be remotely and individually controlled.[16,17]
Nanoscale confinement has long been used as a way to enhance or modify chemical reactivity, as documented in several reviews covering, for example, catalysis,[18–22] photochemistry,[23–27] and charge-transfer processes.[28,29] This work will consider situations where no covalent bonds involving the confined species are broken or formed, and the porous matrix is used essentially as an organizing medium. In such *host–guest* or *inclusion* composites, the guest species are bound inside the cavities or channels of the host by non-covalent forces such as hydrogen bonding, electrostatics and van der Waals interactions. This work aims to give an overview of host-guest materials whose potential applications hold concrete promises in materials science. Composites of this kind for electronics, photonics or sensing, were first obtained by incorporating nanoparticles and photoactive species inside zeolites.[14,17,30] These represent a kind of archetype for other host systems and are the main subject of this story; nonetheless, discussion is extended to newer generations of hosts that have widened the potential application range while presenting new challenges (Figure 1).[31,32] Focus is driven on the molecular-level features of the confined assemblies, whose knowledge is pivotal for progress in applications. In this sense, the relevance of natural porous matrices to probe fundamental facts of host-guest interactions and confinement is acknowledged. Among the many strategies for the realization (and characterization) of composites of potential technological interest, particular attention is here devoted to the use of high pressures.
The concepts of organization and order are not equivalent and need to be defined. *Order* is usually associated to the symmetry and periodicity of crystals (long-range order): for example, the deviation from strict periodicity in crystallography is often called *disorder*. A common feature of composites based on crystalline hosts is that the confining matrix does not impart, in general, its symmetry and periodicity to the incorporated species. This happens because these materials are *non stoichiometric compounds* - hence, "*it is not necessary for guest molecules to occupy every available gap in the host structure before a stable complex is formed*".[33] Very early this fact was recognized by Barrer, that classified host-guest complexes according to the distribution of guest species within the framework and observed that these compounds manifested appreciable departures from stoichiometry.[33] Practically, all materials herein presented fall in this category: because they are not "*strictly periodic*", they are inherently dominated more by disorder rather than by order. Yet the arrangement of the confined guests is far from being random: confinement imposes spatial correlations to the guests, and the supramolecular patterns thus formed, depending on the observed length scales and adopted experimental conditions, often exhibit a certain regularity, usually designed as *correlated disorder*.[34]
Organization stems indeed from the space restrictions imposed by the confining matrix to the included species, and often implies a change in their physico-chemical properties. For example, metal clusters confined in a regular, three-dimensional lattice of pores are *organized* in three dimensional arrays, while chromophores incorporated inside non-intersecting nanochannels are *organized* into one-dimensional arrays. Such *organized* assemblies show electronic absorption, luminescence, and energy transfer properties different from those of a fluid solution or dispersion of the same species. The arrangement of dye molecules in linear arrays, for example, allows for a very efficient and unidirectional FRET (Forster Resonance Energy Transfer)[35] process – a distance-dependent, nonradiative energy transfer mechanism at

[a] G. Tabacchi
Department of Science and High Technology
University of Insubria
Via Valleggio, 9 I-22100 Como (Italy)
E-mail:gloria.tabacchi@uninsubria.it

the basis of solar energy harvesting antenna systems (Figure 1b,d,e).[36,37] Hence, spatial confinement at the nanoscale is *by itself* an organizing agent; accordingly, the arrangement of the confined guests inside the porous matrix will be defined as their *organization*, as common practice in the related literature (see, e.g. Refs.[14,16,37–39])

Organization *does not* imply crystallographic order: besides non-stoichiometry (non-uniform occupancy of the host pores), there are other sources of disorder for the guest species. At the molecular scale, the spatial arrangement of confined guests is determined by a complex mix of intermolecular and host-guest interactions, depending on temperature, pressure and concentration of the guests inside the cavities, among other factors. The confined species generally preserve a certain freedom of movement: for example rotational, or wobbling motions inside cavities, and longitudinal displacement along nanochannels. This atomic-scale dynamics is at the origin of the "dynamic disorder" in crystallography: the refined structure typically features a multiplicity of positions for the guest species with fractional occupancy (as shown e.g. in Figure 1a), and provides only an average picture of the guests. Also, inclusion composites often show "static" disorder – which is related to the symmetry of the guests, their repartition inside the host, andl inhomogeneities of the host, among others. Structural problems of this kind are rather common in these compounds and should be properly tackled by multitechnique characterization strategies.

Note that most of the composites here discussed are *functional* in spite of disorder: for example, the electronic transition dipole moments of the included dyes in Figure 1b are *approximately* aligned, ensuring thus an extremely high speed for exciton transport.[40,41] Technically, this is good enough for use in solar energy concentrators, sensors or solar cells.[29] Of course, there is still room for improvement, and that is why we need a thorough characterization of the material at atomistic level detail. In spite of the great advance of experimental techniques (schematically presented in ***Chapter 2***), important details still remain very difficult to capture especially when fine movements of molecules or groups of atoms are the main characters of the play. The fundamental contribution of computational approaches in revealing these aspects is highlighted in the remainder of this paper, which is structured as follows.

Chapter 3: confining matrices are instrumental in the organization of the included species. This part provides an overview of common porous scaffolds - zeolites, clathrates, silica mesopores, framework materials.

Chapter 4: ***confined nanostructures*** (metal clusters, quantum dots, nanowires, etc) played a key role in the development of nanoporous-based materials for advanced applications[14,42,43] and are now experiencing impressive advances.[44,45]

Chapter 5: ***confined water and water-ion clusters*** is a topic of both historic and fundamental value (see ref.[46,47] for a review) – here, the focus is on water-cation assemblies in natural zeolites.

Chapter 6: confined halogen molecules in nanochannels form relatively simple composites, yet endowed with interesting properties, such as semiconductor behaviour.[48]

Chapter 7*: organic chromophores* encapsulated in nanosized containers show exceptional optical properties (Figure 1). Confinement dramatically enhances their emission intensity by contrasting the formation of undesired aggregates.[49,50] These materials find application in solar energy harvesting,[51] photonics,[52,53] and nano-diagnostics technology.[54] Here, the focus is on the arrangement of dye molecules and the dynamic guest/guest host-guest interactions at the basis of the optical anisotropy of the materials.

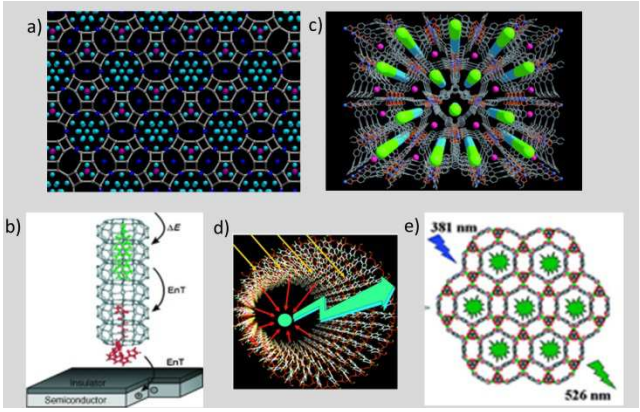

Figure 1. ***Confining matrices and light-harvesting applications***. a) X-ray structure of the perlialite mineral[55–57] ($K_8Tl_4[Al_{12}Si_{24}O_{72}]\cdot 20H_2O$) - a natural zeolite isostructural to zeolite L[58] (LTL framework type)[57,59]. Cationic and water sites have fractional occupancy. Color code: grey, framework (Si or Al); dark blue, K^+ sites; purple, Tl^+ sites; light-blue, water sites. [Illustration created with VMD, using X-ray positions from Refs[56,57]] b) zeolite L antenna system.[60] A luminescent donor dye (in green) inside zeolite L (in grey) functionalized with an acceptor dye (in red) at the crystal termination and interfaced with a semiconductor. Upon irradiation, the composite undergoes FRET[35,40] and transfers the excitation to the semiconductor. [Reproduced by permission from Wiley-VCH].[60] c) Schematic illustration of pyridinium hemicyanine chromophores (green balls) incorporated into a MOF, yielding a material with non-linear optical properties.[61] [Reprinted from ref.[61] with permission from Wiley-VCH]. d) A periodic mesoporous organosilica (POM) bears organic chromophores within its pore walls and strongly adsorbs light. Energy is transferred to the acceptor dye in the channel (green dot), yielding 100% emission enhancement. [Reproduced by permission from Wiley-VCH].[62] e) This zeolitic metal-organic-framework (MOF) features nano-sized cages, within which dyes (green spots) are adsorbed. The resulting composite shows efficient light-harvesting properties. [Adapted from Ref.[63] with permission from The Royal Society of Chemistry]

Chapter 8: ***hyperconfinement*****,** i.e. the use of high pressure to drive molecular species inside nanoporous materials.[64] In this case, the self assembly process is controlled by both the confining matrix and the imposed pressure. Recently observed phenomena such as pressure-induced polymerization[65] or formation of complex supramolecular patterns[66] candidate hyperconfinement as an intriguing route to new materials.

1.1. Short history

The use of porous matrices to create new composites is not a new idea. The first of those materials was realized by the Maya (Figure 2).[67–69] By the inclusion of the indigo dye in the pores of a clay mineral palygorskite,[70] these ancient craftsmen obtained a pigment of exceptional resistance to harsh conditions, whose color could be finely tuned *via* a suitable choice of the process conditions.[70] Only much later it was recognized that the stability of the pigment was due to the inclusion of the dye inside the cavities of the clay:[71–73] In particular, the main stabilizing host-guest interaction is the coordination of the carbonyl group of

indigo to the Al^{3+} ions at the edge of the palygorskite cavities (Figure 2), while similar Mg^{2+}−dye interactions can also be present.[71] Such computational analyses also suggested that the thermal treatment employed in the pigment preparation eliminates some structural water molecules coordinated to the Al^{3+} ions in the clay, thus allowing for the binding of indigo.[74] Maya-blue mimics based on clay minerals are now of relevance for the environmentally-friendly production of colorants, and a fertile soil for advanced materials and sustainable applications alike.[75–78]

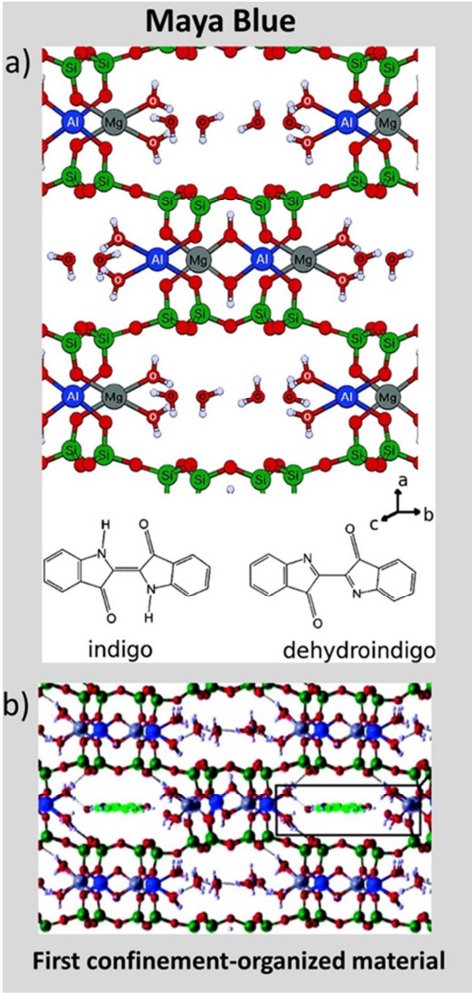

Figure 2. ***The Maya Blue pigment***. a) The inorganic and organic components (top) of Maya blue. The palygorskite clay: O atoms of structural water bound to Al are labeled in white, while O atoms of zeolitic water are labeled in black; (bottom) chemical formula of the indigo and dehydroindigo dyes. b)The Maya Blue pigment, which manifests an extraordinary resistance to humidity, heat, and chemical/photochemical attack, is most presumably formed by the intercalation of indigo in the palygorskite channels upon loss of water. [Adapted with permission from Ref.[71] Copyright 2009 American Chemical Society]

Among the first supramolecular compounds, *clathrate hydrates*[79] occupy a leading position: they were first reported by Davy, Faraday and probably Priestley, over 200 years ago, and are likely the host-guest materials best characterized. They are crystalline solids formed by guest molecules trapped in cages of hydrogen bonded water molecules.[80] Gas hydrates are also found naturally (offshore, under permafrost and in glaciers),[81] and these ones are minerals, according to the American Geological Association. Due to the long history of the field, and to the high relevance of hydrates for industrial and environmental issues,[82] an impressive amount of structural and thermodynamic data has been gathered,[79] which also makes them a choice model for the study of host-guest interactions from a fundamental viewpoint. The field developed around the 1950's, when single crystal structures of hydrates became available.[83] Barrer made prominent contributions to the understanding of these compounds,[33] – but also to the first zeolite synteses[84] and metal incorporation experiments.[85]

The idea of thoughtfully exploiting porous materials as ordering matrices for advanced optoelectronic functionalities was the thesis of a seminal work envisioning the technological potential of zeolites in electro-optical devices.[14] Such roadmap was followed by other accounts reporting on the use of zeolites in sensing devices, and on new appealing zeolite properties, like ionic conductivity[16,17,86,87] This advance was paralleled by great progress in the synthesis of zeolites.[88,89] Porous aluminophosphates,[90,91] oxides,[92] and chalcogenides[93–97] were realized and tested as nanocontainers of photoactive molecules, metal clusters, quantum dots and quantum wires. The resulting materials exhibited non-linear optical behavior, such as second harmonic generation,[98] and were used to build devices like zeolite-based lasers[99] or sensors.[94]

Nanotubes,[100] periodic mesoporous silicas,[101,102] and organosilicas[103] – broadened the size range of guest species. Those materials have larger pore openings, suitable for incorporating macromolecules and nanoparticles. The rise of framework materials[104–106] brought further variety of shapes and composition, structural flexibility, and structures that could undergo reversible changes upon the application of controlled stimulations, such as light or mechanical pressure.[107–109]

In the search of new frameworks,[110] considerable effort has focused on mimicking functionalities of biological systems through biomimetic chemistry.[1] However, mineralomimetics - the counterpart of biomimetics - has been successful as well. According to Iwamoto, this term indicates *the chemistry of building mineral-like structures using materials that never give stable minerals in nature.*[111–113] For example, by recognizing the structural similarity between $Cd(CN)_4$ and SiO_4, the group realized *clay-mimetic and zeolite-mimetic* cyanocadmate inclusion compounds through a crystal-engineering strategy .[114]

The relationships between man-made and natural materials are profound. Structurally, zeolites can be viewed as composed by small, cation-templated "natural building units".[115] Earlier syntheses of zeolites were inspired by minerals,[89] as in the case of the industrially relevant zeolites X and Y,[116] isostructural with faujasite (Figure 3).[117] Conversely, natural counterparts of synthetic zeolites were discovered *a posteriori*; a striking example is mutinaite (Figure 3),[118] isostructural with ZSM-5, a catalytic landmark in petrochemistry.[88] This interplay holds for clathrates as well: structure H hydrate, was first created in laboratory,[119] and then found in nature.[120] Rare silica minerals similar to zeolites and isostructural with gas hydrates, the *clathrasils*,[121,122] host in their cavities small organic molecules, such as methane, and other simple hydrocarbons,[121] – which recall the templates of synthetic zeolites (Figure 4).[123] Natural zeolites[124,125] exhibit chirality[126] (goosekreechite[127]) or extraordinary structural complexity,[128] like paulingite[129] (Figure 3). A recently

synthesized family of zeolites[130,131] was modeled just upon paulingite, and key for the successful synthesis was the recognition that Mg and Ca cations – found in related zeolite minerals – could be used as auxiliary templating agents for the more complex members of the family.[130]

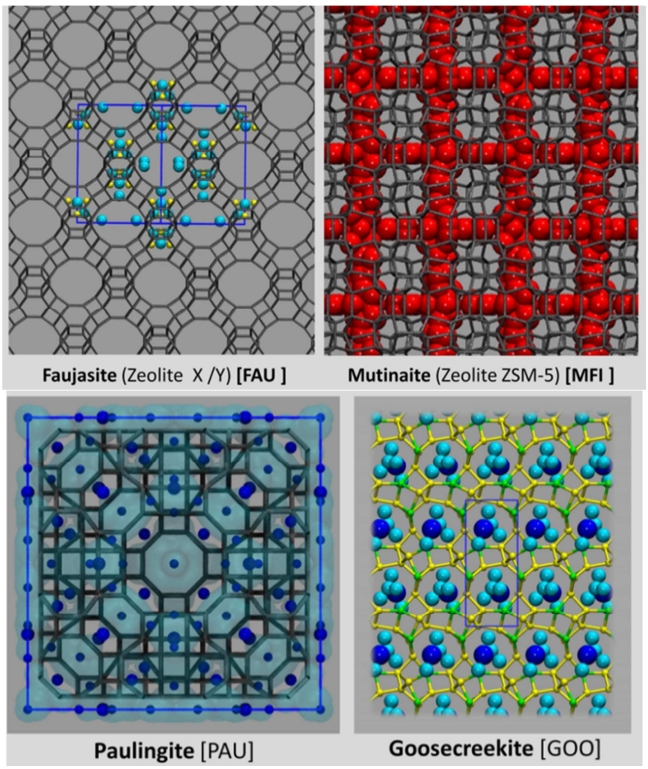

Figure 3. ***Structures of natural zeolites from X-ray diffraction.*** Top: Framework structures ((Si, Al = grey sticks; oxygen omitted for clarity) of the natural zeolites faujasite[117] (FAU) (blue solid lines indicate the unit cell) and mutinaite[118] (MFI), and of their synthetic counterparts (in parentheses). The colored balls are the water and cation sites (with fractional occupancy). [Illustration created with VMD, using the X-ray positions from Refs[117,118]. Framework structure (Si, Al = grey sticks) of natural zeolite paulingite [PAU][129]: the most complex mineral known to date.[128] The colored balls are the cation sites (with fractional occupancy): the size of the ball is proportional to the occupancy of the site. The shaded light-blue regions represent the distribution of the water sites. The blue line represents the unit cell, containing 16 formula units $(Ca_{2.57}K_{2.28}Ba_{1.39}Na_{0.38})[Al_{11.55}Si_{30.59}O_{84}]\cdot 27H_2O$, with minor amounts of Mg (<0.05), Sr (<0.13), Mn (<0.01), and Fe (<0.04).[129] [Illustration created with VMD, using the X-ray positions from Ref.[129]]. Framework structure (yellow = Si, green = Al) and extraframework content (blue= Ca, light blue = water oxygen) of goosecreekite [GOO], the only example of natural zeolite with a chiral framework [idealized formula: $CaAl_2Si_6O_{16}\cdot 5H_2O$]. [Illustration created with VMD, using the X-ray positions from Ref.[127]].

More fundamentally, insight on the interactions of simple, small-sized species like methane, water, and zeolitic cations inside natural porous matrices, is important to better understand the behavior of nano-objects in confined spaces. For instance, natural zeolites contain structured water-ion networks which, under pressure, resist spectacularly or rearrange dynamically,[64] and also the response of the framework is crucially influenced by the water-cation supramolecular assemblies inside the cavities.[132] Fundamental knowledge on the behaviour of such aggregates at high pressure conditions could help to increase the stability range of technologically relevant host-guest materials. For these reasons, care will be taken to compare artificially created inclusion composites with natural systems featuring either relevant similarities or unexpected relationships.

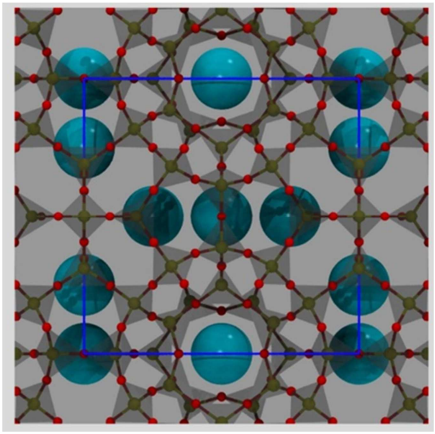

Figure 4. ***Methane naturally confined in a silica mineral.*** Structure of the all-silica mineral melanophlogite, historically recognized as the first clathrasil.[133] The framework is illustrated using shaded grey tetrahedra superposed to a ball-and-stick representation (O=red, Si=yellow). This mineral contains CH_4: the big light-blue spheres represent the experimentally determined C sites.[Illustration created with VMD, using the X-ray positions from Ref.[134]].

2. Characterization techniques

A few characterization methods for the guest species and their pore environment are shortly summarized in view of their widespread use. Many other powerful techniques are however employed to study host-guest compounds.

Structural characterisation of solids is typically performed with approaches based on **Bragg diffraction**, which probe long-range order in periodic solids. Although there are cases where single-crystal/powder measurements are sufficient to solve the structure, in many others the presence of the guest implies a lowering of the symmetry of the host, which hinders structural characterization of the confined species with standard crystallographic methods. In general when deviation from periodicity (i.e., disorder) is present, only a configurational average over all possible disordered states is obtained. Such average structure appears to be more symmetrical that the actual material, because all disorder is reflected back into one unit cell, losing important structural insight. As the unit cell of a disordered material is actually the entire crystal**,** a proper structural description requires also short-range parameters - local geometry, coordination environment, next-nearest neighbors. **Total scattering** measurements do not rely on periodicity and can provide insight into short/medium range correlations (e.g. presence of coordination bonds, or hydrogen bonds) in disordered materials, which typically escape standard diffraction. The Fourier transform of the total scattering structure factor is the pair distribution function (PDF), a weighted sum of probabilities to find atoms of one type at a given separation from atoms of another type. Modern crystallographic techniques can now synergically integrate single crystal, powder, or neutron diffraction data with PDF analyses.[34,135,136] Such advances have

greatly stimulated structural studies of disordered phases, like the recently reported liquid MOFs.[137]

Nevertheless, complex materials like inclusion compounds normally need *multitechnique characterization approaches*. Regarding structural analyses, the combination of diffraction techniques and magic angle spinning (MAS) **solid-state NMR spectroscopy** (SS-NMR) is an excellent strategy, often called ''NMR crystallography''.[138] (see also *CrystEngComm,* 2013,**15**, 8589 for a themed issue). Bragg diffraction and SS-NMR are complementary: whereas diffraction provides an average overview of the long-range structure, NMR does not rely on periodicity and captures detailed "short-range" information on the environment of specific nuclei, including their dynamics and local order/disorder. Because different local geometries imply, in general, differences in the chemical shift, NMR data are widely used in the structural characterization of porous materials. For zeolites, one prototypical case is ^{29}Si, sensitive to bond distances, angles, and next-nearest-neighbor enviroment: its usefulness in probing the Si/Al ordering in zeolites[139] has been long recognized.[140] Besides ^{29}Si,[141] also ^{27}Al plays a key role in many topical issues, for example in the characterization of zeolitic acid sites,[142] or nucleation and growth processes,[143] while ^{33}P[144] is especially relevant for aluminophosphates. Many other nuclei (^{1}H,^{2}H,^{13}C, ^{15}N, etc) are however largely exploited, e.g. for the study of MOF's ligands (see Ref.[138,145,146] for reviews and Ref.[147] for a recent multinuclear characterization of a formate MOF). Also, with the Dynamic Nuclear Polarization approach it is possible to obtain high-quality ^{13}C, ^{1}H, ^{15}N SS-NMR spectra with natural isotopic abundance.[148]

Moreover, with NMR spectroscopy it is possible to probe the uniformity and the connectivity of the pores. ^{129}Xe chemical shift is a good probe of the inner pore surfaces, because it spans a wide range, and is very sensitive to the shape and size of the void. ^{129}Xe NMR has been applied to hydrates[149]and zeolites,[150] but also to MOF's,[151] organic zeolite analogs[152] and silica-based mesopores.[153] In the latter case, for example, the^{129}Xe chemical shift can be correlated with the diameter of the mesopores.[154] With optical pumping techniques it is possible to produce hyperpolarized xenon which allows for a large increase in signal intensity. This high sensitivity has been exploited, for example, to study the distribution of the ibuprufen drug in functionalized mesoporous silicas.[155]

Also the dynamic behaviour of the guests can be studied by solid-state NMR spectroscopy. In this respect, variable-temperature ^{2}H NMR experiments are well-established tools: for example, they have recently allowed to characterize the dynamics of ethylene bound to Ag^{+} site in Ag/H-ZSM-5 zeolite, highlighting two internal rotations of the guest about its symmetry axes.[156]

Other short-range approaches are very fruitful: indeed, **vibrational spectroscopies** (principally, IR and Raman) are prime techniques for investigating porous materials.[157] In particular, infrared spectroscopy of adsorbed probe molecules,[158] like NH_3[159] or CO,[160–162] is highly sensitive to the environment of the absorption site, and has demonstrated to be a powerful method for studying, e.g., Brønsted or Lewis acid centers in zeolitic frameworks. More exhotic approaches, such as photoacoustic IR, enable a precise discrimination of linkers in MOF via the sound produced upon IR irradiation.[163] Raman spectroscopy is widely adopted to gather insight on the orientation of guest species in a broad variety of pressure and temperature conditions (see e.g. examples in chapters 6 and 8). A sophisticated variant, coherent anti-Stokes Raman scattering spectromicroscopy (CARS), is particularly sensitive: for example it has revealed the formation of head-to-tail chains of adsorbate molecules inside the pores of ZSM-5 zeolite.[164]

Most materials presented in this work are of interest for their optical properties. In this respect characterization is performed with **UV-VIS-NIR and luminescence spectroscopies**.[165] The positions of the electronic bands are sensitive to the oxidation state and local coordination environment of the absorbing center. However, only the development of single-molecule techniques such as confocal **fluorescence microscopy**, has allowed to gather insight on the orientation of fluorescent molecules in 1-D zeolite channels. The electronic transition dipole moment of these molecules is normally aligned with their long molecular axis.[30] The technique probes the orientation of the emission dipoles: for example, fluorescence detected upon irradiation with light polarized parallel to the crystal axis (which coincides with the zeolite channel axis) indicates that the molecules are aligned with the channel.[30,165] While this method assumes a homogeneous angular distribution of the encapsulated molecules, such a limitation is overcome by a more recent variant (polarimetric two-photon fluorescence microscopy), which quantified molecular disorder at high concentrations of incorporated dyes.[166]

In general *single-molecule imaging/spectroscopy techniques* have undergone an impressive advance in the latest years (see Refs.[167–170] and special issue of *ChemPhysChem* **2012**, 13, 881–1095). Not only they give insight on the orientation of guests, but they also allow to visualize fine details of pore accessibility and connectivity – a recent example is the demonstration of pore-blocking of zeolite ferrierite during a catalytic isomerization process.[171]

EPR also provides valuable insight on local environment of paramagnetic species. Besides catalytically relevant transition metal centers, it has proved to be particularly effective in the study of zeolite-incorporated metal clusters (chapter 4).

Also **destructive techniques**, like thermogravimetric (TGA) and differential scanning calorimetric (DSC) analyses, as well as mass spectrometry, are widely empoyed for qualitative and quantitative elucidation of the guest content of inclusion compounds, and are particularly useful when combined with non-destructive analyses as the above-mentioned ones.

Finally, the use of **computational approaches** such as quantum chemical and molecular dynamics calculations enables to capture at atomistic level structural and dynamical features otherwise difficult to gather from experiments. Details on the application of computational methods to porous materials can be found in a recent comprehensive review,[172] technical books[173] and MOF-dedicated accounts.[174–176]

3. Empty space architectures

Porous materials can be broadly classified, according to IUPAC, into three categories based on their pore size: *microporous materials* (pore diameters below 2 nm), *mesoporous materials* (pore diameters between 2 and 50 nm), and *macroporous materials* (pore diameters exceeding 50 nm). During the past decades, various classes of porous solids emerged, such as organic clathrates, porous organic cages[177,178] or polymers,[179]

and all-inorganic polyoxometalates,[180] which have further widened the range of possible functionalities and made it hard to select the best material for a given application.[181] Although regular porous solids always exhibit an ordered network of pores, the pore walls may be crystalline (e.g., zeolites), amorphous (mesoporous silica) or broadly periodic (organosilica materials). Transport, adsorption and diffusion processes are not discussed, as they are covered by previous accounts,[46,182–186] including a recent comprehensive review.[187]

The organization inside the pores can be hierarchically extended from the molecular up to the macroscopic scale using assembly approaches in the case of colloidal particles/microcrystals.[188,189] Other common strategies[190–192] imply the attachment or immobillization of the microcrystal on a support. The interfaces (or terminations), of the porous crystals, play a key role in such strategies, but are still relatively little explored.[193] A deep knowledge of the interface regions is fundamental for both host-guest inclusion processes and the final utilization of the prepared material in a functional device.[37]

3.1. Zeolites

Zeolites are microporous crystalline materials mainly made up by aluminum, silicon and oxygen atoms.[57,194] While natural zeolites are important in earth science and mineralogy,[124] synthetic zeolites are ubiquitous in industry and technology.[87,190] Owing to their exceptional thermal stability, selectivity, and activity properties, these materials have been adopted since early 1960s in a wealth of industrial processes involving catalysis, adsorption and ionic exchange, and are key ingredients of detergents and desiccants.[195] Their potential as host matrices for low-dimensionality nanosystems[42] or building blocks for energy harvesting devices has been recognized for long time.[14,30]

Corner-sharing tetrahedra are the *primary building units* of zeolite frameworks and are often designated as TO_4, where T indicates an atom – normally Si or Al - coordinated to four oxygens. The *frameworks* define architectures of channels and cages of nanometer size, which host various *extraframework* species - molecules, ions, nanostructures or supramolecular aggregates – according to the shape and size of the pores.[124]

3.1.1. Structural aspects

To date, the database of the International Zeolite Association (IZA)[59] contains 234 different zeolite structures (each identified by a three-letter code) which may be classified according to the size (i.e., the number of T atoms) of the pore openings, or to the number of dimensions defined by the pores.[57,196] Several structural descriptors have been devised, which provide information on the geometry of the pores,[197] the building blocks of the framework,[198] or the environment of a T atom,[199] as documented in a recent themed review.[200]

The considerable number of zeolite framework types (or "*topologies*") implies that a wide variety of cages and channels, with different geometry and size, are available for the confinement of various guests (Figure 9). The diameters of the pore openings typically range between 0.3 to 0.8 nm, while those of the inner cavities are larger, namely from 0.5 to 1.3 nm.[57]

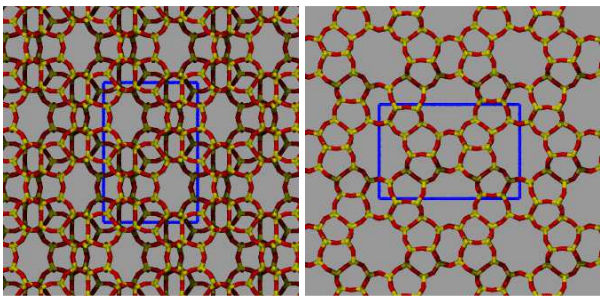

Figure 5. ***The framework structure of silicalite*** (MFI), a zeolite with a 3-D channel system projected a) in the bc plane; b) in the ac plane. Colors: yellow = Si, red = O. The blue line delimits the unit cell. [Illustrations created with VMD, using the X-ray positions from Ref.[57,59]]

Zeolitic channels form one-dimensional – two-dimensional, and three-dimensional arrays of void space. In a zeolite with one-dimensional (1-D) nanochannels, the channels run parallel to one direction and do not intersect with each other. Two-dimensional (2-D) nanochannels cross each other: such intersections, though beneficial in catalytic applications,[201] make the production of sequential arrangements of included species more difficult to control.[37] The same holds for 3-D nanochannels (a typical example is the widespread, industrially relevant MFI framework of silicalite, Figure 5).

Zeolites can also be produced in a two-dimensional form,[202] – a desirable feature for catalysis, which opens new routes to the surface confinement of nanosized species. They are synthesized as zeolitic nanosheets,[203] or ultra-thin films deposited on metal oxides[204] and metal surfaces[205] Other intriguing variants, such as layered zeolites - composed by parallel sheets[206,207] or hierarchical macroporous zeolites[208–210], have been invented in the latest years. These advances allow to "escape from the 10Å prison" of zeolite nanospaces – as aptly termed by Ozin[211] - and broaden the scopes of these materials as organizing scaffolds for diverse nanospecies.

3.1.2. Chemical aspects

All-silica zeolites are formed by Si tetrahedra only, and their framework is neutral. Traditional zeolites are pure aluminosilicates: the framework contains also aluminum, so each Al brings formally one negative charge to the framework. Such a charge is balanced by extraframework ions, mainly alkaline and alkaline-earth cations, hosted in the zeolitic cavities.

Although often considered as perfect and symmetric crystals, zeolites do contain defects; for example, the framework may be occasionally interrupted by hydroxyl groups occupying tetrahedral apexes,[196] or by cracks, as recently revealed by confocal fluorescence microscopy on large crystals of ZSM-5, BEA[212] and FER.[213] Also, seemingly homogeneous crystals are actually constitued by complex crystalline intergrowths.[214] In general, defects randomly distributed over the framework obstacle the fabrication of regular arrays of confined nanosystems.

Another important issue is the so-called structural disorder, which is related to the repartition of the Al atoms over the T-sites of the framework in aluminosilicate zeolites,[196] and affects the positioning of charge-balancing cations. The distribution of the Al atoms over the zeolite tetrahedral sites is normally very difficult to determine by X-rays because Al and Si have very close scattering factors.[196,200] However, the different effects of SiO_4 vs. AlO_4

neighbors on ^{29}Si and ^{27}Al resonances make SS-NMR the technique of choice for determining Si-Al site occupancies and the extent of structural disorder,[138,140] especially when accompanied by computational insight. By ^{27}Al SS-NMR spectroscopy and DFT calculations, for example, Sklenak et al demonstrated that the repartition of Al sites over crystallographic positions in differently synthesized ZSM-5 samples depended on the synthesis conditions.[215] *In silico*, the Si/Al problem is typically tackled by calculating the energy of model structures with different distribution of these atoms on the crystallographic sites[216,217] (same strategy holds for the Si distribution in silicoaluminophosphates).[218]

Along with cations, the pores normally contain water molecules, The interactions of these species with framework oxygens lead to a complex supramolecular network whose structure and connectivity basically depends on the size, geometry, and composition of the zeolite cavity, besides the nature and number of encaged species. For example, while in gismondine (3D-channels) waters are hydrogen-bonded both to the framework and with each other (Figure 6a), in the tight 1D-channels of Li-ABW water molecules prefer to bind with themselves, forming linear chains parallel to the channel axis (Figure 6b).

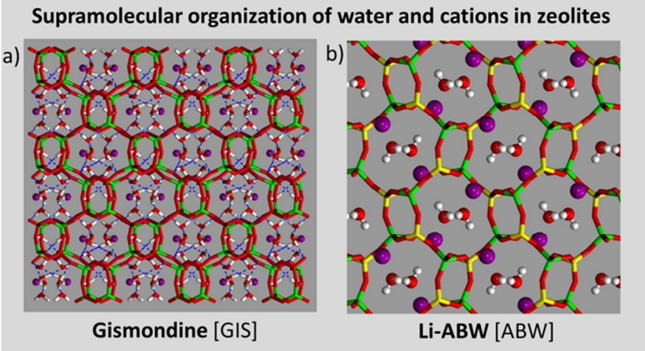

Figure 6. ***Organization of extraframework species*** a) The supramolecular network of calcium cations and water in natural zeolite gismondine (GIS, 3-D channel system). Colors: purple= Ca, green=Al, dark red=Si, red = O, white=H; blue dashed line=hydrogen bonds. b) Water molecules in single file in synthetic zeolite Li-ABW (ABW, 1-D channel system): hydrogen bonds with framework oxygens are very weak. Colors: purple= Li, green=Al, yellow=Si, red = O, white=H. [ICreated with VMD, using the X-ray positions from Refs.[219,220]

Water plays a prominent part in governing supramolecular organization inside zeolites – and in other porous materials as well. Hydrated zeolites undergo dehydration below 400°C and the process is normally reversible.[196] Such ability of reversibly losing and gaining water via dehydration/rehydration processes, , is also useful for tuning the orientation of dye molecules in zeolite nanochannels.[221,222]

Extraframework cations, being non-covalently bonded to the framework, can be exchanged by washing with a concentrated solution of a desired cation, thus making zeolites exceptional ionic sorbents, or exchangers.[190] If the cations are protons (which form covalent bonds with framework oxygens), acid sites are created, whose special reactivity enables to catalyze reactions of substantial relevance for oil industry like cracking of hydrocarbons, or methanol to gasoline processes.[223] Ionic exchange is also used in the ship-in-a-bottle synthesis of zeolite-encapsulated luminescent Ag clusters,[40] as well as for the incorporation of cationic dyes, an essential step in the production of artificial antenna systems and other zeolite-based devices.[30,52]

New framework types, as well as materials with composition different from natural zeolites, are continuously synthesized.[190] The possibility to replace Si and Al with different elements and to control the Si/Al ratio in the synthesis has producedzeolites with fine-tuned exchange, selectivity, and sorption properties exploited in industrial processes.[88,89]

The Si/Al ratio governs the hydrophilicity of the framework. Zeolites with higher Al content host a larger number of cations, adsorb predominantly water, and are used as ionic exchangers, while zeolites with a high Si/Al ratio, being more hydrophobic, have larger affinity for hydrocarbons and are exploited in petrochemistry.[88] Besides applications in industry, agriculture, and environmental protection[19,190,224] the hydrophilic or hydrophobic character of the framework plays a key role in the supramolecular organization inside these matrices.

Zeolites where atoms other than Si and Al occupy tetrahedral sites (*zeotypes*) are important for catalysis:[57] for example, the acid strength of proton-containing zeolites[159,225–230] can be tuned by replacing Al with Ga[231–233] or B.[234] Boron zeolites are much less acidic than Al-ones, and have interrupted frameworks due to the tendency of boron to be trigonal:[235] tetrahedral coordination is recovered upon hydration.[236–238] Aluminophosphates (ALPO)[239,240] generally have neutral framework and large pore sizes[241] – like in VPI-5.[90,91] Elements like titanium, tin, or zirconium impart a Lewis acid functionality to the zeolite,[242,243] while Ge-containing zeotypes exhibit higher flexibility, extra-large pores, and even chirality.[244–247] A peculiar structural weakness of Ge-rich frameworks under hydrolytic conditions is at the basis of assembly–disassembly–organization–reassembly (ADOR), a powerful approach for the synthesis of new zeolites.[248]

Other elements have been incorporated in zeolite frameworks,[249] yielding previously unseen zeolite types and fine-tuning of the chemical properties of the materials.[200,250] Also, the fusion of organic functionalities with a crystalline framework has produced organic–inorganic aluminosilicates with open porosity, also known as “hybrid zeolites”.[251,252] Such variety of shape and composition provides further scopes to the confinement of guest species.

3.1.3. Electronic aspects

Zeolite frameworks are typically classified as insulators. The endeavor of imparting interesting electronic properties to zeolite frameworks has a long history,[16] and has involved both theoretical,[253] and experimental efforts.[93,96] For example, nitridosilicate and nitridophosphate zeolites, owing to their chemical stability, optical transparency, and electronic structure, can be suitable host matrices for Eu^{2+} doping, and have already shown potential as high-performance white-light luminescence materials (Figure 7).[97,254]

Also the titanosilicate ETS-10[92,255] is a remarkable material, featuring a low-dimensionality nanosystem encaged into a zeolite framework. Symmetrically distrubuted TiO_3^{2-} molecular wires occupy zeolite nanochannels, running along perpendicular directions (Figure 8).[256,257] Significantly, the wires displayed neat quantum size effects - band gap dependency on the wire length - and very promising optical properties.[258,259]

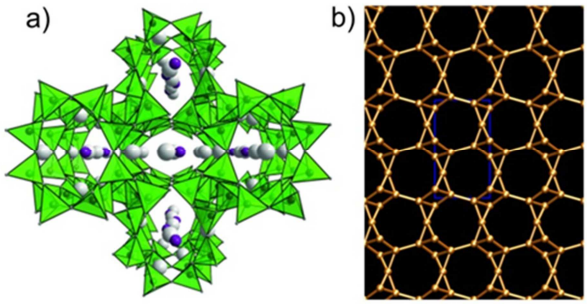

Figure 7. ***A host matrix for high-performance luminescence materials***: a) the nitridophosphate zeolite $Ba_3P_5N_{10}Br$[254] (Br=purple, Ba=gray, PN_4 tetrahedra=green, JOZ framework type[57,59]). It exhibits excellent white-light emitting properties upon Eu^{2+} doping. [Reproduced by permission from Wiley-VCH.[254]] b) JOZ framework structure [Image realized with VMD using the X-ray positions from Ref.[57,59]]

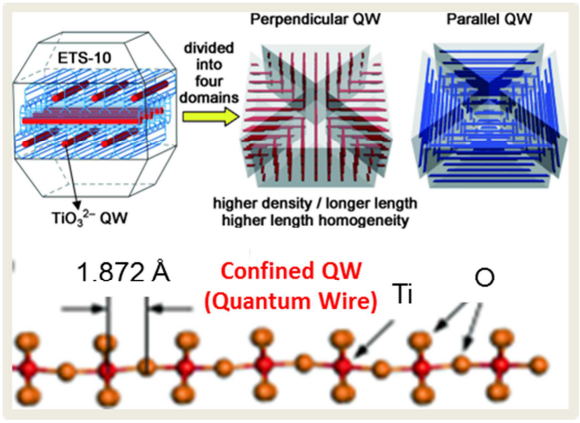

Figure 8: ***An organized lattice of TiO_3^{2-} quantum wires.*** The titanosilicate zeotype ETS-10 hosts in its 2D-channel system (running along the [110] and [1$\bar{1}$0] directions) an unique arrangement of TiO_3^{2-} quantum wires (QWs), characterized by different length. The confined quantum wires feature a symmetrical distribution.[Reproduced by permission from Wiley-VCH].[257]

The fabrication of semiconductive frameworks has focused on the family of chalcogenide zeolites,[95,249] because of their promising behaviour as electronic sensors.[94] Formally, these materials are derived by replacing oxygen with chalcogen atom (S/Se/Te) and Si/Al with tetrahedrally coordinated ions such as In/Ga/Sn/Ge. Recently, Lin et al. fabricated an In–Se chalcogenide zeotype (CSZ-5-InSe) with n-type semiconductor properties, and an ordered distribution of interrupted sites. Such semiconducting zeolite behaved as an effective catalyst for the oxygen reduction reaction, with the In interrupted sites functioning as active centers. The material was then selectively doped with bismuth at the interruption sites, thus allowing for an atomically precise fine tuning of its electronic structure.[260] In spite of the synthetic challenges posed by the fabrication of chalcogenide frameworks, this route seems worth pursuing - not only because the incorporation of semiconductor property into zeolite materials has proved to be possible,[260] but also because the electronic properties of these materials are tunable from metal to insulator by chemical design, as predicted by a recent modeling study.[261] Furthermore, beside their intrinsic relevance as transparent nanoporous semiconductors,[261] these zeolite frameworks could also open totally new application prospects to the confinement of quantum dots,[261] and chromophores (Figure 9).[262] Hu et al recently accomplished an energy transfer process implying the participation of a chalcogenide-based zeolite (coded as RWY) acting as light-harvesting host. The acridine orange dye was encapsulated into the host, and contacted at the pore entrances with another dye (rhodamine B) too large to enter the pores. Upon UV light absorption by the host, energy was transferred to acridine orange, and then to rhodamine B yielding visible-light emission.[262] The energy-funnel behaviour of the RWYhost was confirmed in a second experiment conducted with different dyes (proflavine and pyronine), which highlighted a significant increase of the energy transfer efficiency upon acidification and solvation of the guests.[263] These studies candidate chalcogenide-based semiconductor zeolites as very interesting host materials for energy transfer processes and photocatalysis.[264]

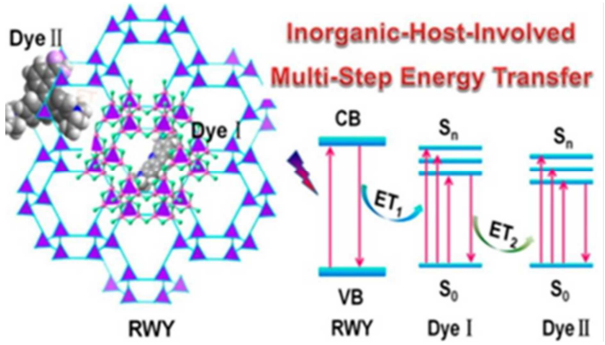

Figure 9. ***Chalcogenide zeolites*** incorporate semiconductive properties directly in zeolite frameworks. **RWY** is a chalcogenide zeolite that can host luminescent molecules and can be directly involved in energy transduction processes: here, the framework absorbs UV-light and transfers the excitation energy to dyes absorbing in the visible range. [Adapted with permission from Ref.[262] Copyright 2015 American Chemical Society]

3.2. Zero dimensional matrices: clathrasils and clathrates

Some silicate minerals are structurally very close to zeolites.[265] These polymorphs of SiO_2 known as *clathrasils* feature regular cavities of sub-nanometer size, but with such small openings to prevent diffusion of molecular species in and out of the pores:[121,133] thus, they might be ideally pictured as inert confining matrices for nanomaterials of zero-dimensionality. Although natural melanophlogite (Figure 4)[134,266–268] contains only very small molecules, like CH_4, CO_2 or N_2,[269,270] bigger hydrocarbons have been found in clathrasils with larger cavities:[121,271] indeed, the recently discovered chibaite,[272,273] hosts methane, ethane, propane and isobutane.[121,271–273]

These minerals (Figure 10) are silica analogs of the well-known natural gas-storage media *methane hydrates*.[274,275] Melanophlogite, for example, is isostructural with the hydrates of „structure I“ (sI) (Figure 10a), which have two kinds of cages: two pentagonal dodecahedra [5^{12}] (with 12-sides) and six tetrakaidecahedra [$5^{12}6^2$] (with 14-sides) in the unit cell (figure 11a). Yet the multifaceted richness of clathrate hydrates goes well

beyond the simple methane hydrate's MEP topology – indeed, they encompass at least six framework types.[79]

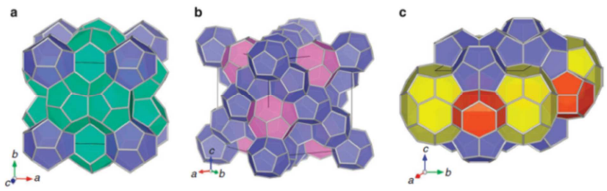

Figure 10. ***Three types of natural clathrasils*** (all-silica minerals): a) melanophlogite (MEP); b) chibaite (MTN) and c) mineral of type DOH as yet unnamed. These clathrasils are isostructural with hydrates of a) structure I; b structure II; c) structure H, respectively [Reproduced by permission from Macmillan Publishers Ltd.]

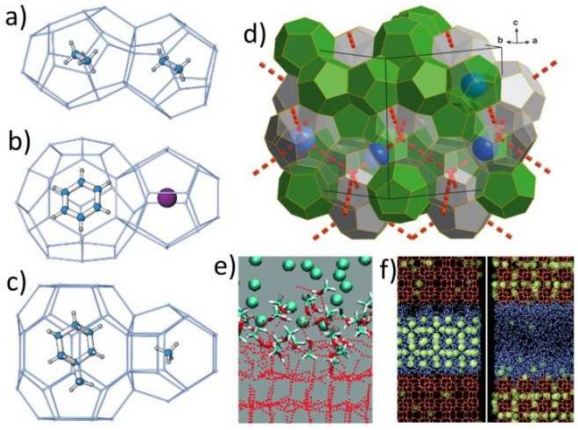

Figure 11. ***Clathrate hydrates*** a-c) Cages of the three main hydrate structures with encaged guests from single crystal X-ray diffraction (only a single position for the guest species is shown in each cage): a) Ethane in the [$5^{12}6^2$] (left) and [5^{12}] (right) cages of cubic structure I; b) cubic structure II, with benzene in the large[$5^{12}6^4$] cavity (left) and a Xe atom in the small [5^{12}] cavity (right); c) Structure H, showing methylcyclohexane in the large [$5^{12}6^8$] cavity (left) and methane in the small [$4^35^66^3$] cavity (right). [a-c) reprinted from Ref. [276]with permission from Elsevier] d) Leaching of Ne atoms (blue) from sII clathrate structure: the atoms move only between large cages (grey) by transiting through six-membered rings of water molecules (the red dashed lines indicate the trajectory of Ne atoms). [Adapted by permission from Macmillan Publishers Ltd.[277]] e) Simulation snapshot illustating the incipient formation of methane hydrate from frozen water/methanol (dots/sticks) solutions exposed to methane gas (cyan balls) at pressures of 30–125 bar and T= 253 K. [Adapted from Ref. [278] with permission from Wiley-VCH]. f) snapshot from MD simulations showing the conversion of a methane clathrate hydrate in contact with all-silica silicalite into methane-filled silicalite (red sticks=silicalite; blue sticks=water; green balls=methane) [Reproduced from Ref.[279] with permission from The Royal Society of Chemistry].

Besides sI, there are two other important structures. One is a cubic symmetry phase, named (sII), of framework type MTN (Figure 10b): its unit cell contains sixteen 5^{12} cages and eight large hexakaidecahedral [$5^{12}6^4$] cavities (Figure 11b). The other phase, structure H (H is for „hexagonal", framework type DOH, figure 11c) comprises layers of 5^{12} cages alternated by layers with small $4^35^66^3$ cages and large barrel-shaped $5^{12}6^8$ cages (Figure11c).[80] Dimethyl ether forms a more exotic hydrate structure, sT hydrate, exhibiting a trigonal crystal structure.[280] The remaining phases appear at elevated pressure. Hydrates are often studied in this harsh regime, and for very good reasons: first of all, their *pressure-induced stability increase.* This allows to reach temperatures around 10 °C (hence, higher than ice melting point) at pressures of 0.1 GPa.[281,282] Note however that there are some hydrates that do not need high pressure, like hydrogen sulfide hydrate, which can exist at ~ 1 atmosphere and 273K.[33]

Most gas hydrates crystallize in sI or sII structures, and the type of structure is determined mainly – but not exclusively - by the size of the guests. Whereas sI is often formed with small molecules (e.g., methane), sII can contain larger guests (Figure 11b). Both large and small guest molecules are needed for sH to form (Figure 11c). However, small molecules like H_2, have been demonstrated to form sII hydrates[283] This happens because: i) sII has more small cages; ii) the large $5^{12}6^4$ cages can accommodate multiple small molecules.

Recall that clathrate hydrates are archetypical non-stoichiometric compounds: it is not necessary for all cages to be occupied. For example, in the ethane hydrate of Figure 11a, the large cage was fully occupied while the small cage was found to be nearly empty (~5% occupancy) yielding a composition of C_2H_6*7.52(1)H_2O.[276] The cage occupancies are thus very different from CH_4 hydrate, where all cages are strongly occupied (large: 100%, small: 90%), and from CO_2 hydrate, where the small cavities are empty.[80]

Fortunately, with single crystal X-ray (or neutron) diffraction it is possible to determine the composition of these phases and their structure, provided that a proper analysis of the guest disorder is performed.[276] For example, the ethane hydrate of Figure 11a is disordered over 8 symmetry equivalent positions: their analysis indicated that the guest are not in the center of the cages, rather they stay close to the walls.[276] The same holds for the benzene molecules in Figure 11 b. This happens because close contact guest-framework allow are to maximize the van der Waals interactions that lie at the basis of the stability of hydrates.

In general, clathrate hydrates are classic supramolecular compounds formed by a framework of water,[79,274,284] in which ions or molecules are encaged (Figure 11a-c). In spite of innumerable studies, these curious forms of ice still remain amazingly surprising. For example, it was thought that they must always contain molecules to avoid collapsing. Yet such rule was broken by a spectacular experiment which accomplished the emptying of a neon hydrate, bringing thus to life the seventeenth phase of ice.[277] This achievement was believed to be impossible, because the stability of hydrates relies only on the very weak interactions between the water framework and its guests. Inspired by the discovery of empty Ge-clathrates,[285] and by previous work suggesting diffusion of H_2[286,287] or Ne[283] through the clathrate lattice, Falenty et al. subjected neon hydrate to continuous vacuum pumping. After 5 days, all guests were gone, and the empty hydrate was studied by neutron diffraction. The empty clathrate was found to resist up to temperatures of ~145 K before decomposing and to undergo a considerable enlargement of its framework with respect to the guest-containing hydrate.[277] The proposed emptying mechanism essentially involves the passage of Ne between the large cages of the sII lattice (Figure 11d), while removal of a Ne from the small cavities would require a "hole-in-the-cage" - i.e. the presence of water vacancies in cage walls.[288,289]

Such experiment underlined the relevance of kinetic effects and host–guest interactions in clathrate hydrates. Similar conclusions were drawn by a recent study on the formation of CO hydrate,

which highlighted the relevance of guest-guest interactions in stabilizing double-CO occupancy of the large cage in structure sII.[290] In general, the physico-chemical origin of hydrate structures should be the solvation of a hydrophobic guest, like those in Figure 11a-c. Nevertheless, hydrophobic interaction is not the only stabilizing cause, because hydrate framework stability depends *holistically* on host-guest interactions: hence, on a balance of the hydrophilic and hydrophobic components. In this respect, methanol is an archetypal case. To the gas companies, hydrates are a real nuisance: to prevent their formation in gas lines, they often add methanol, that acts as „inhibitor": in fact, its hydroxyl group has a distrupting effect on the hydrogen bond network of the hydrate lattice. In spite of this, it has been recently shown that methane clathrate forms very rapidly by exposing frozen water–methanol mixtures to methane gas, using pressures from 125 bars at 253 K.[278] On the basis of simulation results, it was proposed that the methanol hydroxyl group should be involved in a sort of unconventional „catalyst-role" during the formation of hydrates with hydrophobic guests from ice (Figure 11e).[278,291]This could explain the experimentally observed increase in the rate of methane hydrate formation (by up to two orders of magnitude) in presence of methanol.[278]

Also, the recent use of methanol as a helper to obtain more stable NH_4F-containing frameworks[292] via a crystal-engineering approach may be potentially interesting in applications such as gas storage. Indeed, among today's challenges in clathrate research, a major one is understanding the formation and decomposition of hydrates (see Ref.[293] for a review). Computational approaches are instrumental to this aim. For example, the behavior of methane hydrate enclosed between two slabs of hydrophobic silicalite was recently studied by molecular dynamics, showing that the clathrate structure was destabilized by the interaction with the silicalite surface silanol groups.[279] Notably, at low temperature the clathrate structure is basically maintained, while increased thermal motion leads to destruction of the water cages, starting from the interface with the zeolite and proceeding layer-by-layer until complete hydrate decomposition (Figure 11f). Interestingly, the released methane is absorbed by the hydrophobic zeolite pores – an insight that might be useful in the quest of controlled methane extraction from natural hydrates. Despite the existence of intracage diffusion (detected also for methane),[294] according to the Latin word *clatratus*, guest species are trapped, but also protected, "by the bars of a grating". Contrary to hydrates, clathrasils have an exceptional thermal stability at normal pressure. By this virtue, even highly reactive species - such as the methyl radical[295] and the S_2 molecule[296] - can be confined in the cavities of clathrasils. Protected by this inert environment, species can be thorougly characterized spectroscopically:[297] for example, femtosecond pump-probe experiments were able to capture the photodissociation and recombination reactions of iodine molecules inside the cages of decadodecasil-3R (DDR).[298] Such sophisticated experimental analyses in extremely restricted spaces provide, therefore, fundamental molecular-level insight on the dynamics and reactivity of confined molecules - which might be also potentially useful, for example, to the realization of confined quantum dots.

Silica clathrates can be synthesized in laboratory.[299] Dodecasil-3C (MTN framework type) was among the first ones to be produced. Interestingly, this is another case in which the artificial realization of the material[300] came long before the discovery of the mineral,[272] and the same happened to the corresponding hydrate (structure H)[119,120]

Many other framework compositions have been realized leading to new materials for potential optoelectronic, thermoelectric[199] or electrochemical applications,[275,301,302] or perspective catalytic uses.[303] Synthetic clathrates are classified as anionic, cationic, or neutral according to the formal charge of the framework; apart from few remarkable exceptions,[285,304–306] they need to contain a guest in order to be stable.

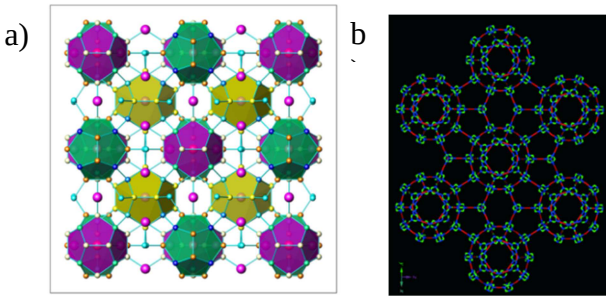

Figure 12. ***The peculiarity of inverse clathrates*** (a) is that the guest species are negatively charged. This one is $Si_{30.3(8)}P_{15.7(8)}Se_{7.930(3)}$ (ordered formula: $Si_{32}P_{14}Se_7$) (MEP framework type): the Se guests are shown as big purple balls. [reprinted from Ref. [307]with permission from Wiley-VCH] ***A MOF clathrate of MTN topology*** (b) containing large cages (volume of about 2.5 nm^3) The MOF $[\{Cd(H_2O)_3\}_{34}(N_4C_6H_{12})_{17}]Cl_{68}\cdot 46\,H_2O\cdot 68$ DMF, DMF=N,N-dimethylformamide] is viewed along the [110] direction. The openings of the six-membered rings measure 12.3×13.1 $Å^2$ (between atom centers), while those of the five-membered rings are 10.4×10.4 $Å^2$. Color codes: Cd=red, N=blue, C=green (O and H atoms are not shown). [reprinted from Ref.[308] with permission from Wiley-VCH]

While negatively charged frameworks (the most abundant ones) trap cations including e.g. europium, the positively charged frameworks of "inverse" clathrates are particularly interesting because, in contrast with most zeolites, they do encapsulate anions - mostly halides, but also tellurium or selenium. For example, a silicon-phoshorus framework can trap Se in a partially covalent embrace, leading to a semiconductive material of potential thermoelectric use (Figure 12a).[307]

Clathrates formed by silicon, germanium, and tin[301,309,310] should have, in principle, neutral frameworks, like silica clathrates or clathrasils; however, charge transfer from the encaged species normally imparts a formal negative charge to their framework.[311,312] Hypothetical guest-free carbon clathrates have been studied for long time[313,314] In 1993, Nesper et al considered all the zeolite and clathrate frameworks known at that time. They replaced each tetrahedral unit with a carbon atom and performed first-principles (Car-Parrinello)[315] molecular dynamics and structural optimization on those structures. Interestingly, calculations predicted that the modification derived from zeolite ZSM-39 (C_{MTN}) and melanophlogite (C_{MEP}) were the most stable hypothetical carbon allotropes after graphite and diamond.[313] Recently, a similar search was performed on ≈600 000 networks,[314] yet no such material has been so far synthesized. Nonetheless, other theoretical investigations suggest that mixed carbon-boron clathrate frameworks filled with lithium[316] or strontium[317] might be thermodynamically stable.

In general, the confinement in clathrate cages allows for the guest species can be studied with multitechnique approaches aimed at

a deeper understanding of their interactions with the host framework. Significantly, this feature is found in other classes of materials; small-caged zeolites such as sodalite (SOD) or ZSM-39 (MTN)[318] are well-known examples.[265] It is also worth noticing that several MOFs have clathrate topologies. The one shown in Figure 12b, for example, was generated by a metal–organic tetrahedral building block TCd_4 (T is a tetrahedrally coordinated molecule) in which the M-T-M angles range from 108 to 120°. Such MOF has MTN topology and exhibits very large cages.[308,319]

3.3. Mesoporous silicas and organosilicas hybrids

Compared to zeolites, mesoporous materials offer the possibility of accommodating larger objects inside their cavites. These materials may be either crystalline – i.e. the arrangement of the pores has long-range order - or amorphous. Only the former category is considered.

3.3.1. Mesoporous silica materials

Regular mesoporous silicas[320,321] and metal oxides,[322] as well as their hybrid organic-inorganic variants,[323–326] occupy a leading place in a variety of applications (for eviews see, e.g., Refs.[320–324,327] and *Chem. Soc. Rev.* **2013**, Issue 9). 3D mesopore systems are more suitable for catalysis because they are less plagued by pore-blocking, while 1D systems are preferred for the encapsulation of biomolecules,[328–331] drugs,[332] and confined nanostructures, such e.g. 1D-metal nanowires.[322,333,334]

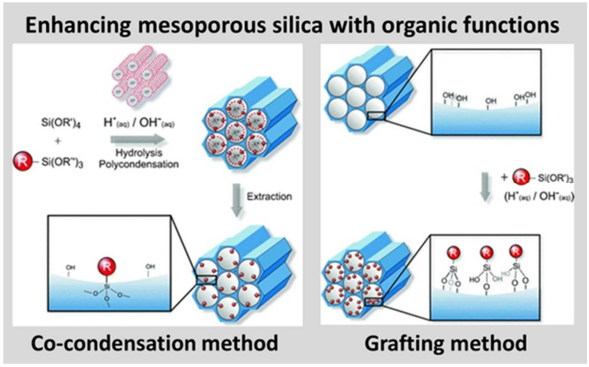

Figure 13. ***Imparting functionality to mesoporous silica.*** The co-condensation method is a "direct synthesis" approach: a trialkoxyorcanosilane R-Si(OR')$_3$ is added to the precursors. R = organic functionality incorporated during the synthesis. The grafting method is a post-synthesis approach, here schematically illustrated by the reaction of a trialkoxyorganosilane R-Si(OR')$_3$ with silanol groups Si-OH on the surface of the mesoporous silica material. [Adapted from Ref.[327] with permission from The Royal Society of Chemistry]

MCM-41[102] and SBA-15[335] have non-intersecting one-dimensional channels with long-range hexagonal order and well-defined diameters (Figure 13). The channel diameter is determined essentially by the template, generally removed by calcination after polymerization.[320,336] By a judicious choice of template and synthesis conditions, it is possible to tune the size of the channel according to the size of specific pre-selected guests.[21,320] Also, mesoporous silicas can incorporate additional functionalities into their matrix via 1) "one-pot" synthesis, i.e. by co-condensation of a functional organosilane with the silica precursor, or 2) "post-condensation", which consists in the binding ("grafting") of the functional organosilane to the walls of the mesoporous material, usually by impregnation or through the vapor phase (Figure 13).[323,337–340] The presence of a great number of surface silanols on the inner pore walls after the condensation step favors post-synthesis functionalization approaches. These are particularly convenient for optimizing the interaction with biomolecules,[341] or the positioning of encapsulated chromophores in artificial antenna system.[342–344] Post-synthesis strategies have also allowed to functionalize mesoporous silica nanospheres with molecular machines, creating intriguing devices for controlled release in drug-delivery.[345–347] For example, by attaching bistable rotaxane molecules to the pore entrances, Zing et al. realized molecular valves which could reversibly open or close the channel entrance commanded by redox chemistry inputs,[348] or sequentially load and release molecules of different size (Figure 14).[349]

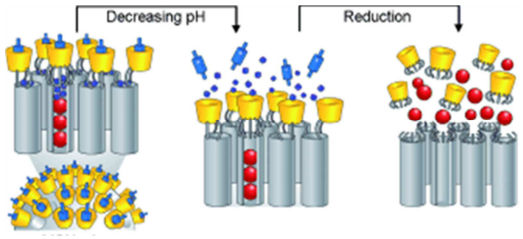

Figure 14. ***A sophisticated mesoporous silica-based drug delivery system***. Pore entrances are end-functionalized so as to release two drugs of different size (blue and red balls) one at a time upon the controlled action of different stimulations. The image illustrates schematically the two-step release process: the smaller molecule (blue balls) is released by lowering the pH, and the larger one by a chemical stimulation (in this case, by addition of a reducing agent). [Reprinted with permission from Wiley-VCH.][349]

3.3.2. Mesoporous organosilica materials

The invention of periodic organosilica[103,350–352] offered the exciting opportunity to do "chemistry *of* the channel walls"[353] of mesoporous materials. Indeed, differently from the silica-based counterparts, the pore walls of mesoporous hybrid organic-inorganic systems are constituted by organosilanes, where silicon atoms are bridged by organic groups.[103,350,353] The organic functionality is, thus, "buried" in the walls as in co-condensed functional mesoporous silica, but in higher concentration and with a uniform distribution (Figure 15).[323] An early example that vividly pictures the "chemistry of the channel walls" in action, is mesoporous methylene silica.[353] The methylene group of the framework could be converted upon chemical stimulation into methyl group grafted on the channel walls, demonstrating the potential of these systems to exhibit a responsive, stimuli-driven behaviour[353]

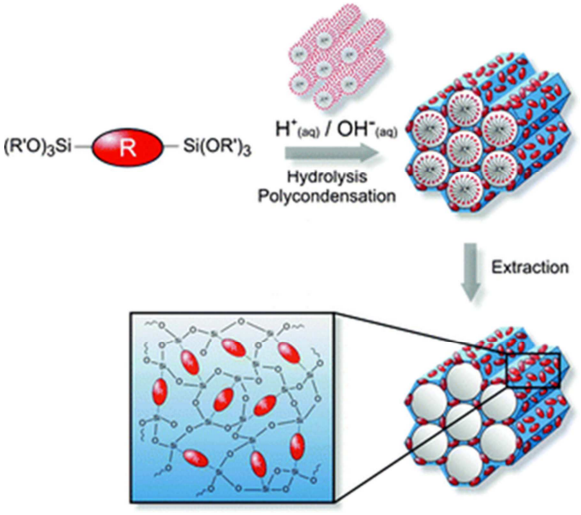

Figure 15. ***Schematic representation of the fabrication of PMOs*** starting from bis-silylated organic bridging units R. [Reproduced from Ref.[327] with permission from The Royal Society of Chemistry]

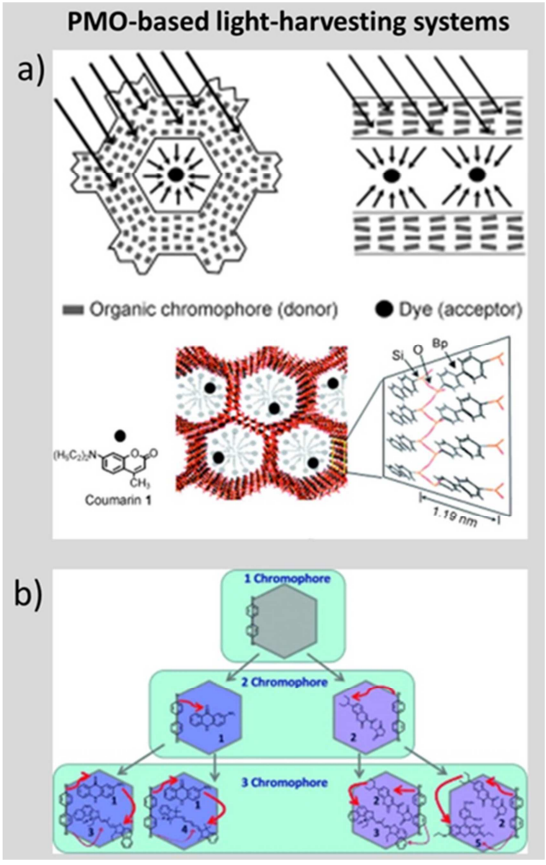

Figure 16. ***Embedding chromophores in the pore walls:*** Energy transfer from the chromophores incorporated in the pore walls of a PMO to the dyes inside the mesochannels. [Adapted with permission from Wiley-VCH.][62] b) schematic representation of the three-chromophore systems with light-harvesting behavior of Ref.[354], for which a two-step-Förster resonance energy transfer process was detected. Energy is transferred from the biphenyl moieties embedded in the pore walls to mediators (indicated as (1)), and then from the mediators to the acceptors (indicated as (3),(4),(5)). The emission wavelength can be varied from 477 to 630 nm by a proper selection of the acceptor dye. [Reprinted with permission from Wiley-VCH.][354]

Both silica and organosilica porous materials offer control over pore size and morphology.[323,355] Yet the possibility to fine-tune the composition of the organosilica pore walls makes these hybrids very versatile materials,[323,326] because of the immense platform of available functional precursors.[52,322,326] Similarities and differences among mesoporous organosilica and their inorganic cousins are thoroughly discussed in a review focused on their use as organizing matrices for advanced applications.[326] In this regard, the incorporation of suitable chromophores in the organosilica walls, along with a proper selection of photoactive guest species is a particularly appealing option, which has already produced materials for light-harvesting devices. (see for some examples).[52,62,331,354] For example, the Inagaki group devised an ingenious light-harvesting system by expoiting the biphenyl bridges in the PMO walls as the light absorbing donors, while the incorporated coumarin dye acted as acceptors (Figure 16a). By investigating the effect of the acceptor loading, it was found that the quantum yield of the material doubled by increasing the coumarin content by 0.8%; the system showed a remarkable FRET efficiency, close to 100%.[62] The idea to use the organic bridges of biphenyl-PMO as donors proved to be successful also when two types of dyes were encapsulated (Figure 16b). Grösch et. al observed two-step-FRET from the biphenyl moieties to a mediator dye, followed by energy transfer from trhe mediator to the acceptor dye, with efficiencies ranging from 70 to 80 % This indicated that the mesochannel structure provides spatial arrangement of chromophore pairs. Interestingly, the wavelength of the emission could be tuned from 477 to 630 nm by a suitable choice of acceptor dye.[354]

3.3.3. The inner surfaces of mesoporous silica materials

The experimentally determined values of the pore thickness in mesoporous materials range between 7 and 15 Å. Pores surfaces may have different degrees of hydrophilicity depending on the surface density of the exposed silanol groups (normally from 1.5 to 7 SiOH/nm^2) and are very difficult to characterize, due to their amorphous nature and to the high density of defects.[356] Computational approaches helped to better understand the surface chemistry of these materials.[356,357]

Models explicitly considering the quantum nature of chemical bonding would be highly desirable, yet this route implies higher computational costs. Earlier first principles studies[356] utilized flat surface models, or nanometer-thick slabs,[358–360] to simulate the walls of mesoporous materials providing valuable insight into their defects. Combined with IR and UV-vis data, those calculations showed that very strained surface defects such as two-membered silica rings are energetically disfavored over non-bridging oxygen defects.[358,359] A similar model was used, jointly with IR and UV-vis spectroscopy, for the vibrational and electronic characterization of the different titanium sites in Ti-grafted mesoporous silicas.[360]Similar slit-pore models, though with the obvious limitation of the absence of surface curvature, have also provided information on adsorption processes dominated by local features of the surface.[356]

Slit-pore models[356] are widely used to study surface defects,[361] functionalization of pore surfaces,[362,363] the interaction with drugs,[364] aminoacids,[365,366] or peptides,[367] and confinement effects on liquids,[368,369] often unveiling intriguing facts. For example, molecular dynamics simulations showed that, in the presence of Na^+ and K^+ cations, a negatively charged peptide

(porcine pepsin) solvated by a water droplet can be attracted by a negatively charged silica surface.[367] The peptide-silica interaction was rationalized thanks to a detailed study of the electrostatic potential of the peptide surface,[370] which exhibited both negative and positive regions.[371] Such model allowed to explain why encapsulation of pepsin in SBA-15 occurs at pH-conditions where both protein and mesoporous silica are negatively charged.[372]
Recently, computational studies with slit-pore models highlighted interesting organizational properties of confined fluids.[368,369,373,374] According to Guo et al, an ethanol–water mixture undergoes a partial demixing within the walls of an hydrophilic pore: while ethanol molecules tend to adsorb on surface silanols, water molecules preferentially interact among themselves, forming wires or clusters (Figure 17a).[368] By attaching to the hydrophilic walls, ethanol creates an hydrophobic coat at the interface, which could explain why water molecules prefer to stay away from the walls and to self-organize in clusters.[368] Partial separation of ethanol and water was also found in model slit pores of graphene and boron nitride. Specifically, Kommu et al. observed a higher tendency of ethanol to selectively adsorb on the pore walls in the case of boron nitride, and showed that the ethanol/water partial demixing was relatively unaffected by the pore width (Figure 17b).[369] Similar microphase-separated tubular structures seem to be a recurrent feature of binary liquid mixtures in mesopores, and are also supported by experimental evidences.[373–376] For example, neutron diffraction experiments on MCM-41 filled with a *tert*-butanol–toluene mixture evidenced an inhomogeneous distribution of the components, suggesting that the pore surface is covered by *tert*-butanol molecules, while toluene preferentially locates in the central region of the pore.[375]

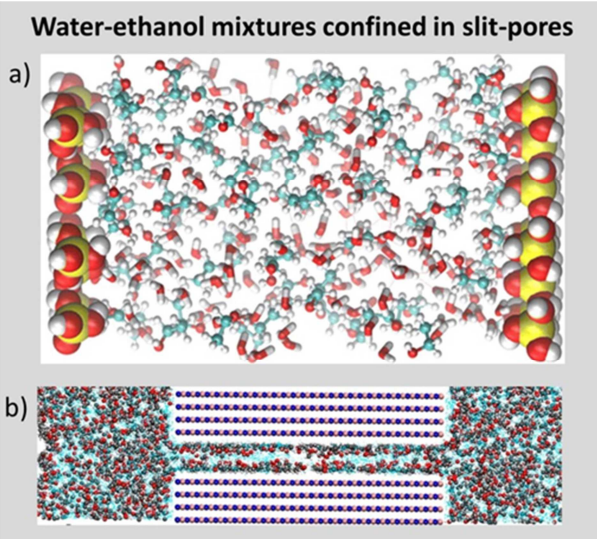

Figure 17. ***Organization of water-ethanol mixtures confined within slit pores*** of a) hydrophilic silica; b) boron nitride. Partial demixing occurs in both cases. a) Color codes: Si=yellow, O=red, C= cyan, H=white. [Adapted with permission from ref.[368]. Copyright 2014 American Chemical Society] b) Spheres represent ethanol atoms (O = red, C=gray H= white). Cyan dots represent water molecules. Boron-nitride layers: B=pink, N= blue. Size of the pore 13 Å. [Adapted with permission from ref.[369]. Copyright 2016 American Chemical Society]

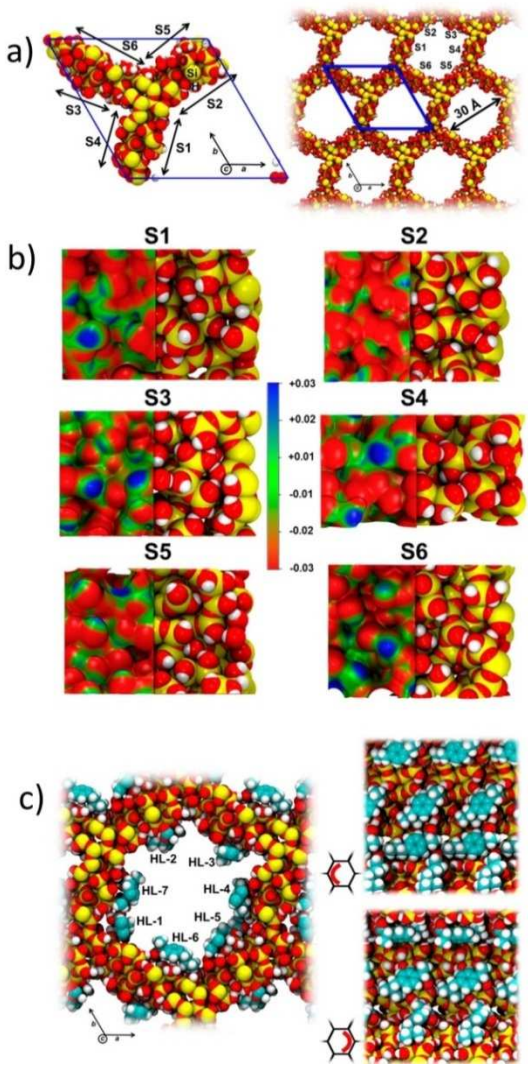

Figure 18. ***MCM-41 "in-silico":*** Unit cell (blue lines) and crystal packing of the MCM-41 model adopted in Ref.[377] to study the adsorption of the widespread drug ibuprofen. Both views are along the *c* axis. The six internal regions of the pore are identified as S1–S6. b) The right panels show the structure on top of which (left strip) the electrostatic potential was mapped on the electron density isosurface (used isovalue: 0.0004 *e*). The color scale indicates the electrostatic potential values. c) MCM-41 with 7 ibuprofen molecules adsorbed within the pore. (left) View along *c* axis. (right) Lateral view showing the two halves of the pore. Color codes: Si=yellow, O=red, C=cyan, H=white. Adapted with permission from Ref.[377] Copyright 2014 American Chemical Society.

Theoretical models well illustrate the fundamental role of surface silanols in the arrangement of the guest species. Ugliengo et al.[378] developed a periodic hybrid-DFT model of the hexagonal MCM-41 pores, (Figure 18), with pore diameter ~30 Å, walls ~10 Å thick, and silanol density ~7 OH·nm^{-2}. Such a model was used to study the absorption of water,[379] drugs,[380] and dye molecules[381] in MCM-41. The accurate treatment of hydrogen-bond interactions between the surface Si–OH groups and the adsorbates,[378] and the inclusion of dispersion[356] allowed to gather a realistic picture of the encapsulation of the ibuprofen drug[377] onto silica mesopores. As SS-NMR experiments

indicated a high molecular mobility of ibuprofen inside the mesopores,[155] to foresee the most favorable absorption sites for the drug, the investigators classified the inner surface in six regions with different silanol density and therefore different electrostatic potential (Figure 18b); in particular, the H atoms of the silanols are associated with positive values of the potential (blue color in Figure 18b), while O atoms with negative values (red color in Figure 18b).[377] Such electrostatic potential maps indicated that all the six sub-regions are hydrophilic and hence capable to adsorb hydrophilic moieties, as the carboxyl group of ibuprofen. Accordingly, the ibuprofen absorbed on all six regions, though with different arrangements depending on the local environment of the site. As a result, the calculated structure, containing seven molecules *per* pore, features a roughly uniform repartition of the drug on the pore surface, but without short-range ordering of the molecules (Figure 18c), because of the amorphous nature of the pore walls.

Experimental evidences support since long time the heterogeneity of the MCM-41 pore surface, which might be imagined to be composed by hydrophilic (silanol-rich) and hydrophobic (silanol-poor) patches.[382,383] A similar picture (Figure 19a) was obtained by modeling with classical molecular dynamics the dehydration process of a cylindrical silica pore *via* the condensation of adjacent silanols.[384] In spite of the initially uniform distribution of surface silanols, after dehydroxilation the silica pore features a slightly elliptical shape, with patches of hydrophobic or hydrophilic character located in high- and low-curvature regions of the pore surface, respectively. According to these simulations, the silanol condensation process and could be at the origin of the non-uniform Si–OH distribution on the surface. A similar deformation of the pore was also found in the simulation, by first-principles, of a silica pore model with a larger diameter, initially exhibiting a perfect cylindrical shape (Figure 19b).[385]

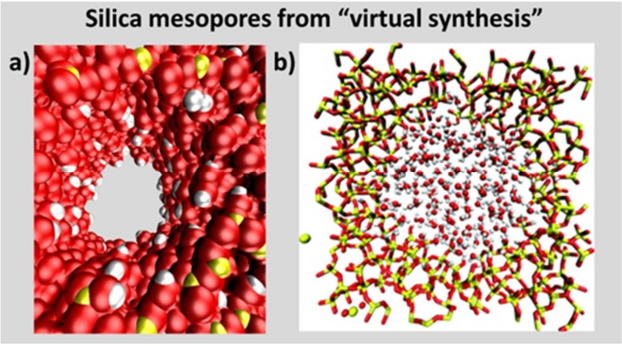

Figure 19 ***Silica mesopores obtained by virtual syntheses*** using a) force-field[384] and b) first principes[385] simulations. In both cases, the pore features an elliptical shape, and silanols are more densely distributed in the flatter rigions of the pore surface. Color codes: Si=yellow, O=red, H=white. In b), the pore also contains water molecules. [Reprinted with permission from Wiley-VCH.][385]

Various procedures allow to build pore models for computer simulations.[386] Nevertheless, the pore surface still remains very difficult to capture at atomistic detail. Whereas the pores of MCM-41 are non-connected, SBA-15 materials are more complex: they have intra-wall disordered microporosities,[387] or small transversal channels connecting the mesopores, as indicated by the evolution of ^{129}Xe NMR chemical shift with xenon partial pressure[153] likely generated by the penetration of the template chains in the SBA-15 silica framework.[388–390]

The connectivity among mesochannels has been visualized by single-molecule fluorescence microscopy (see Ref.[391] for a review). In these experiments, luminescent probe molecules were incorporated in as-synthesized mesoporous silica, and their diffusion along the hexagonally arranged channels was followed with a fluorescence microscope.[392] The passage of dye molecules between channels was detected, thus proving that the pores were connected.[393] Experiments with an orienting electric field and molecules of different size shed light on the local surface features, identifying leaky defects in the walls of the pores.[394]

To summarize, mesoporous materials incorporate guests that would never fit into zeolites: they have tunable pores and are relatively easy to functionalize. However, the amorphous structure of the walls implies that the surface functionalities (and thus the guest molecules) do not have a regular distribution at the molecular scale, and that the behavior of the included molecules is actually dominated by the surface defects. Also, small-sized guests still preserve much freedom of motion, which hinders the formation of uniform and stable supramolecular arrays.

3.3. Metal-organic and covalent porous frameworks

The most familiar examples of crystalline mesoporous materials are metal organic frameworks (MOF) – which are typically constituted by inorganic secondary building units, often containing a transition metal center, and organic linkers, joined through moderately strong coordination bonds.[395] One of them is shown in Figure 20: the peculiar triangular shape of its 1-D channels, very different from the elliptical or circular openings of zeolites or Si-based mesopores, suggests new opportunities for space confinement.[106] Indeed, this MOF was shown to incorporate dipolar dyes by a simple ionic exchange procedure, yielding a composite with high second-harmonic generation intensity.[61]

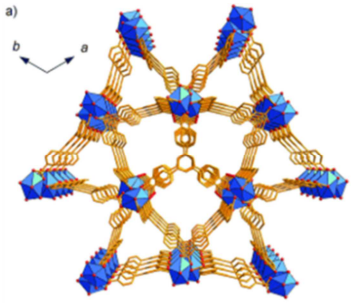

Figure 20. ***A MOF***. Schematic representation illustrating the inorganic building units (blue polyhedra) connected by the organic linkers. The MOF is viewed along the *c* direction (color codes: In=blue polyhedra; C=orange; O=red). By ion exchange, dyes can be orderly encapsulated in this MOF, leading to second-order nonlinear optical (NLO) materials[61] [Reprinted with permission from Wiley-VCH.][61]

A highly popular family is that of covalent organic frameworks, (COF) - which are made only by organic building blocks, and can be considered as the lightweight counterparts of mesoporous silicas or zeolites. They are useful in applications where low

weight and high framework flexibility are required, - with the additional benefit that advanced functionalities, such as chirality or photoconduction,[396] can be directly incorporated into the framework by a proper selection of the ligands and of the synthesis conditions.[397] Two-dimensional COFs, have a layered structure deriving from π-stacking of planar "building units" with extended π-conjugated systems amenable for electronic and optoelectronic applications.[32,396] A nice example is the COF in Figure 21: the stacking of the conjugated units perpendicular to the plane creates a tubular network within which bulky guests can be confined. This was the case of C60, which was incorporated into the COF via sublimation. Because of host-guest size resctrictions, only one C_{60} molecule can pass through the cylindrical pores. Upon irradiation with visible light, the composite displayed photoconductivity and fast response to the light stimulus, making this material particularly interesting for photoswitches and photovoltaic cells.[396]

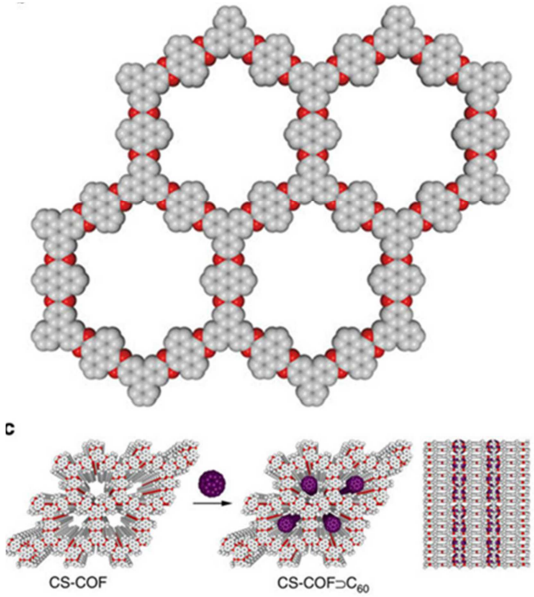

Figure 21. ***A π-conjugated COF***. van-der-Waals representation of one layer of the π-conjugated units (grey: carbon, red: nitrogen, *tert*-butyl groups and H atoms are not shown for clarity). The material is built from the stacking of π-conjugated layers, thus extending the periodic structural ordering of the π-conjugated layers to the third dimension. It can be used as organizing scaffold for bulky guests: for example, by encapsulating C_{60}, the resulting composite displayed a promising photoconductive behaviour.[396] [Adapted by permission from Macmillan Publishers Ltd.[396]]

The Zeolite Imidazolate Frameworks (ZIF) have high robustness and chemical stability.[398,399] Their pore dimensions are generally smaller compared to other MOF families. Although topologically isomorphic with zeolites, ZIF are made up by imidazolate linkers connected to transition metal centers in tetrahedral coordination. Their zeolite-like topologies derive from the fact that the metal-imidazolate-metal angles are close to the Si-O-Si inter-tetrahedra angles in zeolites. Figure 22 depicts one of the most studied members of this family: ZIF-8, with sodalite topology, has excellent mechanical properties and has become an archetypal example of MOF's resilience to high-pressure conditions.[398] These features make it a choice system also for computational studies providing a molecular-level description of the geometry[399] and flexibility[400] of the pore windows, useful in sorption applications.

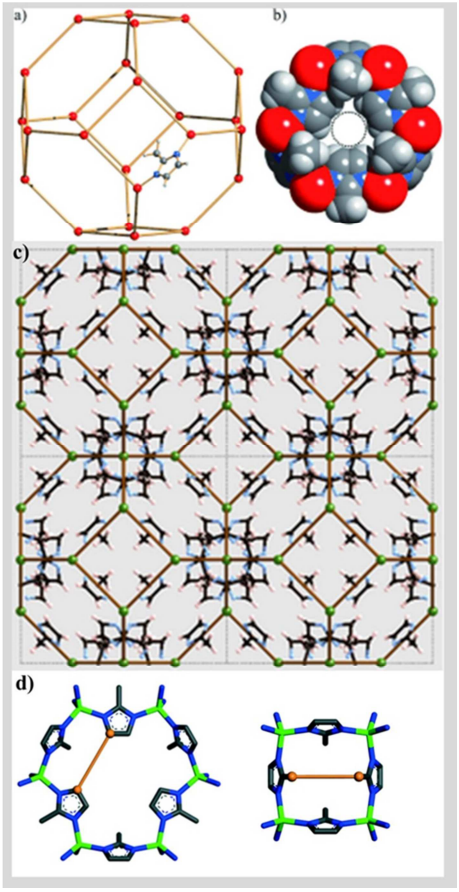

Figure 22. ***A ZIF with sodalite topology***. ZIF-8[398] has composition $Zn(mim)_2$ (where mim=2-methylimidazolate), and sodalite (SOD) topology. a) A topologic SOD cage, showing the typical six-ring (hexagonal) and four-ring (rhombic) windows. A mim ligand connecting two Zn centers (red balls) is also highlighted. b) space-filling representation of a six-ring window of the SOD cage with 3.3 Å diameter. Color codes: Zn=red, N=blue, C=gray, H=white. [Adapted with permission from Wiley-VCH.][398] c) Ball-and-stick representation of a 2×2 supercell of ZIF-8. The SOD topology is highlighted by brown lines connecting Zn^{2+} ions (green balls). [Adapted with permission from Wiley-VCH.][400] d) Ball-and-stick representation of the structure of the six-membered and four-membered rings in ZIF-8. Colors: Zn=green, N=blue, C=black (H not shown). The orange segments indicate the C-C which define the width of the window (4.946 Å and 4.608 Å for six- and four-membered rings, respectively).[399] [Reproduced from Ref.[399] with permission from The Royal Society of Chemistry]

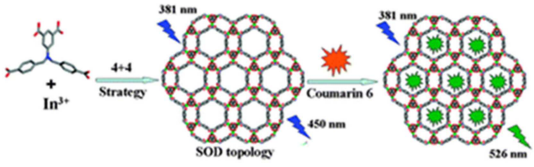

Figure 23. ***A ZMOF with sodalite topology***. This ZMOF, constituted by In^{3+} and a tetracarboxylate ligand, has a negatively charged framework with SOD topology and emits in the visible. By encapsulation of cationic dyes such as coumarin, it becomes an interesting composite for light-harvesting. [Reproduced from Ref.[63] with permission from The Royal Society of Chemistry]

Zeolite-like frameworks can be constructed with other linkers besides imidazolates. The resulting materials are usually termed ZMOF (Zeolitic MOF). As an example, the ZMOF depicted in Figure 23 has the topology of zeolite sodalite. This was obtained using organic building units designed to be the tetrahedral nodes in the final structure, and In^{3+} ions.[401] The ZMOF was loaded with coumarine dye by ionic exchange. Photoluminescence spectra of the composite evidenced that the excitation energy was transferred from the ZMOF host to the guest dyes, indicating an efficient light-harvesting behaviour.

A wide variety of MOFs frameworks has been reported, featuring systems of 1D- , 2D-, or 3D- channels similar to zeolites, and/or isolated cages analogous to clathrates. Cavities of various shape have been designed, and functionality has been imparted to the framework, using for example catalytically active metal centers.[402] Also the linkers often contain active, stimuli-responsive elements, such as rotors,[403] rotaxanes[404] and catenanes,[405,406] or luminescent species[407] Several MOFs incorporate functional elements both within their framework and inside the pores. Figure 24, for example, illustates the possibility to tune the rotor motion of the linkers by CO_2 loading/unloading in the MOF, demonstrated by ^2H SS-NMR spectroscopy. [403]

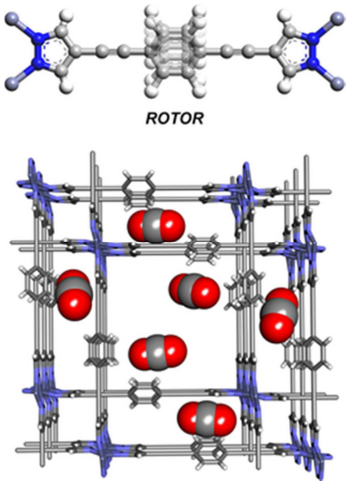

Figure 24. ***A stimuli-responsive MOF framework***, where the rigid rod-like linkers bears a phenylene rotor (top). The spinning speed of the rotors is tuned by the CO_2 entering the MOF. [Reprinted with permission from Wiley-VCH.][403]

The exponential growth of this area (for an overview see e.g., *CrystEngComm,* 2015, issue 2; *Coord. Chem. Rev*. 2016 - Issue 307; *Chem Soc Rev* 2017, Issue 11), has led to the formulation of a new nomenclature and general rules for classifying MOF's structures, which can be retrieved in dedicated databases.[408]

Such functional and stimuli-responsive platforms for the confinement of molecules or nano-objects have opened new perspectives not only to devices (see e.g. Ref.[31] for a review) but also to analytic methodologies. The so-called "crystalline sponge" approach refers to the preparation of composites in which guest molecules, are trapped into MOF cages and then studied by crystallographic methods.[262,409] In practice, carefully selected frameworks absorb target molecules from a solution, thus converting the incoming liquid into an arrangement of confined guest species thanks to the molecular-recognition ability of MOF cavities.[410] In this manner, the geometrical features of the absorbed species could be revealed, along with the host framework, by X-ray analysis of the porous composite material, thus making structure elucidation possible even for compounds very difficult to crystallize.[409,410] Besides the obvious advantages, the method suffers from limitations: i) structure resolution is not always successful, ii) pore confinement in some cases alters significantly the physicochemical properties of both the guest species and the host, as evidenced by a recent study.[411]

4. Clusters of metals or semiconductors: organization of zero-dimensional nanosystems

Zeolites have been elected as ideal matrices for creating ordered arrays of clusters of metal or semiconductors since the early 80's.[14] If we consider, for example, semiconductor nanoclusters, widely known as quantum dots, it is easy to understand why they are an ever-green topic in material science: they offer the unique opportunity of synergically combining quantum size effects - useful for optoelectronic applications, with an exceptionally high fraction of exposed surface atoms, that would be much desirable for catalysis. Unfortunately, the latter feature is usually accompanied by a too high reactivity of the clusters, and by the unwanted formation of larger aggregates. Confinement in porous matrices was early recognized as a viable solution for those problems, hence zeolite frameworks - chemically inert and characterized by remarkable thermal and mechanical stability – were immediately exploited to this aim. Ideally, both the high reactivity and the growth of the clusters would be limited by the small and regular size of zeolite pores. Practically, the implementation of this concept encountered several difficulties, which hindered the fabrication of regular, ordered architectures of clusters in zeolite cavities until very recent times. Although many other approaches to the production of uniform, low-dimensionality nanostructures were implemented over the years,[189,412] fabrication in confined spaces never lost its appeal. In particular, the improvement of synthesis and characterization techniques[413–417] combined with the insight from computational studies[45,418,419] fostered this decade's tremendous progress.[44,420]

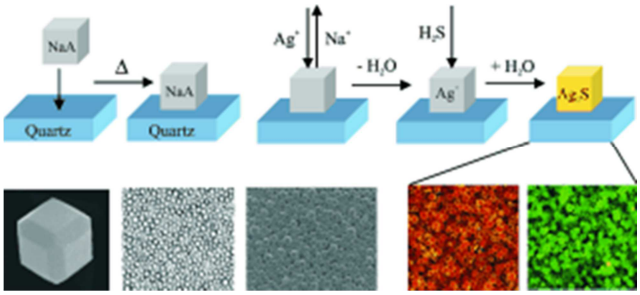

Figure 25. ***Ship-in-a-bottle" synthesis of confined nanoclusters***: 1) physisorption of monolayer of zeolite A crystals on quartz; 2) fixation of the monolayer by heating (600 °C); 3) insertion of Ag^+ via ion-exchange; 4) dehydration and exposure to H_2S vapor, which reacts with the encapsulated Ag^+; re-hydration and formation of stable $(Ag_2S)n$ clusters in zeolite. A. The images show the zeolite crystals during the various stages of this process. [Reprinted with permission from Wiley-VCH.][40]

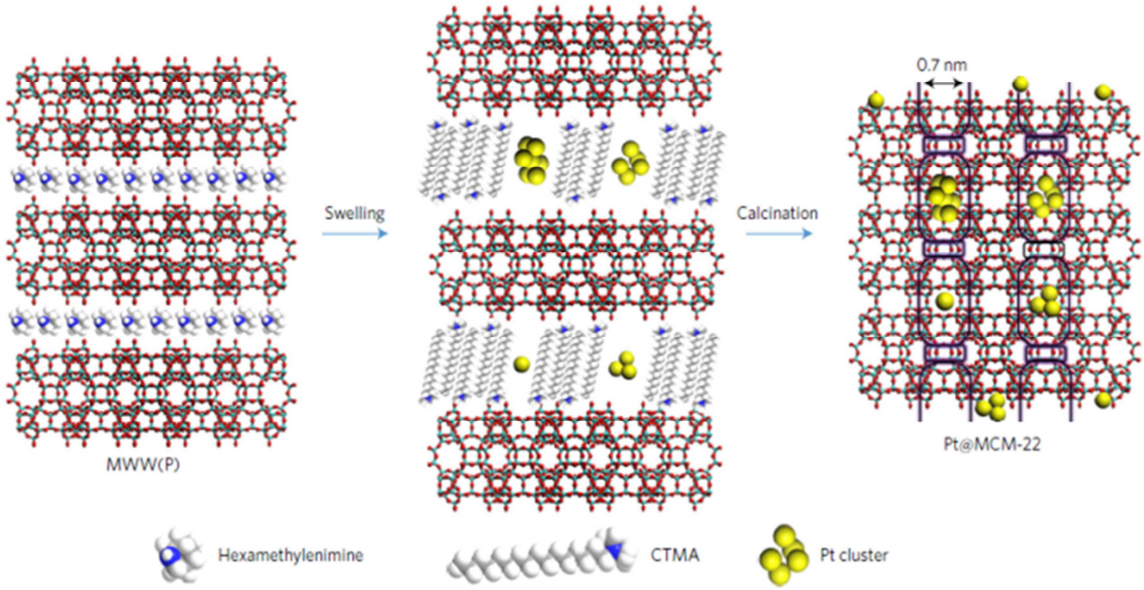

Figure 26. ***Fabrication of Pt-nanocatalysts confined in zeolite*** MCM-22 (MWW-framework type).[57,59] A Pt-containing solution is added during the swelling process of the pure-siliceous layered zeolitic precursors, in which the 2D-zeolite sheets are expanded using a common organic surfactant (hexadecyltrimethylammonium, $CTMA^+OH^-$). Smaller Pt species are also encapsulated inside the channels of each zeolitic layer. Removal of the template leads to the Pt@MCM-22 composite material, featuring supercages of ~0.7×1.8 nm size, loaded with Pt single atoms or subnanometric Pt clusters. Reprinted by permission from Macmillan Publishers Ltd.[130]

Common synthetic strategies for confined nanoclusters are vapor deposition methods with suitable precursors,[14,16] or "ship-in-a-bottle"[421,422] approaches allowing for the *in-situ* synthesis of compounds in a host matrix. In the latter case, the reactants are molecules and ions sufficiently small to penetrate inside the host nanochannels, leading to products too large to escape from the cavities. This concept is illustrated in Figure 25 for the "ship-in-a-bottle" fabrication of luminescent silver sulfide clusters in supported zeolite A monolayers.[40] In practice, silver ions enter zeolite cages via ionic exchange, and self-assemble into clusters upon heating or irradiation with light in a process usually called "activation".

A new strategy for the fabrication of zeolite-confined nanocatalysts was recently proposed by the Corma group, based on the incorporation of Pt during the transformation of a two-dimensional into three-dimensional zeolite.[423] The idea was to entrap Pt clusters inside the hemi-cages of a layered zeolite precursor during the condensation step (see Figure 26). Besides outstanding thermal stability and catalytic activity, the obtained composite material actually featured a distribution of confined Pt-species, comprising both individual atoms and nanoclusters up to 1 nm in size. This example clearly showcases how difficult it is to synthesize arrays of confined clusters with atomic-level order. Irrespective of the nature of the nanostructures and fabrication strategy, perfectly ordered arrays of e.g. nanodots would be obtained only if the pores were uniformly occupied – thus, in practice, only if the confining matrix were completely filled by species of the same size. This objective is very hard to achieve even by using zeolites with a single type of pores of small size, such as sodalite – which is constituted only by small-sized cavities called beta-cages (see Figure 26).

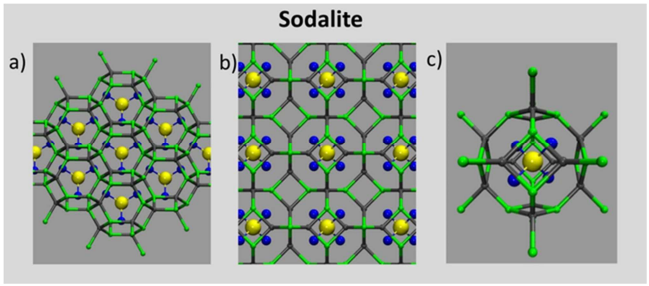

Figure 27. ***Natural sodalite*** (SOD framework tipe). a,b) Two representations highlighting: a) the six-membered-ring windows of the cavity; b) the cubic symmetry of the framework, entirely constitued by the infinite replication of a sodalite-cage (shown in c)). Color codes: Si=grey; Al=green; Cl=yellow; Na=blue (the framework oxygen atoms are not shown for clarity). [Illustration created with VMD, using the X-ray positions from Refs[57,59]]

Syntheses inside mesoporous matrices were also plagued by analogous problems for a long time: even though clusters or nanowires of noble metals or metal oxides were successfully realized since end 1990's,[424] in most cases, the pores were only partially filled, and consequently, the resulting distribution of clusters or nanorods in the mesoporous-silica matrix was quite random.[334] Nonetheless, perfect order is not required for most applications, including catalysis or sensing.

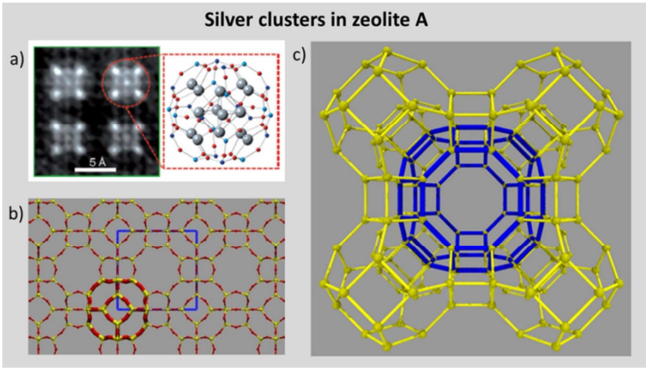

Figure 28 ***The void-space architecture of zeolite A*** features cages of different size, among which silver cluster of outstanding luminescence can be hosted. a) scanning transmission electron microscopy image of the arrangement of isolated Ag ions and Ag clusters of six atoms in zeolite A. The sodalite cage is shown in the left inset. [Reprinted by permission from WILEY-VCH[413]] b)Ball-and-stick representation of the framework structure (yellow = Si, red = O) of zeolite A (LTA)[57,59] with the unit cell shown as solid blue lines. The sodalite cage, highlighted in licorice representation, is a composite building block of zeolite A. c) Representation of the LTA framework highlighting the sodalite cages (yellow) and the alpha-cage (blue) [Illustration created with VMD, using the X-ray positions from Refs[57,59]]

4.1. Nanoclusters in sodalite cages

No surprise at all that the pioneering efforts to synthesize nanoclusters in zeolites chose sodalite as their favourite playground (Figure 27).[14] Its beautifully symmetric body-centered arrangement of perfectly equal cavities - the truncated-octahedral beta cages – also captured the attention of Linus Pauling, who first described its structure in 1930.[425] The sodalite structure builds up the most numerous zeolite family, counting about 900 members, i.e. over 18% of all published zeolite structures,[426] among which lazurite[70,427,428] – the main component of lapis-lazuli, and *natural* tsaregorodtsevite - a rare mineral hosting a tetramethylammonium organic cation in its cages.[429,430] Besides the abundance and diversity of sodalite-type structures, the beta-cage is a constituent block of many other zeotypes, such as the catalytic cornerstone zeolite A (Figure 28), or zeolite Y (Figure 29), and a widespread structural motif in metal-organic framework materials.[63,431,432]

Also the first computational studies aimed at gathering insight on the structural and electronic properties of confined nanoclusters were performed on sodalite,[433–435] which still remains a very attractive model system for theoretical investigations.[436] For example, theory indicates that the electronic properties of isolated quantum dots are mainly transferred to the confined species, and that the zeolite environment just modulates their electronic transitions.[436,437] Zeolite frameworks therefore act as confining dielectric media, that protect the clusters without compromising their optical properties.[436,438]

Since 1990's[42,43,439,440] A and Y zeolites have been used to stabilize silver cluster, and the appealing optical properties of the resulting composites have been thoroughly investigated. The observation that, upon high vacuum activation, the originally white-colored silver-exchanged zeolite A turned yellow at room temperature and brick red at 200 °C was particularly important because it revealed that the optical properties of the composite depended on hydration.[43] The reversible, stimuli-induced change of colors of silver zeolites was correlated to ligand-to-metal charge transfer transitions from the oxygen atoms of the framework to the vacant 5s orbital of the Ag ions.[43] In later experiments, individual Ag clusters were activated by a laser beam, producing intense luminescence,[414] while other investigations demonstrated that the color of the emission of Li-substituted silver–containing zeolite A could be tuned by water; specifically, while partially hydrated composites generated a blue emission, a green/yellow color was detected upon full hydration.[441] XRD and scanning transmission electron microscopy analyses on silver-zeolite A composites revealed that silver forms octahedral clusters inside the sodalite cages, surrounded by eight cations, each located in the center of a 6-membered-ring (Figure 28a).[413] However, the size of the confined clusters depends, in general, on silver loading and on the preparation history of the sample. For example, operating at relatively mild conditions, cationic aggregates composed by 3, 4, 6 silver atoms – namely, Ag_3^{n+}, Ag_4^{n+}, Ag_6^{+} could be obtained; such clusters were experimentally characterized by EPR spectroscopy, testing also their reactivity towards small species such as ethylene,dioxygen and nitrogen oxide.[442,440,443,444]

Nowadays, silver-containing zeolites can be synthesized with tailored optical properties:[44] they can emit in the whole visible spectrum[445] and with remarkable quantum efficiencies.[446] Zeolite-Y works particularly well, because the luminescent clusters are hosted in well-separated hexagonal prism cages.[44,447] In zeolite A, the clusters are located in adjacent sodalite cages, (Figure 28)[448] yet they still feature excellent stability and efficiency.[447] By this virtue, silver exchanged LTA zeolites hold great promise for practical applications such as optical encoders[416] or bright emitters in OLEDs.[417] Further progress in this field could be greatly stimulated by deeper insight on the structural and electronic properties of these confined aggregates obtained by first-principles studies.[45,449] Also, since silver cations located at different zeolitic sites have different enthalpies of adsorption,[450,451] the use of thermodynamic models capable to predict the repartition of Ag^+ cations in the confining medium upon ion exchange, and hence the organization of the Ag-cluster in the final composite, could greatly contribute to advance the preparation procedures of these materials *via* a knowledge-based approach.[450,452]

Other metals have been successfully incorporated - for example platinum, leading to confined nanoclusters composed by up to 13 atoms[453] with interesting magnetic properties,[453–455] and even confined nanoalloys can be produced.[456]

Chalcogenide clusters have been extensively studied as well, in particular using zeolite Y as a matrix.[420,457,458] As observed for the Ag-clusters, the structure of the confined aggregates and the properties of the resulting materials are strongly dependent on the composition of the framework and on process parameters, such as the degree of hydration.[458] In principle, the clusters can form both in the sodalite cage and in the supercage of zeolite Y (Figure 29a,b). Recently, a structural model based on X-ray diffraction data (Figure 29c) has been proposed, suggesting that a Cd_4S^{6+} ion of tetrahedral structure (similar to natural sodalite, see Figure 27) is formed in the sodalite cage, while a larger tetrahedral ion $Cd(SHCd)_4^{6+}$ is located in the supercage.[459] A recent review thoroughly discusses the synthetic strategies to achieve, for example, the selective occupation of only one type of cages, and the broad spectrum of potential applications of these

composite materials.[38] For instance, photovoltaic solar cells based on CdS and PdS quantum dots encapsulated in zeolite Y have been realized, and the performance of such devices was found to depend, besides from the chemical nature of the nanospecies, on the homogeneity of their distribution inside the zeolite matrix.[460]

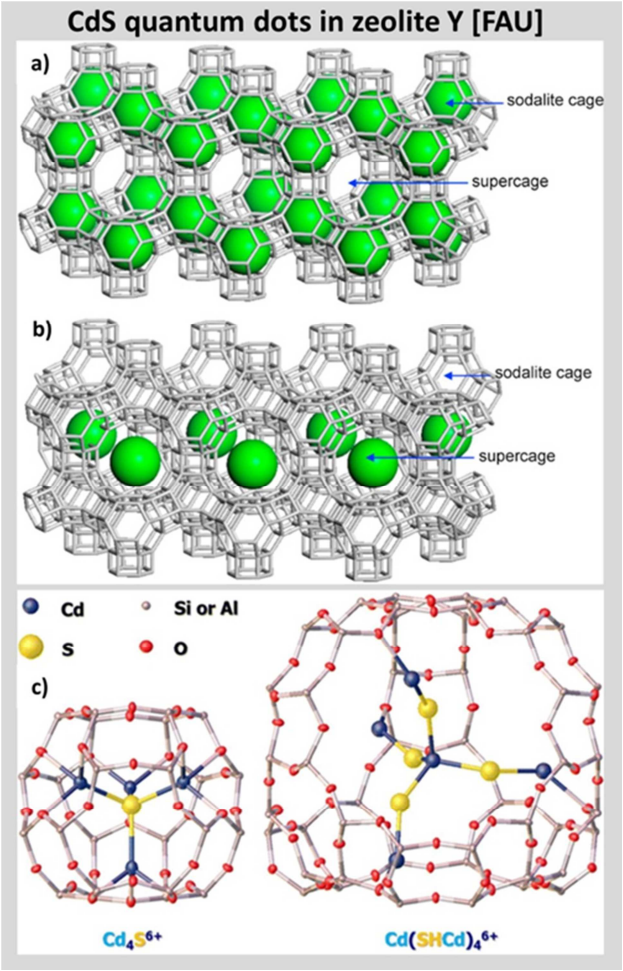

Figure 29. ***CdS quantum dots*** (schematically represented as green spheres) confined in zeolite Y located a) in both sodalite cages and supercages; b) in the supercages. [Reprinted by permission from Elsevier[38]] c) X-rays structure of tetrahedral Cd_4S^{6+} ion in the sodalite cage (left) and tetrahedral $Cd(SHCd)_4^{6+}$ ion in the supercage (right) of zeolite Y. [Adapted with permission from Ref.[459] Copyright 2016 American Chemical Society.]

Chalcogenide nanoclusters have been also encapsulated into a chalcogenide-based semiconductor zeolite.[461] Specifically, the host–guest hybrid system contained MnS clusters - as confirmed by UV-Vis, IR and Raman measurements. The aggregation state of the cluster, probed by EPR, suggested different morphologies according to degree of loading and temperature. Interestingly, the MnS clusters showed two emissions peaks (at 518 nm and 746 nm) whose photoluminescence intensity depended on loading level and temperature.[461] Indeed, the second peak was never found in previous experiments on MnS clusters in other hosts, raising thus interest toward the potential use of semiconductor zeolites as hosts for luminescent nanoclusters.

4.2 Nanoclusters and quantum wires in mesopores

Owing to their large, and tunable pore size, mesoporous silicas are attractive scaffolds for confining quantum nanostructures, also because the host matrix, like most zeolites, is an insulator, and acts as an effective barrier between individual wires.[462] Obtaining mesoscopic ordering of the confined nanomaterials is, in general, more difficult than in zeolites, because low crystallinity, or presence of unwanted macropores in the silica matrix may lead to the formation of nanoparticles greater than the nominal pore size and to their sparse incorporation within the matrix.[424] In spite of these difficulties, advances in the fabrication procedures made it possible to realize, for example, arrays of highly ordered zinc-manganese sulphide quantum wires within MCM-41 and SBA-15,[462] or magnetic Fe_2O_3 nanoparticles with regular, finely controllable sizes confined into hexagonally ordered mesopores (Figure 30a).[463]

Recently, intriguing alternatives to standard quantum dots, such as nanosized perovskites, have become very popular in the photophysics community due to their excellent optical properties and photovoltaic performances.[464] Whereas the photophysical properties of conventional quantum dots (chalcogenide nanoclusters), are very sensitive to surface defects, in these new materials the surface dangling bonds do not create trap states that detrimentally affect photoluminescence.[465] Because of such peculiar defect-tolerance, perovskite nanocrystals do not need to be passivated. The Kovalenko group took advantage of this fact and implemented a facile template-driven synthesis of lead halide perovskite nanocristals in hexagonal mesoporous silica.[466] The investigators impregnated the pores of various commercial mesoporous materials, such as MCM-41 and SBA-15, with perovskite precursor solutions and, after drying, they observed the formation of ordered arrays of perovskite nanocrystals compatible with the pores size of the adopted template. The confined nanoparticles showed photoluminescence properties dependent on the pore-diameters of the template and improved processability over non-templated fabrication routes.[466]

Despite the difficulty of tuning simultaneously the size, composition, distribution, and uniform dispersion of the encapsulated clusters, also MOFs frameworks have been used as confining matrices for nanoparticles of various nature, including quantum dots.[467,468] For example, strategies for the controlled incorporation of capped nanoparticles of various shape, composition and size into a ZIF can produce composites with good catalytic, magnetic and optical properties derived from the encapsulated nanoparticles.[469] Another emerging strategy is the use of atomic layer deposition approaches.[470,471] Self-assembly methods have been successful in achieving the confinement of nanowires with electron donor character into the periodic pores of electron-poor MOFs acting as acceptors. This strategy has led to donor–acceptor hybrid materials composed by semiconductive MOFs containing ordered arrays of semiconductive nanowires (Figure 30b).[472]

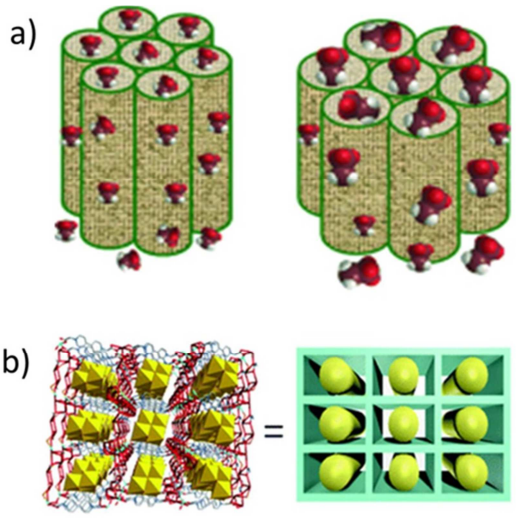

Figure 30. ***Confined nanostructures in mesopores and MOFs***: a) Fe_2O_3 nanoparticles of uniform sizes fabricated inside mesoporous supports of tunable diameter [Reproduced from Ref.[463] with permission from WILEY-Wch]. b) semiconducting iodoplumbate nanowires (in yellow) regularly organized in the pores of semiconductive pyridinium MOF [Reproduced from Ref.[472] with permission from The Royal Society of Chemistry]

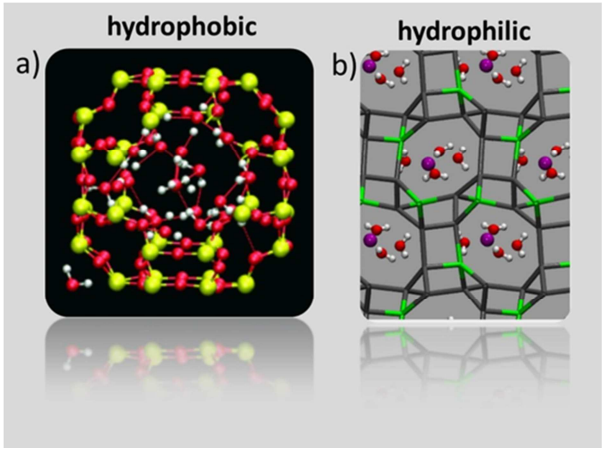

Figure 31. ***The different organization of zeolitic water*** in a) hydrophobic and b) hydropylic frameworks. a) water in the sodalite cage of all-silica LTA: the leading interaction is hydrogen bonding between water molecules. Colors: Si=yellow, O=red, H=white [Adapted from Ref.[503] with permission from WILEY-Vch] b) water and calcium cations in natural zeolite yugawaralite: calcium cations are coordinated to both Al-bonded framework oxygens and water, and water molecules form hydrogen bonds with both themselves and Al-bonded framework oxygens. Colors: Ca=purple, Si=grey, Al=green, O=red, H=white. Framework oxygens and hydrogen bonds are not represented for clarity. [Illustration created with VMD; X-ray positions of Ref.[505]]

5 Supramolecular organization of water and cations in confined spaces

Mainly because of their impact on catalysis, the location and distribution of the extraframework cations in hydrophilic zeolites has been object of many experimental[117,473–476] and computational[477–484] investigations over the years.[485,486] Also the organization of water confined in hydrophilic or hydrophobic environments has been intensively studied,[487–495] often uncovering unexpected supramolecular patterns, such as nano-helices (in natrolite)[487], triple helices (in VPI-5),[91,496] cyclic hexamers (in the 12-ring cages of NaY zeolites, Figure 29)[497,498] or even nano-worms (in hydrophobic silicalite, Figure 5[499,500] along with the more common nanospheres (in zeolite A, Figure 28)[501] and ice-like nanotubes (in $AlPO_4$-5 and SSZ-24).[502] The general message emerging from these studies is that the behavior of water in hydrophobic and hydrophilic zeolites differ significantly (Figure 31).

Water molecules can be introduced in hydrophobic (all silica) zeolites by applying a moderate pressure; once encapsulated, they form hydrogen bond among themselves and interact with the framework walls only weakly. Although such weak interactions are actually non-negligible and perturb the hydrogen-bond network and dynamics,[500] water aggregates confined in hydrophobic zeolites might be considered, at least as a first approximation, somewhat similar to “isolated” water clusters or water droplets, depending on the size of the channel.[495,503,504] In this case, the size and shape of hydrophobically confined water aggregates is mainly determined by the geometric shaping effect of the confining matrix, with its empty channel and cages.

On the contrary, in hydrophilic frameworks, the interaction of water with both charge balancing cations and framework oxygen atoms can be very strong and specific, and - along with the water-water interactions - determines the resulting organization of the confined species. Assemblies of water and ions in hydrophilic cavities cannot be regarded as “isolated species”, neither as a first approximation: rather, jointly with the framework, they create a single supramolecular architecture extending indefinitely in the three dimensions up to the macroscopic scale.

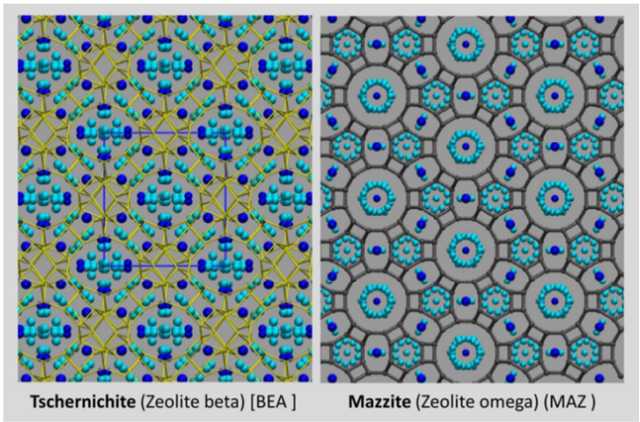

Figure 32..***Nature-made supramolecular organization:*** Framework structures of the natural zeolites tschernichite (BEA)[506,507] and mazzite (MAZ)[508] (and of their respective synthetic counterparts (in parentheses)). The colored balls show the water and cation sites (with fractional occupancy). The blue solid lines are a guide for the eye and illustrate the unit cell, as exemplified for BEA. [Illustration created with VMD, using the X-ray positions from Refs[507,508].]

The fascinating patterns of water and cations in natural zeolites are generally very complex, and also very difficult to study via diffraction experiments: the extraframework sites have often low occupancy, and a multitude of symmetry-related positions are possible.[56,118,129,476,507,509,510] A further obstacle is the possible co-presence of two crystalline phases, for example the tetragonal and monoclinic polytypes of tschernichite, the natural analog of zeolite beta (Figure 32).[507] Also, in large-pores zeolites (like mazzite, Figure 32) it is especially challenging to locate, in practice, all the water molecules, even with the knowledge of the preferential location of Al (obtained *via* ^{27}Al SS-NMR).[508]

Yet those averaged positions provide hints on the arrangement of extraframework species, and if they are graphically represented together (as in Figure 32), the striking complementarity between the framework and the confined guests emerges in its full significance. This relationship is much more profound than a simple geometric effect, dictated by shape-volume constraint, because the framework and its content are tightly bound together by an intricate network of electrostatic, coordinative and hydrogen bond interactions, which is very difficult to disentangle from a conceptual viewpoint, and lies at the origin of the impressive stability of natural zeolites.

An appealing way to gather insight on the responsivity properties of these naturally organized arrangements is to study their behavior under an external perturbation or stimulus: for example, temperature or pressure. Whereas an increase of temperature normally causes an increase of disorder of the hydrogen bond network, and ultimately dehydration, pressure effects are far less straightforward. When zeolites are compressed hydrostatically (with non-penetrating media),[64,511–514] the organization of water and cations change responsively and the framework undergoes the less-energy costly structural change: without internal distortion, the tetrahedral units rotate around their hinges and the channels deform.[512,515]

The extraframework species play a crucial role in governing the deformation of the zeolite framework.[64,513]. Under high pressure, the formation of water dimers in scolecite triggers a phase transition,[516] and the coordination network of the cations could guide, as a sort of template, the distorsions of the framework, as exemplified by calcium in natural zeolite yugawaralite.[505,517] Such a “template” role of the extraframework cations, which also explains the resistance to dehydration of tightly-coordinated zeolitic water,[129] may be visually captured by looking at Figure 33, which evidences how precisely the naturally confined species, taken as a whole, fill the network of empty spaces. A similar template role of the guest molecules has been first proposed and demonstrated for clathrasils. In particular, the pressure-induced amorphization of dodecasil-3C (characterized by cage voids), and decadodecasil-3R (with 2D-channels) were studied by IR spectroscopy, X-ray diffraction experiments and molecular dynamics simulations, evidencing that amorphization is fully (dodecasil-3C) or partlially (decadodecasil-3R) reversible only when guest molecules occupy the clathrate lattice.[518] Hence, the guests act as „organizing centers“, making the lattice resilient to much higher pressures compared to guest-free clathrasils.[518]

A surprisingly simple architecture of water and cations was found inside a rare mineral, called bikitaite.[519] This aluminosilicate is a natural zeolite which hosts in its mono-dimensional channels linear assemblies of water molecules coordinated to the extraframework lithium cations (Figure 34).

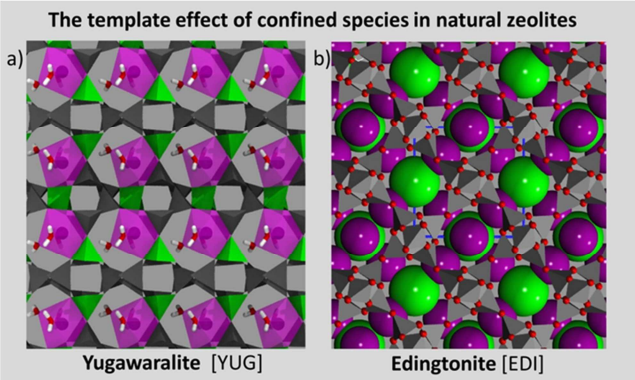

Figure 33. ***The organization of extraframework species in natural zeolites*** a) yugawaralite and b) edingtonite. a) The coordination polyhedron formed by the calcium cations (purple) is linked to the negatively charged AlO_4 tetrahedral units (green). SiO_4 tetrahedra are in grey, water molecules in red and white (framework oxygens not shown). b) Cl (green) and Ba (purple) alternatively occupy the center of the edingtonite cage. All tetrahedral atoms Si, Al are represented in grey, framework oxygens as red little balls (water molecules not shown). [Illustration created with VMD, using the X-ray positions from Ref.[505] (YUG); Ref.[57] (EDI).]

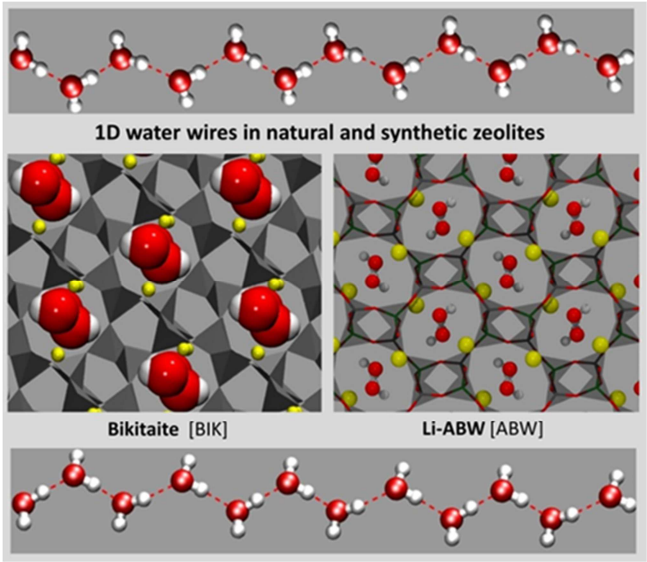

Figure 34. ***Water wires*** occupy the one-dimensional channels of natural bikitaite (left) and synthetic zeolite Li-ABW (right): the water molecules are coordinated to the Li cation (yellow balls) and do not form hydrogen bonds with the framework oxygens. The two zeolites (and the confined water wires) are viewed along the channel direction. In-plane views of the water wires are shown in the top and bottom panels. [Illustration created with VMD, using the X-ray positions from Ref.[520] (BIK)[57,59] and Ref.[521] (ABW) [57,59]].

Such unusual 1D organization was termed “one-dimensional ice”[520,522] because of its solid-like behavior, evidencing impressive stability towards high-temperature[523]/high-pressure[524–527] conditions and absence of translational/rotational motion of the individual molecules irrespectively of the Al/Si ordering in the framework.[522] This knowledge was obtained by multitechnique analyses including computational studies[230,522,528,529] neutron-[519] and X-ray diffraction,[520] single crystal polarized Raman,[530,531] and ^{1}H SS-NMR relaxation

experiments.[532] The latter ones, performed in the temperature range 224–418 K, identified one single dynamical relaxation process: a 180° flip-flop motion of water exchanging the positions of its protons,[532] analogous to the librational twist of water in solid hydrates.[533] The water filipping motion was reproduced by molecular dynamics simulations,[528] that, in line with the NMR experiment, did not observe any water diffusion in that temperature range. Other simulation studies proposed a two-step mechanism for the dehydration process: the first and rate determining step is water escape from its site followed by a fast jump to an empty site.[523] The Li cations assist water migration from site to site, lowering the free energy barrier of the process.[523] It is clear that such a single-file diffusion in 1-D channels can occur only if one water site is empty, i.e. if the water wire has „defects".

Notably, the 1D-water chain in bikitaite is not hydrogen bonded to framework oxygens, but it is only anchored to the extraframework Li^+ cations via strong coordination bonds (Figure 34). Also the synthetic zeolite Li-ABW has 1-D channels, in which linear water assemblies are confined.[534–536] Yet such water wires are easily perturbed upon compression: namely, the molecules tend to form hydrogen bonds with framework oxygens and their linear organization gradually disappears upon increasing pressure.[220]

The reason why the water wires in the two zeolites have different behavior under mechanical stress lies in the different framework topology: the electric polarization of the framework is much stronger in bikitaite compared to Li-ABW, and this implies a greater electrostatic stabilization to the water architecture.[534] Also importantly, the water chain does not form when Li is replaced by Na, as demonstrated for the zeolite Na-ABW, because of the lower polarizing power and binding capacity of the sodium cation towards water and framework oxygen atoms.[535] This example evidences the delicate interplay of host-guest interactions in hydrophilic zeolites: fine differences in the framework structure, or in the nature of the extraframework cations, may affect significantly the stability and dynamic behavior of the confined supramolecular assembly. Such an interplay underlies also the supramolecular organization of guest species bearing technologically appealing functionalities, for example lanthanides,[53] luminescent complexes,[537,538] or dye molecules, in hydrophilic hosts.[539–542]

6. Organization of linear molecules confined in 1-D channels

The encapsulation of halogen molecules in various types of porous confining matrices[298,543–548] has been extensively studied over the years,[549–551] especially because of the environmental relevance of toxic gas capture.[48,552]

Some of these studies, however, also focused specifically on the organization of these simple diatomics under confinements, trying to unravel not only the molecular-level structure of the supramolecular aggregates, but also how such an organization could be influenced by different factors: for example, size and concentration of the guests,[553] structural and chemical features of the confining matrix,[546,553] presence of cosolvent,[554] and changes in temperature and pressure.[549,555]

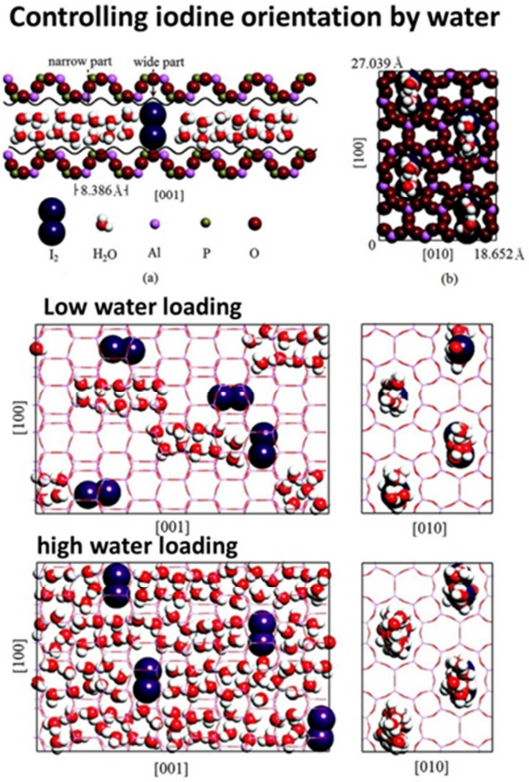

Figure 35. ***The role of water in the organization of iodine*** inside the 1D channels of ALPO4-11 (AEL). The top panel represents: a) a schematic view of a I_2-containing nanochannel of the AEL aluminophosphate (I_2@AEL) at high water loading. The channel features an alternance of wide parts and narrow parts with a periodicity of 1/2 *c* (*c* = 8.386 Å corresponds to the AEL lattice parameter along the channel axis, while the dimensions of the narrow part are 4.3 Å × 6.1 Å). b) Projection in the (110) plane. The middle and bottom panels depict two configurations (viewed in the (101) and (110) planes) from molecular dynamics simulations of I_2@AEL at low water loading and high water loading conditions, respectively. [Adapted with permission from Ref.[554] Copyright 2012 American Chemical Society.]

In general, small molecules confined in small zeolitic cages, like those of sodalite (Figure 27), may have some freedom of movement: in particular, rotational motions - which may be more or less frictioned according to the size of the guest, but are normally very fast.[556] In zeolite channels, if the guest species are allowed to rotate, their orientation with respect to the channel axis may change. This happens, for example, when bromine or iodine molecules are confined within the channel of aluminophosphates with AEL and AFI framework type.[543,544,549,550,554,557–559] In particular, the rotational barriers are greater for the confinement in AEL-type channels, which not only have an elliptical shape but also show an alternance between wide regions and narrow regions (see figure 35). Basically, these studies, based on raman spectroscopy data, revealed that the confined molecules could be either aligned, or perpendicular to the channel axis. Along limited portions of the channels, the molecules may actually have a uniform orientation; however, such organization is often interrupted by molecules oriented perpendicularly to the other ones. As a result, only short chains are formed.

More specifically, Liu et al. exploited the monodimensional channels of the zeolitic matrix AlPO4-5 (AFI framework type) to realize stable bromine molecule arrays by introducing under

vacuum Br_2 vapor into the selected host. Raman spectra evidenced that the Br_2 supramolecular chains were nearly aligned to the channel axis of AFI single crystals, and also an appreciable proportion of individual molecules were oriented parallel to the channels.[558] Interestingly, such a proportion of uniformly aligned molecules could be further increased through the use of high pressures,[560] as discussed in section 10.

To explore the effect of temperature, the confinement of iodine molecules in the 1-D elliptical channels of $AlPO_4$-11 (AEL) crystals has been studied down to −196 °C by Chen et al.[555] Combined raman experiments and molecular dynamics simulations indicated that, upon decreasing temperature, the thermal motion of the confined molecules slowed down, thus inducing a change of molecular orientation. The proportion of iodine molecules laying along the channel axis increased: hence, longer I_2 chains were formed, with a higher degree of ordering. Nonetheless, such a cooling-induced order enhancement was not preserved after recovery to room temperature.

The reversibility of the iodine orientation inside ALPO channels is mainly due to the fact that the interactions between the iodine molecules and the walls of the confining matrix are noncovalent, non-specific, and weak. One now might wonder what would happen if such molecules were forced to share the channel space with another guest – water, for example. In such a case, the orientation of the confined guests should reasonably depend on how much water is present. While at low water loading I_2 mainly lyes along the axis, after further hydration, the iodine molecules are found in a perpendicular orientation (see Figure 35). Such an organization – with the water-solvated iodine molecules standing in the widest portion of the channel - is actually the most energetically favorable state of this system at room temperature and full hydration.[554]

This study clearly showed that the close geometrical match between the host cavities and the guest is not sufficient to achieve orientational ordering of the guest molecules: because of thermal motion, the guests still preserve some orientational freedom, which might be reduced by imposing additional constraints. In this case, confinement is enhanced by water, resulting into a uniform “standing” orientation of the iodine molecules (Figure 35). Such organizational role of water is also responsible of the orientation (and optical anisotropy) of some dyes commonly used in zeolite-based antenna systems, as discussed in chapter 7.[221,222,561,562]

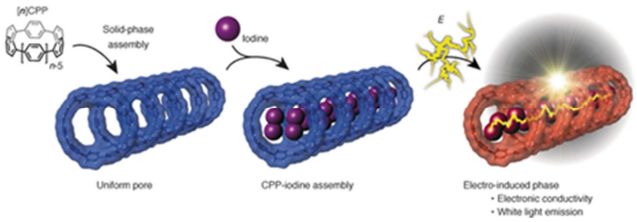

Figure 36. ***1-D Iodine chains confined in an organic nanocylinder*** made up by cycloparaphenylene (CPP) rings. Electrical stimulation of this host-guest assembly generates electronic conductivity (from the iodine chain) and white light emission (from the organic confining matrix).[Reprinted with permission from Wiley-VCH.][547]

Beside interesting structural aspects, small molecular species, when forced to organize into confined spaces, may reveal quite unexpected phenomena, especially when the confining matrix is stimuli-responsive. In one such matrices – formed by condensed organic nanorings, iodine chains similar to those in zeolites were formed, and, activated by an electric field, showed electronic conductivity, ascribed to polyiodide chains formed by charge transfer from the organic nanoring-pore (Figure 36). Though the polymerization mechanism has not been clarified yet, conductivity was found to depend on the size of the ring, suggesting also that the dynamics of the confined iodine molecules may play a relevant role in the process.[547]

Nevertheless, technologically appealing properties may appear even when iodine is confined in zeolites, for example in the familiar silicalite (Figure 5), where I_2 forms a nice three-dimensional supramolecular network with semiconducting behavior (Figure 37).[48]

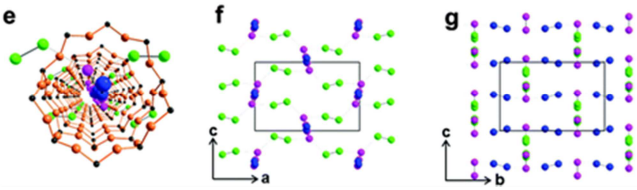

Figure 37. ***Semiconducting I_2 network in silicalite.*** Vision along the channel axis of the straight *b*-channel of hydrophobic silicalite incorporating all three types of crystallographically different I_2 molecules. A row of iodine molecules is oriented parallel to the *b*-axis (in blue). The full 3D-network of confined I_2 molecules, viewed in the ac plane (center) and in the bc plane (right). [Reproduced from Ref.[48] with permission from The Royal Society of Chemistry]

So, it seems that these halogen molecules, when they are confined, do exhibit interesting electronic behaviours. This holds also for chlorine. For example, the first excited state of gas-phase molecular chlorine is a triplet,[563] yet experiments on confined chlorine molecules[564] suggest that the excitation should occur, instead, on an unbound singlet state relatively close to the triplet, causing thus the dissociation of the molecules.

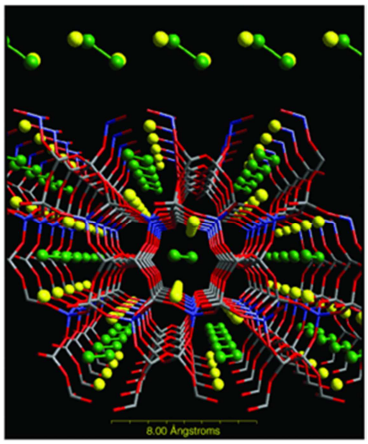

Figure 38. ***Linear organization of chlorine molecules*** in the 1-D channels of zeolite bikitaite. Color codes: Cl=green, Li= yellow, Si=grey, Al=blue, O=red. [Reproduced from Ref.[565] with permission from WILEY-VCH].

By first principles modeling,[565] Medici et al. simulated the electronic excitation of a wire of chlorine molecules confined in the 1D-channels of bikitaite (Figure 38).[566] Zeolite confinement, and the organization of Cl_2 in supramolecular wires, could favor collisions of the excited molecule with the adjacent ones, triggering the excitation-transfer. Indeed, the calculations showed that the excitation was localized on a single Cl_2 molecule, which dissociated into two neutral Cl atoms. Moreover, collision of such atoms with the adjacent molecule along the wire led to of the electronic excitation transfer, with the net result that another molecule dissociated, and a new Cl-Cl bond was formed. The excitation transfer along the confined supramolecular wire occurred at picosecond-time scales via a Dexter[567] mechanism, and may be viewed as a displacement of the Cl-Cl bonds along the supramolecular chlorine wire.[565] Such insight could be of help for understanding electronic excitation transfer along ordered arrays of confined molecules.

7. Organization of complex species in 1D

The previous sections showed that small linear molecules, even if confined in zeolites with 1D-pore systems, do not form, in general, perfecly ordered one-dimensional structures, especially when the size of the channel is large enough to allow for a certain rotational freedom of the encapsulated species. Yet, irrespective of the type of guest, confinement in one dimension still remains the easiest solution to the organizational problem, because: i) the number of possible supramolecular patterns is limited, and ii) the organization processes could be more easily designed and controlled.

For this reason, one-dimensional porous matrices have been heavily exploited to confine any possible kind of system of nanoscopic dimension, from inorganic to organic, from biological to hybrid bio-inorganic: fullerenes have been placed inside mesoporous oxides,[568,569] MOFs,[32,394] or COFs,[396] natural pigments, such as clorophyll,[570] or light-harvesting complexes of photosyntetic bacteria, like LH2, were confined in mesoporous silica,[571,572] and extra-large pore MOFs with 1-D channels were invented to encapsulate enzymes (Figure 39).[573,574]

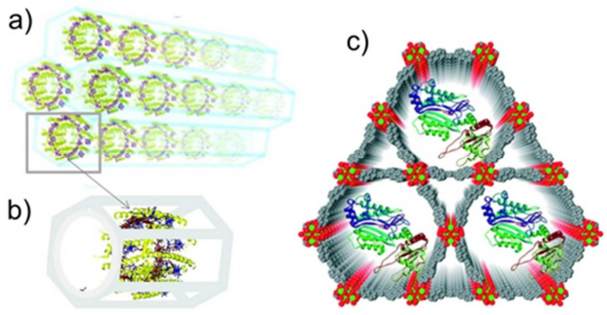

Figure 39. ***Mesochannels*** for 1-D organization of huge molecules a) Schematic view of the hybrid inclusion composite of the photosynthetic complex LH2 inside the channels of a mesoporous silica; b) zoomed view of a confined LH2 molecule. [Adapted with permission from Ref.[571] Copyright 2006 American Chemical Society.] c) Schematic representation of an enzyme encapsulated in a channel-type MOF. [Reproduced from Ref.[574] with permission from The Royal Society of Chemistry]

The dimensions of the pore openings are an extremely important parameter, because they dictate the size of the molecules that may enter the pores and be organized within their spaces. However, molecules are flexible, and can often manage to pass through the pore orifices even if they have nominally a larger size.

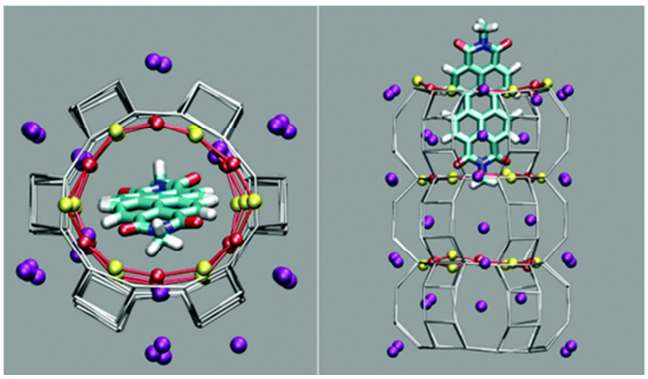

Figure 40. ***Difficult entrance*** of a guest into a channel: the molecule has van der Waals diameter slightly greater than the pore opening. The process can only occur if both the host matrix and the putative guest deform in a cooperative manner.[575] Here, the guest is a perylene-diimide dye and the host is the 1-D channel framework of zeolite L (framework type LTL[57–59,576]): the channel entrance becomes transiently elliptical when the dye passes through. The confinement of such dyes in zeolite L leads to the production of a family of useful hybrid composites: it occurs at high temperatures thanks to the favorable interaction of the carbonyl group of the dye with the zeolite K^+ cations, and to the cooperative vibrational motion of the two partners which allows overcoming the steric constraint of the channel. The motion of the dye inside the porous matrix has an asymmetric free energy profile,[575] which makes the entrance process favored over the exit, in analogy to what observed for the passage of a diazobenzene dye through a crown-ether ring.[577] Color code: Si and Al atoms of zeolite L framework = gray sticks. C=cyan; H=white; N=blue, carbonyl O=red; K^+=purple. The red and yellow balls on the channel aperture, highlighting the elliptical deformation of the opening at the passage of the molecule, represent framework oxygens.

Framework flexibility, which is a distinctive feature of MOFs such e.g. ZIF-8,[398–400,578,579] may also play a key role in facilitating the penetration of oversized guests *via* a window-swing effect.[400] Contrary to common expectations, also zeolites manifest a surprising extent of structural flexibility, which allows for the vapor-phase incorporation of relatively bulky molecules, like perylene-diimide dyes, within sub-nanometric channels, such as those of zeolite L (Figure 40).[575]

In spite of the enormous advances in the fabrication and characterization of hybrid materials based on confining porous matrices, the molecular level understanding of the mechanisms of the confinement process, as well as of the host-guest interactions determining the macroscopic properties of the composites, is still in its infancy - mostly because of the generally overwhelming complexity of both the encapsulated species and the confining matrix. One remarkable exception is the family of hybrid composites produced by the inclusion of chromophores in zeolite L[58,576] (Framework type LTL). The fabrication of these hierarchically organized photoactive materials and their use as artificial antenna system, pioneered by the Calzaferri group[30,37,40,51,539,580–586] has been thoroughly investigated and the acquired knowledge played a seminal role, for example in extending the applicability scope of these composites to

biomedical uses.[587–592] Also importantly, the successful concept of dye-zeolite L hybrids stimulated the quest of a multitude of new host matrices for supramolecular luminescent assemblies and antenna systems: not only zeolitic frameworks of diverse shape and compositions,[262,593–599] but also mesoporous silica and organosilica,[62,343,354,600–602] 1-D macrocycle channels,[39,603] and finally MOFs.[61,63,604–612]

7.1 Dye-zeolite L composites as prototypes of artificial confined organization

Zeolite L (Figures 40, 41) has been so popular as a confining matrix because the size and shape of its one-dimensional channels are particularly suitable for the encapsulation of a broad variety of dye molecules, either in neutral or in cationic forms. In this way, one can obtain guest-host composites with remarkable organizational patterns, up to 1-D end-to-end sequenced chains of different chromophores.[30,37,41]

Another remarkable advantage is the relative facile synthesis of zeolite crystals of tailorable aspect-ratio[613–615] and the selective functionalization of their external surfaces, either at the base or at the coat regions.[584] These features enable to obtain, for example, zeolite-L crystals self-assembled via coordinative linkers,[616] arranged in close-packed monolayers,[617] integrated with external devices,[60] and even connected with living systems such as bacteria,[618] which could then be selectively targeted and killed upon red-light irradiation.[619]

Nonetheless, the atomistic-level structure of these versatile compounds often remains unexplored, as suggested by the scarce number of available diffraction studies.[620–627] Fortunately, computational studies may come to the rescue.[172] An *in-silico*-based atomistic picture would be especially useful to understand the processes that occur at the channel entrances (Figure 41), which govern the formation of the organized material,[575] as well as its potential practical uses. Channel entrances are particularly important because they can be functionalized; for example, with stopper molecules (traditionally defined as “stopcocks”), that, by preventing the leakage of the chromophores and the entrance of undesirable species,[628] preserve the inner supramolecular organization and functionality of the material (Figure 42).[583,629,630] The specific modification of the channel openings via the grafting of alkoxysilane moieties is also fundamental to realize macroscopic organization of zeolite crystals (by covalent attachment to a support, for example)[540,631,632] and to add further functionalities. The new functionalities could carry specifically selected magnetic[633,634], optical and photo/electroresponsive properties[41,53,538,635,636] such as those of phtalocyanine dyes[637] and iridium(III) complexes,[638] or even take part to molecular recognition processes involving the binding of gold nanoparticles to the zeolite crystal extremities.[639]

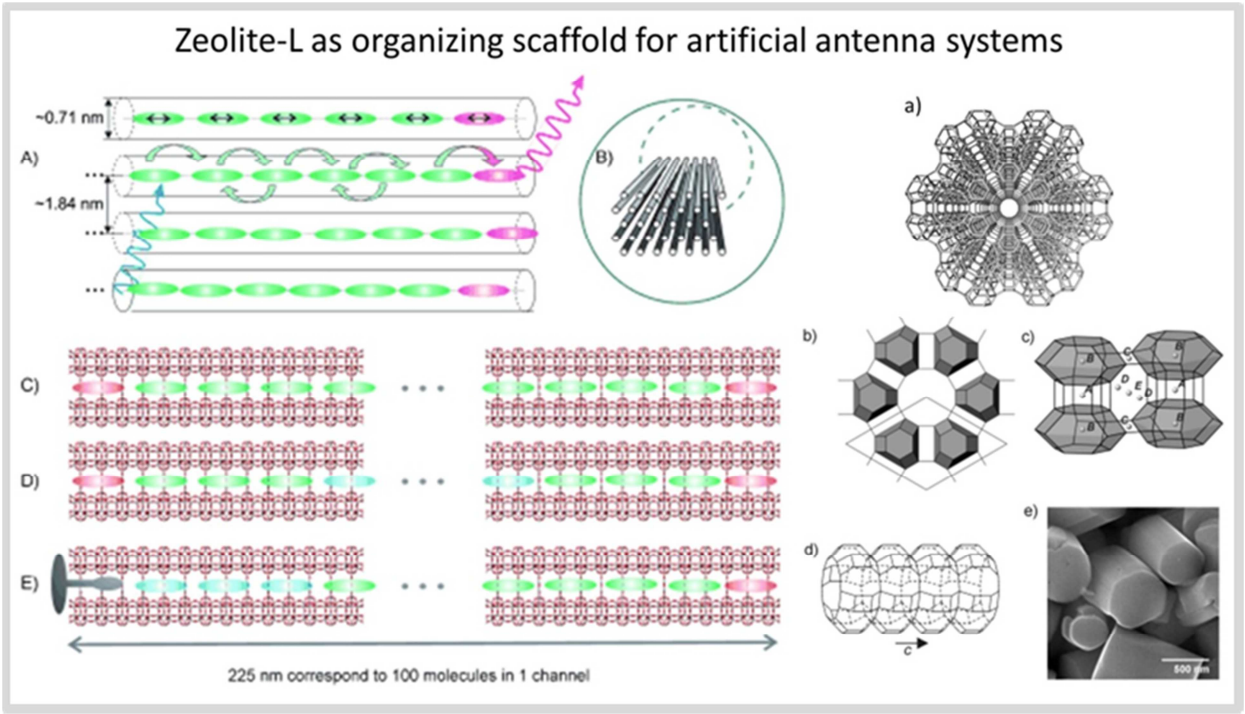

Figure 41. ***Artificial antenna systems*** based on zeolite L are schematically illustrated on the left side of the figure. A) Donor dyes (green) absorb light and transfer their excitation energy by Forster resonance energy transfer (FRET) to acceptor dyes (magenta) placed at the channel end. The electronic transition dipole moments (ETDM) of the dyes are indicated by double arrows. B) Arrangement of parallel nanochannels. C,D) Sequential organization of two- (C) and three- (D) types of chromophores. E) Unidirectional antenna system: energy is transported only one-way, from left to right. The left side of the channel is blocked by a molecular stopper (the “stopcock”),[629] represented in gray. Commonly adopted perilene-dimmide-based dyes[640,641] are typically about 2.25 nm long, and can even be longer, see, e.g. Ref. [628] for a thorough account. [Reproduced from Ref.[642] with permission from WILEY-VCH]. ***The zeolite L framework*** is shown on the right side of the figure: a) view along the channel axis (corresponding to the *c* axis); b) the cancrinite cages are shown as polyhedra, c) the different positions of extraframework cations (A to E); d) one 12-membered ring channel of zeolite L viewed along the *c* axis, e) SEM image of hexagonal crystals of zeolite L. [Adapted from Ref.[30] with permission from WILEY-VCH].

The specific modification of the channel openings via the grafting of alkoxysilane moieties is also fundamental to realize macroscopic organization of zeolite crystals (by covalent attachment to a support, for example)[540,631,632] and to add further functionalities. The new functionalities could carry specifically selected magnetic[633,634], optical and photo/electroresponsive properties[41,53,538,635,636] such as those of phtalocyanine dyes[637] and iridium(III) complexes,[638] or even take part to molecular recognition processes involving the binding of gold nanoparticles to the zeolite crystal extremities.[639]

Cationic or neutral dyes are commonly incorporated in the zeolite via ion-exchange or vapor phase methods, respectively.[30,643–646] An alternative strategy is the ship-in-a-bottle method, where dyes are incorporated directly into the porosities of the matrix during the synthesis step.[540] As schematically shown in Figure 48, the well-defined geometry of the 12-membered ring channels of zeolite L (7.1 Å diameter) should force the confined molecules to self-organize in a single file, providing thus an efficient transfer of excitation energy along the chain.[585,642,647]

Achieving supramolecular organization in such a confining environment is, however, not as a simple task as it might appear. Besides the topology and composition of the framework, organization depends on several factors, among which the size, shape, charge, and concentration of the guest; moreover molecules other than the chromophores may be present as well - typically, zeolitic water. Nonetheless, many experimental and theoretical analyses over the years have shed some light on how the host−guest, guest−guest, and guest−zeolitic water interactions govern, at a fundamental level, the resulting supramolecular organization, its stability, electronic absorption - excitation properties, and hence the optical behavior of the composite, also suggesting possible ways to improve these materials through a molecular-basis approach.

The considerable number of chromophores encapsulated in zeolite L could be classified in two broad groups, namely, cationic and neutral dyes. Basically, it can be said that while the electrostatic potential of the zeolite plays a key role in the organization of cationic dyes, neutral chromophores can become orderly arranged by forming localized, specific, and strong interactions with the host – for example, coordination bonds.

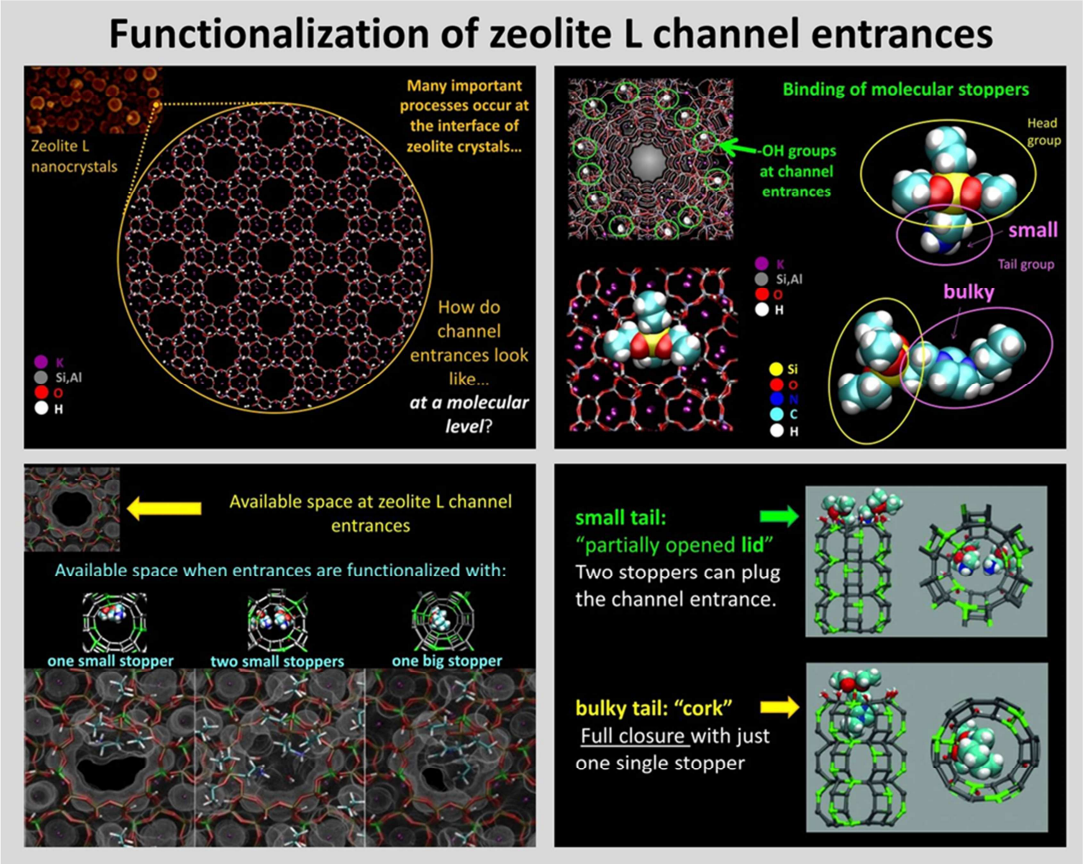

Figure 42. ***Tuning the pore openings*****:** To master supramolecular organization in the confined spaces of zeolites, microscopic insight on the pore entrances (of zeolite L microcrystals, in this case) is needed. Modeling can provide useful information a-b) on the structure of the zeolite L channel entrances and (b,c,d) on their functionalization with, e.g., alkoxy-silane moieities to prevent leaking of guest species from the zeolite pores.[193] Attachment of these molecular stoppers (or "stopcocks") to the channel entrance drastically modifies the accessibility of the zeolite pores according to the type and size of the selected stopper. Bulky stopper molecules, bearing an imidazolate tail group, can fully seal the channel entrance acting similarly to a cork on a bottle. [Adapted from Ref.[193] with permission from WILEY-VCH].

7.2 Neutral dyes: is confined organization imposed only by the space constraint of the matrix?

Let us first consider neutral guests – for example, perylene-diimide dyes, widely used in functional materials because of their outstanding optical properties.[640,641,648,649] Because of their size, these dyes must align to the channel axis to be confined in zeolite L (Figure 43). In this case, the organization is dictated by the space constraints of the matrix, but it is fine-tuned by the geometry of the dye;[650,651] for example, the spacing between adjacent molecules can be engineered via a proper choice of the perylene-diimide end-substituents.[652] Moreover, also the carbonyl groups have an important role in the organization, which can be better captured by analyzing another carbonyl dye, of much smaller size: fluorenone.

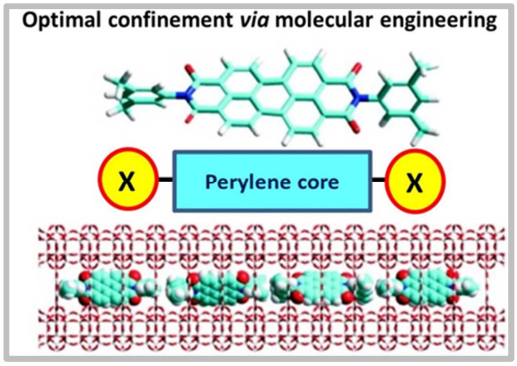

Figure 43: ***Perylene-diimides*** are a family of dyes that fit exactly into zeolite L channels. By a judicious choice of the end-substituents (schematized as yellow balls)**,** the organization of the dyes - in particular their spacing - may be tuned in a molecular engineering fashion.[586,628,650] The figure shows, for a typical dye of this family, the structural formula, the schematic representation, and an illustrative scketch of the organization of the confined chromophores. Color codes: C=cyan, N=blue, O=red, H=white, Si/Al=grey. [Adapted with permission from Ref.[650]. Copyright 2011 American Chemical Society.]

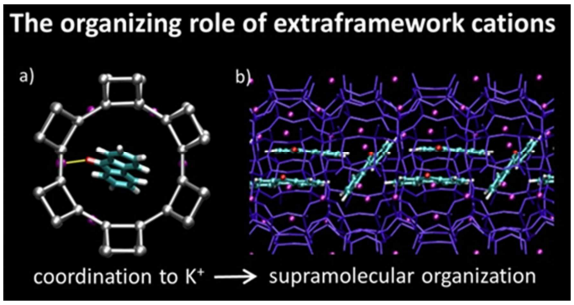

Figure 44. ***Molecules bearing carbonylic functionalities*** tend to coordinate K^+ when confined in zeolite L.[653] At high loading (b), the extraframework potassium cations cope to induce the self-organization of the dye into a regular, one-dimensional ladder-like arrangements.[624] Color codes: C=cyan, O=red, H=white, K=purple, Framework=grey (a) or blue (b).

Due to its size, fluorenone has some freedom of movement inside the channels; yet it forms unexpectedly stable adducts with zeolite L, also at humid conditions,[643] because it is bound to the extra framework potassium cations *via* its carbonyl group. Such a strong interaction explains not only the stability, but also the optical anisotropy of the composite.[653,654] Indeed, the coordination to K^+ ensures that the molecules, on average, are correctly oriented for giving resonance energy transfer.[343,582] This composite clearly exemplifies how zeolitic extraframework cations can be instrumental in directing the supramolecular organization of the confined dyes. Organization, here, is not just a matter of steric constraints; rather, it is clearly dominated by a specific and strong attractive interaction.[653] When the concentration of the dye increases up to a close-packing regime (Figure 44), such an interaction still remains important, and drives the formation of a peculiar space-filling arrangement of regularly organized chromophore molecules.[624]

7.3 Charged dyes. Role of electrostatics, water, and flexibility

Chromophores bearing a positive charge - from the simplest ones like thionine,[580,597,625,655] xanthene dyes,[221,582,613,625,656–658] acridine (and derivatives),[222,562,659,660] to more complex molecules like methylviologen[621] or bodypy-dyes,[41,658,661] - are naturally prone to be incorporated by a zeolite framework via straightforward ion exchange, a practice which is also used for dye encapsulation into anionic MOF nanochannels.[61,63] As a consequence, cationic dyes are very popular as luminescent guests, and their encapsulation has been widely documented by experimental, theoretical, or combined investigations.
Taken as a whole, these studies indicate that cationic dyes normally form stable composites with zeolite L, and are arranged anisotropically inside the zeolite nanochannels - which is a necessary condition to energy transfer.[30] As for neutral dyes, anisotropy arises because the confined molecules are not randomly oriented, but show some preferential orientation due to the spatial restraints of the channel and host-guest interactions.[37] Irrespective of the nature of the dye, such a preferential orientation is also determined by the electrostatic potential inside the channel, which is especially important for charged guest species, and may become the dominant factor when the composite is dehydrated.[221,222]

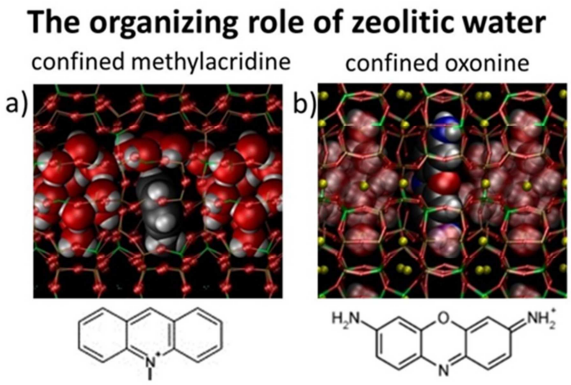

Figure 45. ***Confined water may impart organization***. Structures of hydrated zeolite-L composites containing a) methyl-acridine and b) oxonine dyes. Both dyes are located in the wide part of the channel, oriented with their long axis perpendicular to the channel axis, and surrounded by water. The water molecules are arranged like in perlialite, the natural analog of zeolite L. Colors: C=grey, O=red, H=white, N=blue, K=yellow, Al=green, Si=brown [in a), K is omitted for clarity]. [Adapted with permission from a) Ref.[222] Copyright 2013 American Chemical Society; b) Ref.[221] Copyright 2012 American Chemical Society]

That water – normally present in zeolitic cavities – could drastically influence both the electronic properties of framework sites,[662] and the emission of guest chromophores[561] was long recognized,[663] yet the fundamental role of water in determining the orientation and organization of the dyes in confined spaces was discovered and understood only recently.[221,222] Due to its tendency to hydrogen-bond with itself, water tends to confine small dyes, into the widest parts of the channel, and oriented perpendicularly to the channel axis (Figure 45). Therefore, as in the case of iodine, water has an indirect yet prominent role in the arrangement of small chromophores: basically, their confinement is enhanced by the water self-organization in the zeolite environment. Actually, the water molecules surrounding the dye are arranged into the same supramolecular pattern formed by water in perliarlite, the natural analog of zeolite L.

To understand and control supramolecular organization of confined dyes, it should also be kept in mind that neither chromophores, nor the host framework are rigid objects. Various studies highlighted an impressive structural flexibility of the encapsulated species. The confinement in 1-D nanometric channels poses severe restrictions to the geometry of the guests: to meet such requirements, molecules may deform spectacularly. Changing conformation is rather easy for methylviologen,[621] or cyanine dyes:[660] they have a single bond, around which the rigid parts of the molecule may rotate, in order to better fit to the constraints of the channels. What it is indeed surprising, is that also fully π-conjugated chromophores such acridine-,[222,659,660] xanthene-,[221] and even BODIPY dyes,[661] may exhibit unexpectedly large fluctuations from their typical gas-phase planar structure (see Figure 46). Also remarkably, such deformations have generally only minor effects on the absorption and emission properties of the dye assembly, and hence on the potential applications of the composites (Figure 46b).[661]

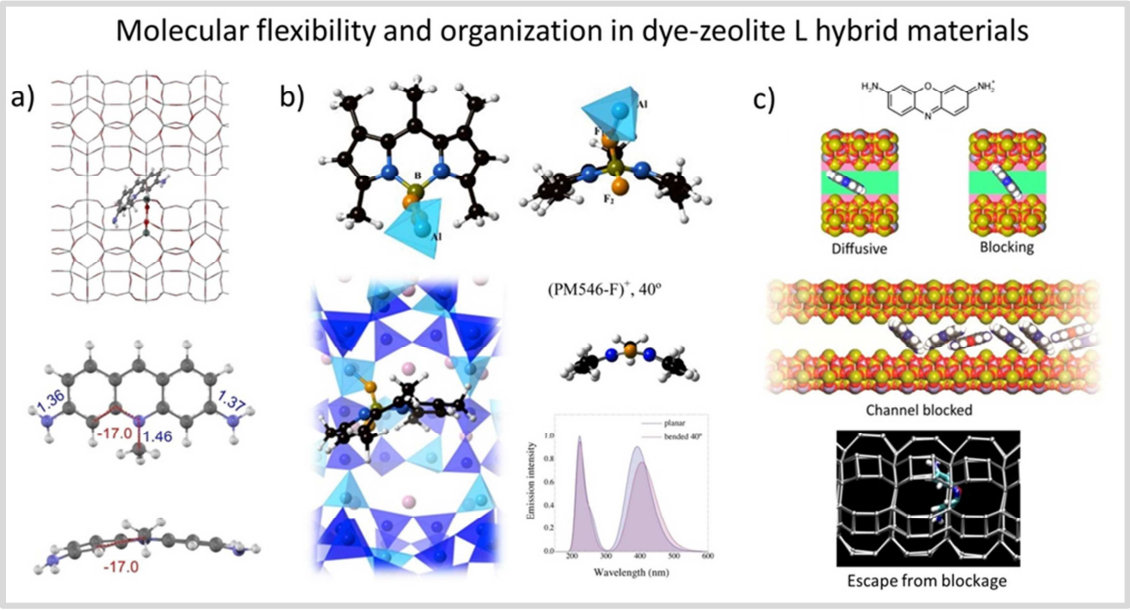

Figure 46. ***Confinement-induced molecular distortions***: a) DFT-optimized geometry of the acriflavine molecule inside zeolite L (side view along the LTL channel) and calculated values for selected geometrical parameters of the confined molecule, with distances (Å) and dihedral angle (degrees) shown in blue and red colors, respectively. [Adapted from Ref.[664] with permission from Elsevier]. b) Configuration of a BODIPY dye adsorbed in zeolite L taken from a molecular dynamics (MD) simulation of the composite. The representations highlight the arrangement of the dye inside zeolite L (viewed along the channels): a fluorine atom from the BODIPY is coordinated to an Al atom from the zeolite. The calculated absorption spectra of the dye in the planar configuration and at the maximum bending angle are also shown. Color codes: C= black, H=white, N=blue, B=green, F=orange, Cs=pink, SiO_4=dark blue, AlO_4= light blue. [Adapted with permission from Ref.[661] Copyright 2013 American Chemical Society]. c) Schematic illustrations of different configurations of oxonine guests leading either to diffusive regime or to blocking, and of a collective blocking mechanism in the zeolite channel, which may hinder the diffusion of the chromophore. [Adapted with permission from Ref.[657] Copyright 2016 American Chemical Society]. A possible escape mechanism from the blocking configuration, implying a prominent distortion of the dye from its planar structure[221] is shown in the black inset. [Illustration created with VMD].

Also, framework flexibility, molecular flexibility, and exceptionally large transient distortions of the molecular geometry, might play a pivotal role in favoring the encapsulation and then the diffusion of the confined dyes along the nanochannels. For example, flexibility might favour the escape of molecules from "blocking" configurations. The trapping of the dye into such states actually "plugs" the channel (Figure 46c), as evidenced by a recent computational investigation on the dye distribution inside the host.[657] According to such study,[657] the "blocking" configurations should be the main responsible of the so-called "traffic-jam effect", which hinders the diffusional motion of the dyes, and may make the preparation of the composites quite a time-consuming task.[37]

7.4 Effects of the framework type

The above-mentioned dyes, among with several others, have been incorporated in many hosts other than zeolite L. Aluminophosphate-zeolites, which do not contain extraframework cations, have been widely used as organizing

scaffolds for luminescent materials, yielding, for example, one of the first hybrid composites with laser dyes.[665] More recently, a series of studies[594,595,666,667] was performed on a selection of aluminophosphate hosts with different pore size, with the aim of finding the framework that would fit "like a glove" to the selected guest species (Figure 47).[594] Pyronine, for example, has dimensions of 13.7×6.2×3.2 Å, and is expected to be confined into the three candidate hosts of Figure 47 always with its main axis nearly parallel to the channel direction, similarly to perylene dyes in zeolite L – leading to composites with optical anisotropy.

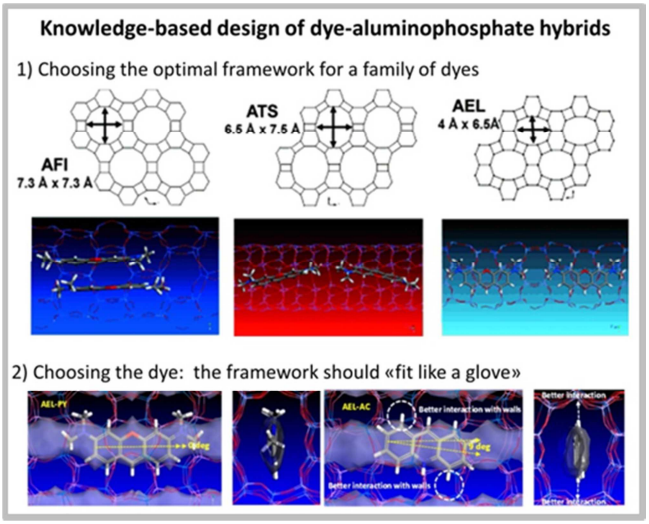

Figure 47. ***Optimizing organization inside porous aluminophosphates***: 1) selection of the best candidate among three frameworks (AFI, ATS, AEL) for the encapsulation of pyridine dye. The pertaining optimized structures calculated from DFT are also reported, and suggest that the framework that best suits to pyronine should be that of the AEL. [Adapted from Ref.[667] with permission from WILEY-VCH]. 2) choice of the dye: PY (pyronine, left) and AC (acridine, right) confined in the 1-D channel system of the aluminophosphate AEL. The angles formed by the molecular axis with the channel axis are an estimate of the alignment of the dye: The white shaded regions indicate the free space in the channel. [Adapted with permission from Ref.[666]. Copyright 2014 American Chemical Society.]

Unfortunately, the AFI-type channels are circular and can allow pyronine molecules to pack together, because of the favorable guest-guest interactions, into undesirable H-aggregates, with detrimental effects on the luminescence properties. Things went better with the second host, ATS, whose elliptical channels spatially disfavor the formation of H-aggregates, but not that of close end-to-tail arrangements of dye molecules, called J-aggregates. The third matrix, AEL, led to the composites with the best fluorescence properties, owing to the smaller size of the openings and to the channel topology (Figure 47), that not only matches the geometry of the dyes, but also forces them to be well-separated from each other, thus preventing them to aggregate.[594]Going a step further, the investigators found by calculations that acridine adjusted even better than pyronine into the AEL channels, and with more favorable interactions, rationalizing thus the higher loading of such dye found experimentally.[596] Such knowledge-driven selection of the optimal dye-zeolite pair led to a hybrid material with high fluorescence efficiency and anisotropic effects, hence amenable for various optical applications.[666,668]

The detailed knowledge of the interactions governing the supramolecular assemblies inside zeolitic nanochannel has been of crucial relevance for widening the scopes and improving the functionality of optical devices based on dye zeolite hybrid composites. The gathered insight might help to address the complexity of the newer generation of photoactive hybrid materials: understanding their structure and inner working mechanisms from molecular-level bases would be one of the future challenges of this area.

8. Organized materials by high pressure confinement

The intellectual attractiveness of the realm of high pressures has captured scientists for a long time – when matter is compressed at the extremely harsh conditions of few megabars, "strange things happen" - as illustrated, for example, by a monumental review[669] aptly entitled "*The chemical imagination at work in very tight places*". Of course, earth scientists are well accustomed with the power of pressure – maybe not so harsh to strip electrons out of atoms, or turning insulators into metals, but still very high for our standards. More precisely, to study phase transitions or amorphization of minerals, geologists work "in the GPa range" – i.e., with kilobar-to-megabar pressures. In this regime, unusual and fascinating facts emerge by compressing porous materials with molecules small enough to penetrate into their channels. With the help of high, or even just moderately high pressures, these molecules may be driven into unfavourable environments: for example, hydrocarbons can fill hydrophilic frameworks and water hydrophobic cavities. Also, oversized or overcrowding guests can be fitted into cages or channels, and stable species might be forced to react. Most importantly for our scopes, this tremendous power, combined with the shaping effect of the matrix, can provide access to a new multitude of otherwise unfeasible supramolecular organization patterns.

The intrusion of new molecules in a porous material is usually enforced using a diamond anvil cell (DAC)[670,671] – an apparate in which the sample is compressed hydrostatically *via* a pressure transmitting medium loaded into the DAC.[672] At normal conditions, the pressure transmitting medium may be in liquid, solid, or gas state; in the latter case, it is either liquefied before loading, or directly injected at high pressure into the DAC using a gas-loading device.[64,511,512] The transmitting medium plays, therefore, a key role in the experiments, because it is the potential content of the pressure-created material, which should be "shaped" by the framework architecture. Particular care should be taken in choosing the composition of the pressure fluid, especially when mixtures are used, because the penetration process depends on many factors other than the relative size of the host cavities and the potential guests.

A considerable number of experimental and computational evidences indicates that not all frameworks are penetrated by

new species coming from the pressure-transmitting fluids – namely, intrusion may not occur although the molecules of the pressure media are small enough to pass through the pore entrances. For example, many hydrophilic frameworks, including those of natural zeolites, do not typically welcome the penetration of new species, because they already host supramolecular aggregates at room pressures.[132,511,673] Hence, the uptake of molecules from the pressure media depends also on the species already present in the pores at room conditions, as well as on various experimental parameters: the maximum pressure and the rate of pressure increase, the surface/volume ratio of the crystallites in the sample, the temperature at which the experiment is performed.[64,511,674] All these factors, together with the purely geometric "shaping effect" of the framework, play an important role in governing not only the pressure-driven penetration and organization of molecular species, but also the reversibility/irreversibility of the process. Their influence should be further investigated and deeply understood at atomistic level in order to gain control over the process. Nevertheless, empty frameworks are generally preferable to already filled ones for fabricating organized materials with the help of high pressure. To this aim, hydrophobic all-silica zeolitic frameworks – after removal of the template used in their synthesis – offer a wide platform of robust void-space architectures, and weak interactions with guest species: such features make them ideal candidates as confining matrices for pressure-assisted supramolecular organization.

8.1 Pressure-induced water insertion and cation exchange

Water was the first species to be introduced through high-pressure into zeolites,[675] yet the first structural reports on pressure induced hydration (or overhydration) came many years later.[676,677] Since then, many studies have discussed the pressure-driven injection of water inside hydrophobic[504,678–680] or hydrophilic[681–684] matrices, including aluminophosphates, which have advanced our understanding of water organization in very tight spaces, and are analyzed systematically in dedicated accounts.[64,132,511,512] As regards hydrophobic frameworks, the forced intrusion of water was often attained using a porosimeter – an apparatus operating at pressures lower than those of DACs.[685] This approach has also been applied to force the intrusion of electrolytic solutions.[685,686] Such studies, already surveyed by a recent review,[685] were aimed at the possible application in energy storage devices of water intrusion/extrusion process in porous systems,[687] provided a thermodynamic description of hydrophobically confined water,[679]and played an important role in the development of the field.[685]

Basically, high-pressure overhydration studies on hydrophilic frameworks, mostly conducted with DACs, evidenced that insertion of water molecules drastically perturbs the pre-existing arrangement of the extraframework species, leading to the appearance of new organizational patterns.[511,688,689]

The pressure-driven formation and evolution of water supramolecular aggregates in the monodimensional channels of a synthetic potassium gallosilicate LTL framework[678] nicely illustrates the combined effects of high pressure and space confinement (Figure 48).

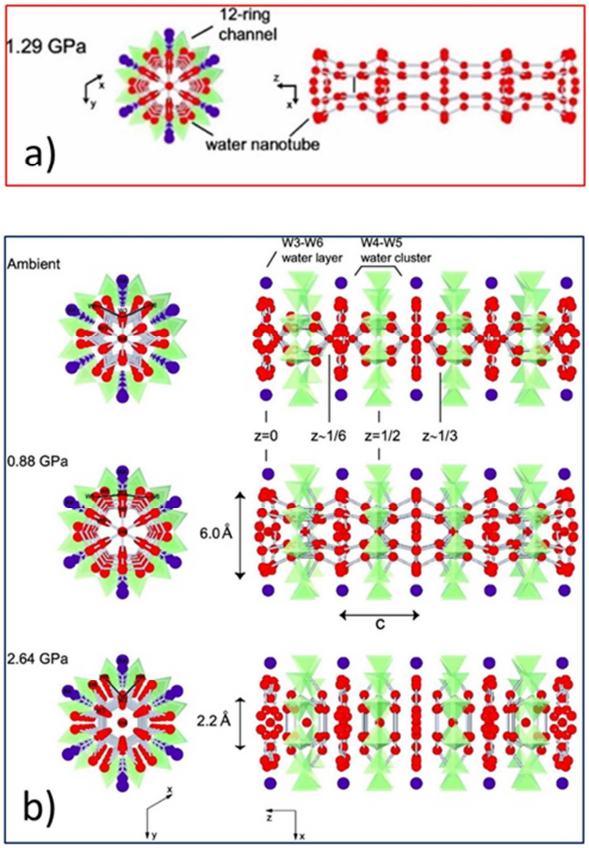

Figure 48. ***Water nanotubes*** in the 1-D channel system of an LTL-type potassium gallosilicate. a) X-ray structure at 1.29 GPa, representing the fully-formed nanotube. b) Different water nanostructures form inside the 12-membered-ring channels of K-GaSi-LTL upon increasing pressures. Water layers and water clusters, separated at ambient conditions, join together to form a tube at 0.88 GPa. At higher pressure (2.64) GPa the interactions of water with the LTL walls become predominant and the nanotube disassembles into individual clusters. Color codes: The 12-membered ring channel windows are highlighted as green polyhedra, while red and blue balls indicate oxygen atoms of water, and K^+, respectively. The grey bars between oxygen atoms represent possible hydrogen-bond interactions (distances between 2.55 and 2.9 Å). The heights of the water nanostructures along the *c* axis are also reported. Vertical arrows indicate the size of the entrance of the water nanotubes: the access is closed at 2.64 GPa. [Adapted with permission from Ref.[678]. Copyright 2007 American Chemical Society.]

At ambient pressure, the confined water molecules mainly form hydrogen-bonded clusters separated by water sheets, as in natural perlialite,[56] while at higher pressures (0.88 GPa) the water clusters and the sheets join together to form hydrogen-bonded water nanotubes inside the zeolite nanochannels. By further increasing pressure, from 1.29 up to 2.64 GPa, the confined nanotube is gradually disrupted into isolated species interacting with the host matrix. This experiment demonstrated the potential of pressure to create regular water structures inside zeolitic channels, but also that an exceeding high compression

may damage or destroy the confined supramolecular architecture.

High pressure-induced ionic exchange may be a further way to exert control over the type of guests encapsulated within hydrophilic frameworks,[690] allowing thus to place oversized cations, like europium,[691] in zeolites that do not normally undergo ion-exchange, like natrolite. Such counterintuitive phenomenon can occur because natrolite is an auxectic material, i.e., it expands perpendicular to the stretching direction, thus causing its narrow pores to increase their volume under hydrostatic compression.[692] When pressure is applied, the elliptical channels of natrolite are gradually converted into nearly circular ones: in this way, larger cations enter the pores and remain trapped after pressure release (Figure 49). As predicted by DFT calculations,[693,694] ion-exchange is energetically unfavorable, and must be driven by pressure - not surprisingly, the extent of Eu^{III} exchange increases with compression.[691] Hence, pressure-induced ionic exchange can lead to materials where structure and composition of the original zeolite are radically altered.

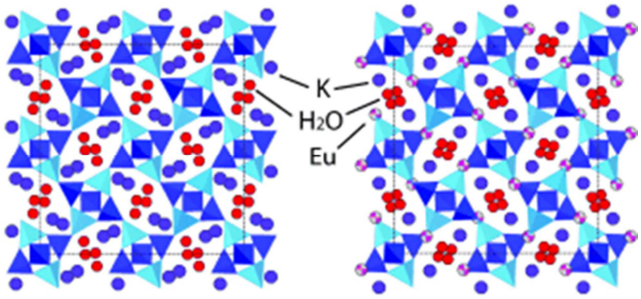

Figure 49. ***Pressure-driven ionic exchange***. The x-ray structure of zeolite K-natrolite is shown a) at room pressure and b) compressed at 1.5 GPa with a 1.0 M Eu^{III} nitrate solution as pressure-transmitting medium and cation-exchange solution The zeolite is viewed along [001], i.e. the channel axis. Upon compression, europium cations (pink) are found in a site different from the potassium cations (blue balls) and water molecules (red balls) sites. The application of high pressure also induces a significant re-organization of water and potassium cations inside the void spaces of natrolite. Dark (light) tetrahedra represent an ordered distribution of Si (Al) atoms in the framework. [Adapted from Ref.[691] with permission from WILEY-VCH].

8.2 pressure-driven polymerization as a limit case of confined organization

Pressure-assisted polymerization may be considered as an extreme case of organization under spaces restrictions. Bulk-phase polymerization under high pressures,[695,696] and polymerization in confined environments at ambient conditions[697] were both well-known phenomena, yet their combination was documented only recently. By compressing the all-silica zeolite silicalite (MFI framework type, Figure 5) in supercritical ethylene up to 1.5 GPa, and irradiating the sample with UV light, Santoro et al.[698] reported in 2013 the formation of photopolymerized ethylene. Optical spectroscopy and X-ray diffraction data confirmed that the ethylene-silicalite host-guest compound, after ambient pressure recovery, contained polyethylene chains and had a greater bulk modulus with respect to silicalite due to the filling of the pores (Figure 50a). Using the same zeolite as confining matrix, the same group performed the pressure-driven-only polymerization of acetylene: compression up to ~ 4 GPa (without light irradiation) induced the penetration of the molecules in silicalite and their polymerization to polyacetylene chains running along the zeolite channels (Figure 50b).[65]

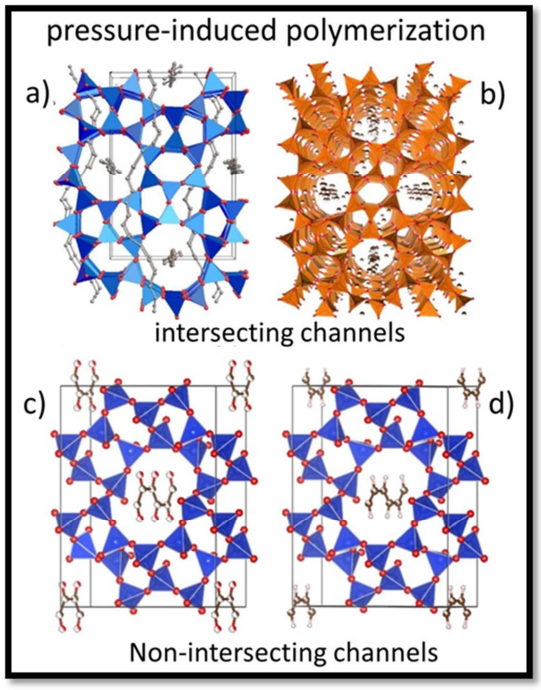

Figure 50. ***Pressure-fabricated confined polymers***: a) strained polyethylene chains in all-silica silicalite (MFI framework type) (Color code: blue = SiO_4 tetrahedra; red balls=O atoms; small grey spheres=C atoms, while H atoms are not shown). [Adapted by permission from Macmillan Publishers Ltd.[698]] b) polyacetylene in silicalite; b) polyacetylene and polycarbonyl in ZSM-22. Color codes: a) silicalite framework: Si = orange tetrahedra O=red balls. The white balls are the positions of C atoms of polyacetylene from in situ high-pressure X-ray diffraction. Reprinted with permission from Ref.[65] Copyright 2014 American Chemical Society. c,d) ZSM-22 framework: Si = blue tetrahedra; O= red balls. c) Polycarbonyl: grey (C) and red (O). d) Polyacetylene: black (C) and white (H). Adapted with permission from Ref.[699] Copyright 2016 American Chemical Society.

Now, the question arises as what happens if we use the same "mould" – the zeolite framework - and change its potential content - the pressure medium. To answer this question, the above experiment was repeated using carbon monoxide, which formed a polycarbonyl species $[-(C=O)-]_n$ inside silicalite.[700] The investigators compressed mixtures of solid CO and silicalite in a DAC, and adopted a joint experimental-computational characterization to evidence the formation of the polymer: in particular, they found that the IR spectra were compatible with the structure obtained by DFT calculations. Experimental data suggested that no covalent bond were formed between the

zeolite and the encapsulated polymeric moiety, while ex-situ analyses proved the irreversibility of the process. Unfortunately, as silicalite has a three-dimensional pore system (Figure 5), the CO molecules penetrated and polymerized into the smaller channels as well; as a consequence, the obtained polymer was not perfectly monodimensional. To solve the branching problem, the researchers chose a zeolite with a mono-dimensional channel system: the all-silica ZSM-22 (TON framework type), which was compressed up to 5-10 GPa using as pressure media CO and acetylene, in two successive experiments.[699] Also in this case, the applied pressure led to the irreversible formation of polycarbonyl and poly-acetylene, but the use of a 1D-channel framework greatly improved the linear organization of the polymerized guests, highlighting thus in a very effective way the relevance of the purely geometrical "shaping effect" of the confining medium (Figure 50c,d).

A confining matrix with 1-D channel network – namely, zeolite $AlPO_4$-5– was also recently chosen by Liu and coworkers to study the pressure behavior of confined bromine.[560] By high-pressure Raman and X-ray diffraction experiments, the researchers found that, with respect to previous studies of Br_2 encapsulation,[558] the use of high pressure led to the formation of longer bromine chains. Although a true polymerization did not occur, the distance between confined molecules gradually became comparable to the Br-Br intramolecular bond length with increasing pressures, suggesting that the dissociation of the bromine molecules and the formation of a Br_n confined polymer should occur at even higher pressures – namely, above 24 GPa.[560] Also iodine was found to exhibit a similar pressure-driven self-organizing behavior when confined into the same framework.[701] Such pressure-created $(I_2)_n$ chains showed an interesting, unexpected photoluminescence behavior under compression – which was absent in solid iodine, and was attributed to the unique 1D structure of the formed chains.[550]

These experiments showcase how the pressure-induced polymerization reaction is, actually, the ultimate consequence of the "hyperconfinement" regime: when confinement in nanospaces is combined with compression, intermolecular interactions may become competitive with intramolecular covalent bonds, and even dominant if the applied pressure is high enough.[669] Also, remarkable properties may simply emerge from the higher degree of order imposed by compression, without the need of breaking or forming covalent bonds, as demonstrated by the promising observation of pressure-induced photoluminescence of confined iodine chains.[550] In such cases, however, the appealing properties acquired via compression should be maintained upon pressure release - i.e. the process should be irreversible - in order to be more easily exploitable in applications.

8.3 Pressure-driven organization of a single type of guests

The framework composition profoundly affects the uptake of the pressure transmitting medium in the zeolite channels, as demonstrated by several experiments.[673,691,702]

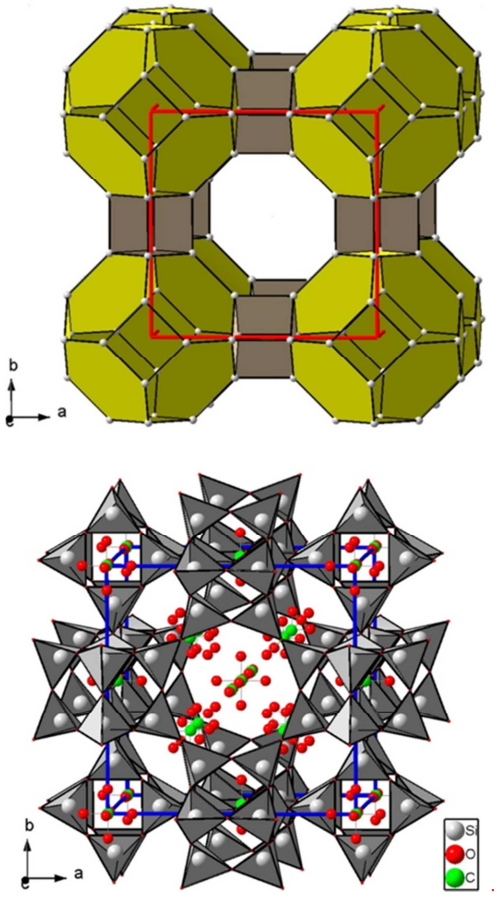

Figure 51. ***High-pressure–induced organization of CO_2*** in the host framework of ITQ-29, an all-silica zeolite with the LTA topology. (top) The sodalite cages and the cubic cages composing the framework are colored in yellow and gray, respectively. (bottom) The CO_2-filled framework structure showing the connectivity between the SiO_4 tetrahedral units and the location of CO_2 molecules at 0.5 GPa. Gray, green, and red balls represent Si, C, and O atoms, respectively. [Reproduced with permission from Ref.[703] Copyright 2017 American Chemical Society.].

Whereas it was not possible to encapsulate ethanol and methanol inside Na-mordenite – which already contained six Na^+ and 19 H_2O in the unit cell,[683,704] Arletti et al.[705] reported the intrusion of these molecules into the empty pores of all silica mordenite.[57,59] These researchers also compressed the all-silica mordenite framework by using ethylene glycol as pressure-transmitting medium. They observed that the intrusion of the glycol molecules greatly enhanced the stability of the zeolite framework against pressure-induced amorphization. Importantly, the insertion of ethylene glycol occurred already at moderate pressures - namely at 0.1 GPa, and showed features of irreversibility upon decompression.[705] The experiment indicated, therefore, that it is not necessary to use extreme pressures to introduce organic molecules in zeolites, a desirable feature for the scalability of such approach. This finding was in line with what observed for the intrusion of pure water in hydrophobic ferrierite[679] and for the pressure-driven encapsulation of other inorganic species, such as ammonia borane. Indeed, by using

Raman spectroscopy, Richard et al.[706] proved that this molecule, solid at normal conditions, could be inserted in hydrophobic silicalite (Figure 5) already at very low pressures (about 0.1 GPa), and showed a greater orientational disorder of the $-BH_3$ and $-NH_3$ groups with respect to bulk ammonia borane crystals. X-ray diffraction analysis on the ammonia borane-silicalite composite evidenced the formation of guest-molecule chains due to the spatial constraints, suggesting that each pore in the unit cell should contain between 2 and 3 molecules of ammonia borane.[706]

Confinement and supramolecular organization of simple molecules, like carbon dioxide, in nicely symmetric three-dimensional patterns, can be achieved also by using frameworks with large void spaces, like ITQ-29,[707] an all-silica analog of zeolite A (Figure 51). Santamaria-Perez et al. studied the behavior of this system up to 20 GPa, establishing that the intrusion of CO_2, which occurred below 0.5 GPa, stiffened the structure and actively prevented the amorphization of this large-pore zeolite.[703] Notably, the intruded fluid is actually tailored by the void-space-network: among the 13 encapsulated molecules *per* unit cell, twelve occupy the large α-cage in an organized arrangement, and only one the small sodalite β-cages. The filling of the α-cage by the organized CO_2-assembly is presumably the reason why this zeolite framework did not collapse under the extreme pressures used in the experiment.[703]

8.4 High pressure as driving force for supramolecular organization of multiple species

Up to now, we discussed the intrusion of a single type of species either in one- or in two/three dimensional channel systems. The complexity of the molecular organization problem drastically increases when the species to be confined have different chemical nature, i.e. if the pressure medium is a mixture.

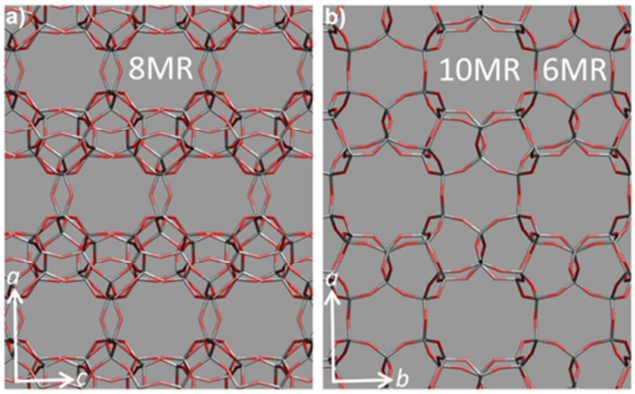

Figure 52. ***Ferrierite*** (FER framework type) has a two-dimensional system of intersecting channels, into which molecular species may be organized in 2-D patterns. The image shows two views of the FER framework a) in the ac plane, showing the eight-membered ring channels, b) in the ab plane, showing the ten- and six-membered ring channels (O=Red sticks; Si=grey sticks). [Adapted from Ref.[66] with permission from WILEY-VCH]

This is, for example, the case of an electrolytic $MgCl_2{\cdot}21H_2O$ solution injected by Arletti et al. in all-silica ferrierite.[664] This zeolite features a two dimensional system of intersecting channels: specifically, eight-membered ring channels running in the y direction cross two parallel channel systems of different diameter, defined by six- and ten- membered rings, which develop in the z direction (Figure 52). The six-membered ring cavities are also named ferrierite cages.[708]

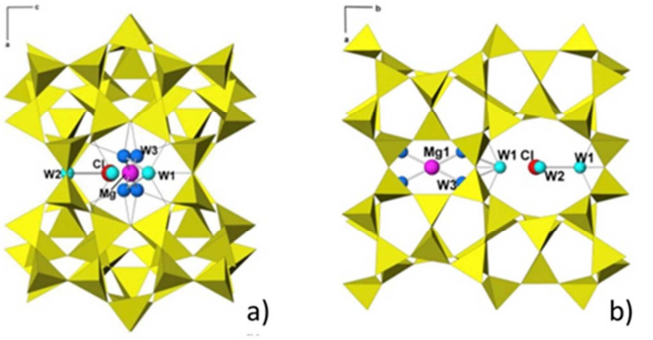

Figure 53. ***Organization of Mg, Cl, and H_2O in the 2-D channel system of ferrierite***. Both ions and water molecules present in the $MgCl_2$ aqueous solution used as pressure-transmitting media are intruded in ferrierite: Mg in the 6-membered ring cage and Cl in the ten memebered ring channels. Atom positions are obtained from refinement of the data collected at 0.28 GPa. FER framework is represented as yellow tetrahedra. [Adapted from Ref.[664] with permission from Elsevier].

Aim of the investigators was to ascertain whether both ions and water molecule could penetrate in ferrierite. Indeed, the insertion took place at relatively low pressures (below 0.2 GPa) and was reversible, as demonstrated by diffraction experiments. The refinement showed that all the components of the pressure fluid penetrated in the zeolite. A two-dimensional pattern emerged, featuring Mg at the center of the ferrierite cage, surrounded by four water molecules in a square planar symmetry, and chlorine in the ten membered ring channels, interacting with two water molecules (Figure 53). One remarkable finding was that the location of the Mg cation perfectly matched that observed by Alberti et al. on a natural ferrierite sample from Sardinia, in which the Mg cations coordinated six water oxygens in a perfect octahedral geometry.[709] In spite of the different nature of the extraframework species, the identical placement of the bivalent cation in the mineral and in the pressure-created material is striking and underlines how the realization of new supramolecular patterns through high-pressure confinement could benefit from the knowledge of the supramolecular organization of water and cations in natural zeolites.

Water-alcohol mixtures of different composition are often used as pressure transmitting media. Mixtures of methanol:ethanol:water in relative proportions 16:3:1 are commonly adopted, and were also used in two high-pressure investigations[674,710] on siliceous ferrierite. This confining matrix, according to experimental/computational studies,[711–713] should be one of the most selective frameworks for the

separation of water/alcohol mixtures – an important step in bioethanol production.[714] Indeed, separating molecules of similar size has always been a challenge for industry and technology, especially if they form hydrogen bond networks – like e.g., in water/methanol/ethanol mixtures. In both high-pressure studies on Si-ferrierite, however, only water molecules penetrated into the framework,[674,710] already at moderate pressure values (0.2 GPa) – similar to what observed with the intrusion of pure water in the same zeolite.[679]

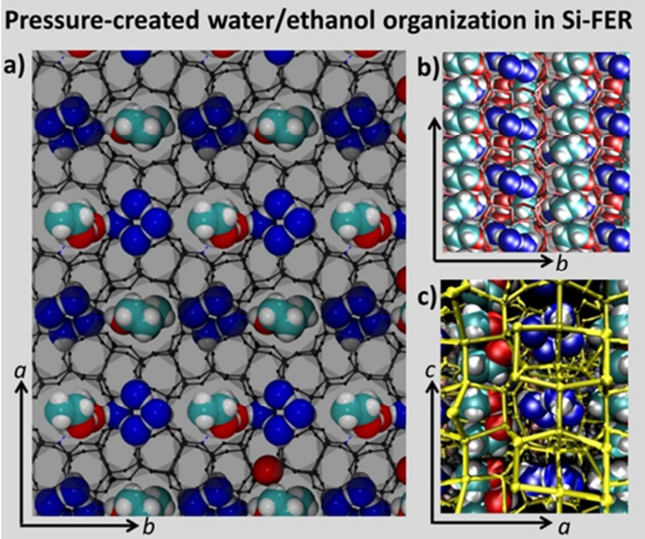

Figure 54. ***The two dimensional pattern of water and ethanol*** obtained by compressing Si-FER with a water-ethanol mixture up to 1.3 GPa. The three different views highlight, in particular: a) the water tetrameric squares; b) the chains of ethanol dimers; c) the confinement of the supramolecular architecture inside the zeolite. This pattern is maintained after recovery to ambient pressure, showing how pressure-enhanced confinement in nanospaces ("hyperconfinement") can turn liquid mixtures of simple molecules into organized materials. (water=blue and white; ethanol=red,cyan and white. FER framework: a) grey sticks and tetrahedra; b) red-gray sticks, c) yellow ball-and-sticks.) [b): Adapted from Ref.[66] with permission from WILEY-VCH].

Let us see what happens if we use the same framework and change the composition of the pressure medium by increasing the water content. Arletti et al.[66,715] compressed hydrophobic ferrierite[57] in an ethanol:water = 1:3 mixture up to 1.2 GPa and detected penetration of the fluid already at relatively low pressures. X-ray powder diffraction data combined with first-principles modelling showed that the ferrierite framework had separated the ethanol–water mixture into nearly isolated ethanol dimer wires and water tetrameric squares, forming a confined two-dimensional pattern of alternating supramolecular units (Figure 54), which remained stable even upon recovery to normal conditions.[66] Geometric analyses of these units and of the ferrierite cages indicated that the 6- and 10-membered rings channels have the right size and shape to host, respectively, the water tetramers and the ethanol dimers. Hence, the shaping effect of the ferrierite framework plays a key role in the organization of water and ethanol.

In general, the irreversibility of the pressure-induced transformation is relevant for potential applications of materials obtained in this way. Although a moderate compression can be sufficient to achieve penetration,[679,710] higher pressures seem to be necessary for irreversibility. In this case, they might have also contributed to organization.[66] The inherent preference of water molecules to congregate together, both in hydrogen-bonded liquid mixtures[716] and under confinement (as discussed throughout this review), is most likely the main molecular-level origin of the separation of water and ethanol in supramolecular blocks perfectly tailored by the void spaces of ferrierite.

8.5 High pressure and MOFs

The mechanical stability of MOFs, generally lower than zeolites, may represent a big practical problem for certain applications. Nonetheless, by virtue of the immense structural versatility of this family of materials, MOF frameworks might actually be optimized to improve their stiffness. Of course this task would be easier if we knew how they respond to harsh pressure conditions. Although the high-pressure behavior of MOFs is still relatively little explored, significant examples of diffraction experiments have been reported and nicely surveyed by a recent review.[717] Studying the response of MOFs to pressures which can push the resistance to the frameworks to their limits would provide precious information for the design of more robust frameworks with potential applications in processes requiring high-pressure conditions. A recent example is the so-called "retrofitting" of MOF-520, that amorphizes at 2.81 GPa, with an extra bridging ligand which allows the retrofitted material to remain crystalline up to 5.5 GPa (Figure 55).[718] Moreover, unique mechanical effects - such as negative linear compressibility[719] or reversible pressure-induced amorphization[720] could be uncovered. The acquired knowledge would be a significant asset for devising new supramolecular confined systems.

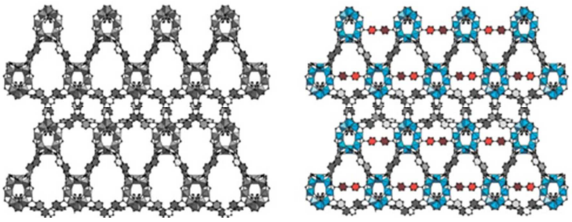

Figure 55. ***MOF retrofitting to withstand compression***: The original MOF-520 (in gray), represented on the left, was "retrofitted" by introducing an extra 4,4′-biphenyldicarboxylate ligand, which acts as a "girder" and improves the mechanical stability of the material (MOF-520-BPDC, right). [Reproduced with permission from Ref.[718] Copyright 2017 American Chemical Society.]

However, molecular inclusion in MOF's confining spaces can be obtained also at lower pressures, as shown recently by Im et al,[721] that, at 0.3 GPa, selectively replaced, in the as-synthesized hydrophobic MOF MIL-47(V), the terephthalic acid (TPA) with methanol using a methanol/ethanol/water

mixture as pressure transmitting fluid (see Figure 56, left). The system was then compressed up to 1.91 GPa, and, upon pressure release, methanol remained into the 1D-channels of this MOF.[721] Instead, by compressing the MOF with water, the exchange occurred at higher pressures (1.0 GPa) and water incorporation was reversible (Figure 56, right). Such a different behavior was attributed to the hydrophobic nature of the framework: actually, the exchange of TPA with methanol occurs also at ambient pressure simply by pouring methanol solution into the MOF.[721] This study evidenced that the pressure-induced incorporation depends strongly on the molecules composing the pressure medium, in line with what found in many experiments on zeolites, as previously discussed. Also note that here the starting system (the as-synthesized MOF) contains already a supramolecular assembly, formed by the TPA molecules. Such a system is readily disassembled upon pressure-intrusion of methanol molecules, which self-assemble into a new confined architecture (Figure 63).

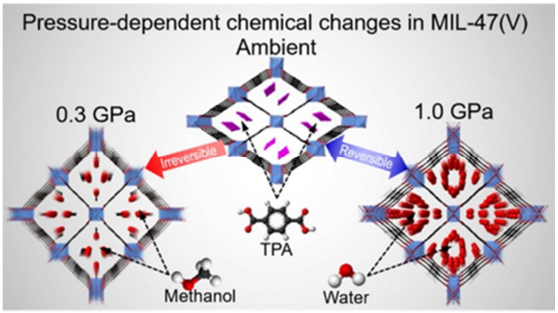

Figure 56. ***Pressure-induced guest exchange***: At moderate pressures, in the 1-D channel MOF MIL-47(V), (at the center) the terephthalic acid (TPA) molecule can be exchanged with methanol molecules (left), which are ordered with either the C or O atoms directed toward the VO_6 octahedral nodes of the MOF (sketched in blue). Much higher pressures are needed to induce water intrusion into such hydrophobic MIL-47(V) framework (right). Color cores: O=green, C=grey, H=white. [Reproduced with permission from Ref.[721] Copyright 2016 American Chemical Society.]

To gather insight into such intriguing processes, the contribution of modeling studies, especially when combined with experiments, could be invaluable.[722–724] Methodologies for determining elastic constants and other strain-related properties[725] at a high level of accuracy have been implemented[726,727] – and applied in order to improve our understanding of the mechanical response and stability of this topical family of materials.[176] Tan et al, for example, used *ab initio* periodic density functional theory to study the elastic behaviour of two nanoporous zeolite-imidazolate frameworks with the same chemical composition but different topological features, thus highlighting important relationships between their differences in structure and elastic properties.[728] In a subsequent study, Ryder et al investigated theoretically the bulk modulus of a class of zirconium MOFs in order to assess the mechanical resistance of the framework against the imposed hydrostatic pressure, thus determining the average mechanical response of the materials to compression.[725] Such an insight will become even more important in the future, particularly in designing new applications of these materials and stimulating further development of this vibrant research area that has contributed to change "our perception of the solid state".[729]

9. Conclusion and perspectives

The organizing behaviour of molecules, ions or nanoparticles in regular porous matrices was the subject of this work, which was aimed to show how the organization of guest species under nanospace confinement is a multifaceted and complex problem. From tight clathrate cages, to zeolite channel architectures, up to the tunable mesopores of organosilicas or MOFs, *organization under confinement is not simply a matter of shape, size and geometry.*

Geometry – in particular the size-shape matching of host and guest - certainly helps in selecting species to be incorporated in a given host, and vice-versa. However, small molecules can form organized patterns even within oversized cages, provided that there is a *further organizing stimulus* – for example, specific, host-guest interactions; an external pressure or field; presence of other species (e.g. solvent or template molecules) – that impartsn*additional confinement*. Conversely, molecules can be introduced into undersized spaces thanks to the *structural flexibility of both host and guest*. This factor strongly influences and often determines how organization is achieved and maintained, destroyed or converted - especially under tight space restrictions. Organization is in itself a *dynamic process*.

The *time variable* is crucial in spatially-restricted (re)organization processes: efforts should be directed towards further understanding how organized assemblies dynamically form, and evolve in time – which is particularly important for host materials characterized by a high framework flexibility.

A prominent common feature of the hosts is the *presence of an interface with the guest molecules*: the inner pore surface. Though weak in some cases, interactions of the incorporated species with the interface atoms – van der Waals, electrostatic, hydrogen bonding, or coordination – finely influence the dynamics and molecular response properties of the confined aggregates. Moreover, guest species may interact significantly with point defects of the pore surface.

Obviousy, all those system have in common also the *interface with the rest-of-the-world:* the external surface, and particularly pore entrances. The entrance of guests in confined spaces is often the first step of their assembling processes. Functionalization of pore entances offers the opportunity to control the organization process and then to transfer hierarchically the organization to the macroscale.

All confined organizations, irrespective of the matrix, are stimuli responsive. Useful information on their stability, and their dynamics can be obtained by studying their changes upon application of a stimulus – e.g. electromagnetic, thermal, mechanical. This work focused on the latter one, because the combination of high pressure and regular porous matrices has emerged as an appealing route to confined supramolecular organization - whose molecular-level bases remain largely

unexplored. The perspectives are particularly exciting: new materials have already been synthesized in this manner – for example, starting from an economically convenient precursor, a new zeolite has been obtained by high pressure treatment, showing significantly better catalytic performances than the parent material.[730]

In general, striving to dissect the subtle mechanisms of molecular organization would be instrumental in achieving a better control over them. This is suggested, for example, by the increase in scope of several applications - such as luminescent clusters, quantum dot arrays, or antenna systems - initially devised in zeolites and then implemented in MOFs or mesoporous materials: such an extension has certainly benefitted, either directly or indirectly, from the expertise acquired with zeolites. A profound knowledge of the host-guest interactions would facilitate the realization of pre-designed confined molecular superstructures to be used, ultimately, as active components of functional devices. In this sense, multitechnique studies of the organization of guest species in natural zeolites, clathrate hydrates and other minerals at different pressure/temperature conditions will greatly enhance the fundamental understanding of the host-guest interactions that govern, for example, mechanical stability. In this sense, "*paleo-inspiration*"[731] - is gaining increasing momentum in the scientific community. The idea is that of transferring into modern materials the environmental resilience and other interesting properties of ancient materials, like Roman cements, or the archetypal Blue Maya pigment, typically based on minerals. Indeed inclusion compounds of engineered clays[49] are beginning to show actual potential as eco-friendly functional materials.[732–736] Such progress was also fostered by modeling studies – that suggested, for example, to contrast the worsening in the mechanical properties of the clay (caused by the incorporation of dyes) *via* the co-adsorbption of surfactants in the interlayer space of the clay.[75,77,737] Taking inspiration from Blue Maya, the indigo molecule was recently encapsulated into zeolite L microcrystals yielding an exceptionally robust colorant:[738] the insight from simulations[193] was instrumental for the successful blockage of the crystal extremities. A better knowledge of natural porous matrices is also important for converting them into new materials using sustainable fabrication approaches; for example, using a vapor-induced approach the direct synthesis of zeolites starting from clay minerals has been recently performed.[739]

Concerning the concrete use of these composites in optoelectronic applications, the distribution of the guests inside the porous matrix, and the related changes in the photophysical properties remain major issues, nearly for all the considered cases. In the endeavour to attain a more uniform distribution of the luminescent centers, an accurate characterization plays a key role. Though obviously limited to luminescent guest or probes, single-molecule optical spectroscopy techniques are perhaps best suited to address the microscopic characterization of hybrid complexes – especially when combined with other experimental techniques (e.g. NMR, Raman) or computational modeling. These approaches have already been instrumental in probing the pore structure and diffusion dynamics in mesoporous materials as well as the optical anisotropy in zeolite host-guest materials.

The appealing luminescent properties of zeolite-encapsulated metal clusters have been disclosed only relatively recently. The latest advances, concerning particularly Ag-zeolites, raised great expectations for their applications in photonics and as phosphors in lighting, which are showcased in two very recent reviews.[44,417] Further amelioration efforts are however necessary for their actual use and commercialization e.g. as LED phosphors. For example, the emission and excitation/absorption properties of rare-earth or organic-based phosphors are still superior, as the Ag zeolites are normally activated with wavelenghts below 375 nm – a wider excitation range would be preferable. On the bright side, besides outstanding luminescence, they display comparable quantum efficiencies, thermal behaviour and also stability. Indeed the zeolite confinement is very effective as a protective environment, but the composites still remain very sensitive to humidity, that alters dramatically their photophysical properties. Viable solutions may involve the embedding of Ag-loaded clusters in polymeric matrices, or the sealing of the zeolite channel crystal terminations with suitable functionalized stopcocks.

The shortcomings of the uneven distribution of clusters in the crystalline porous matrix are somewhat mitigated in catalysis and sensing uses. For example high stability combined with the extraordinary luminescence properties of silver clusters in zeolite microcrystals will be of great advantage for applications such as bio imaging and bio sensing.[740] Also, recent promising attempts of realizing exceptionally effective environmental sensors make use of crystalline zeolite nanoparticles in the fabrication of photonic structures.[741]

Zeolite L-based antenna materials guarantee a maximum loading of the donor molecules – which results in an extremely high speed for exciton transport – and a low loading of acceptor molecules, thus minimal self-absorption losses: the acceptors can nearly quantitatively capture the excitation energy.[628] Though the composites are technically suitable for use in solar cells and sensing applications (Chapter 7), acidity inside the zeolite L channel is still a limiting factor towards attaining maximum concentration of donor molecules inside the host.[586] Nevertheless, these composites have proven to be thermally and mechanically robust, the host matrix is easy to synthesize in form of disc-shaped crystals, for which a uniform filling of dye molecules along the channels can be accomplished.

One aim of this review was to sketch the usefulness of computational methodologies in connecting macroscopic properties of functional host-guest compounds with their molecular level structure and behavior. An important advantage of modeling is that it is possible to dissect the complexity of the real system and evaluate the separate effects of different variables (composition, temperature, concentration, etc) on the macroscopic property of the system. However, although theoretical studies do provide insight and predictive ability, it is still not possible for computational models to reproduce the complexity of the real material. Though in different manner, all of the systems presented herein show an impressive degree of complexity: the number and type of guest species, their

distribution in the pores, the structural defects of the porous matrix, the effects of temperature on the guests' dynamics and framework flexibility, just to name a few. The experimental data (e.g., the photophysical response of the material) depend on all these factor in very complex manner. Experimental and computational scientist should endeavour to design together and jointly adopt integrated strategies to address the set-up of a model able to capture the essential features of the real system. Similar approaches for the elucidation of molecule-to-material conversion processes have made progress thanks to the combined endeavours of experimentalists and computational researchers. As evidenced by the presented examples, the information obtained by molecular simulation has already helped to design host-guest materials with improved optical properties. The integration betwen experiment and theory is particularly advanced in clatrate hydrate research. Calculations have become important to characterize disordered systems such as zeolite-metal clusters compounds. Nevertheless, the effort should be systematic to bridge the still existing gap between the need of a quantum mechanically consistent description and the complexity of the actual system. A truly combined experimental–theoretical approach would be based ideally on the joint simplification of the experimental system and augmentation of the computational model. In this sense, the availability (ideally) defect-free crystals or lower-dimensionality systems, for example 2D-zeolites, would be particularly helpful for a combined characterization.The understanding thus gathered could foster substantial improvements of the current fabrication/characterization techniques, and help envisioning new directions for the practical application of these materials.

I am a Computational Chemist and I teach Physical Chemistry at the Insubria University in Como, Italy. My research activity includes the simulation of molecules, materials, and interfaces at both normal and high pressure/high temperature conditions. I find porous materials and their guests especially challenging and captivating.

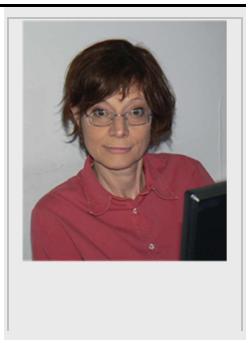

Acknowledgements

I gratefully thank the ChemPhysChem's Editorial Team and particularly the EIC Dr. Greta Heydenrych for inviting me to contribute. Rossella Arletti, Gion Calzaferri, Salvatore Coluccia, Ettore Fois, Aldo Gamba,. Diego Gatta, Gianmario Martra, Simona Quartieri, Giovanna Vezzalini are acknowledged for the work done together, as well as for the excellent discussions and exchanges of ideas that inspired this work in many different ways. Italian MIUR projects ImPACT and Zapping and Uninsubria FAR2017 are acknowledged for funding.

Keywords: clathrates • host-guest interactions • zeolites • mesoporous materials • metal-organic framework

[1] J.-M. Lehn, *Supramolecular Chemistry*, Wiley-VCH Verlag GmbH & Co. KGaA, Weinheim, FRG, **1995**.
[2] J.-M. Lehn, *Angew. Chemie Int. Ed. English* **1988**, *27*, 89–112.
[3] V. Balzani, A. Credi, F. M. Raymo, J. F. Stoddart, *Angew. Chemie Int. Ed.* **2000**, *39*, 3348–3391.
[4] P. Ceroni, A. Credi, M. Venturi, *Chem. Soc. Rev.* **2014**, *43*, 4068–4083.
[5] S. Kassem, T. van Leeuwen, A. S. Lubbe, M. R. Wilson, B. L. Feringa, D. A. Leigh, *Chem. Soc. Rev.* **2017**, *46*, 2592–2621.
[6] J.-M. Lehn, *Angew. Chemie Int. Ed.* **2013**, *52*, 2836–2850.
[7] D. Philp, J. F. Stoddart, *Angew. Chemie Int. Ed. English* **1996**, *35*, 1154–1196.
[8] G. M. Whitesides, J. P. Mathias, C. T. Seto, *Science (80-.).* **1991**, *254*, 1312–1319.
[9] C. Cheng, J. F. Stoddart, *ChemPhysChem* **2016**, *17*, 1780–1793.
[10] R. D. Astumian, S. Mukherjee, A. Warshel, *ChemPhysChem* **2016**, *17*, 1719–1741.
[11] C. Pezzato, C. Cheng, J. F. Stoddart, R. D. Astumian, *Chem. Soc. Rev.* **2017**, *46*, 5491–5507.
[12] V. Balzani, A. Credi, M. Venturi, *ChemSusChem* **2008**, *1*, 26–58.
[13] G. M. Whitesides, B. Grzybowski, *Science (80-.).* **2002**, *295*, 2418–2421.
[14] G. A. Ozin, A. Kuperman, A. Stein, *Angew. Chemie Int. Ed. English* **1989**, *28*, 359–376.
[15] L. V. Interrante, M. J. Hampden-Smith, *Chemistry of Advanced Materials : An Overview*, Wiley-VCH, **1998**.
[16] G. A. Ozin, *Adv. Mater.* **1992**, *4*, 612–649.
[17] M. E. Davis, *Nature* **2002**, *417*, 813–821.
[18] E. G. Derouane, J. C. Védrine, R. Ramos Pinto, P. M. Borges, L. Costa, M. A. N. D. A. Lemos, F. Lemos, F. Ramôa Ribeiro, *Catal. Rev. - Sci. Eng.* **2013**, *55*, 454–515.
[19] J. Weitkamp, *Solid State Ionics* **2000**, *131*, 175–188.
[20] A. Corma, C. Corell, J. Pérez-Pariente, *Zeolites* **1995**, *15*, 2–8.
[21] A. Corma, *Chem. Rev.* **1997**, *97*, 2373–2419.
[22] A. Corma, *Angew. Chemie - Int. Ed.* **2016**, *55*, 6112–6113.
[23] N. J. Turro, *Acc. Chem. Res.* **2000**, *33*, 637–646.
[24] J. C. Scaiano, H. García, *Acc. Chem. Res.* **1999**, *32*, 783–793.
[25] S. Hashimoto, *J. Photochem. Photobiol. C Photochem. Rev.* **2003**, *4*, 19–49.
[26] A. Corma, M. T. Navarro, F. Rey, V. R. Ruiz, M. J. Sabater, *ChemPhysChem* **2009**, *10*, 1084–1089.
[27] V. Ramamurthy, Y. Inoue, *Supramolecular Photochemistry: Controlling Photochemical Processes*, Wiley, **2011**.
[28] V. Ramamurthy, P. Lakshminarasimhan, C. P. Grey, L. J. Johnston, *Chem. Commun.* **1998**, *0*, 2411–2424.
[29] N. Alarcos, B. Cohen, M. Ziółek, A. Douhal, *Chem. Rev.* **2017**, acs.chemrev.7b00422.
[30] G. Calzaferri, S. Huber, H. Maas, C. Minkowski, *Angew. Chemie -*

Int. Ed. **2003**, *42*, 3732–3758.
[31] I. Stassen, N. Burtch, A. Talin, P. Falcaro, M. Allendorf, R. Ameloot, *Chem. Soc. Rev.* **2017**, *46*, 3185–3241.
[32] D. D. Medina, T. Sick, T. Bein, *Adv. Energy Mater.* **2017**, *7*, 1700387.
[33] R. M. Barrer, in *Non-Stoichiometric Compd.* (Ed.: L. Mandelcorn), Academic, New York, **1964**, pp. 309–437.
[34] D. A. Keen, A. L. Goodwin, *Nature* **2015**, *521*, 303–309.
[35] T. Förster, *Ann. Phys.* **1948**, *248*, 55–75.
[36] M. M. Yatskou, M. Meyer, S. Huber, M. Pfenniger, G. Calzaferri, *ChemPhysChem* **2003**, *4*, 567–587.
[37] G. Calzaferri, *Langmuir* **2012**, *28*, 6216–6231.
[38] H. S. Kim, K. B. Yoon, *Coord. Chem. Rev.* **2014**, *263–264*, 239–256.
[39] L. Maggini, D. Bonifazi, *Chem. Soc. Rev.* **2012**, *41*, 211–241.
[40] C. Leiggener, G. Calzaferri, *ChemPhysChem* **2004**, *5*, 1593–1596.
[41] L. Gartzia-Rivero, J. Bañuelos, I. López-Arbeloa, *Materials (Basel).* **2017**, *10*, 495.
[42] T. Sun, K. Seff, *Chem. Rev.* **1994**, *94*, 857–870.
[43] R. Seifert, A. Kunzmann, G. Calzaferri, *Angew. Chemie Int. Ed.* **1998**, *37*, 1521–1524.
[44] E. Coutiño-Gonzalez, W. Baekelant, J. A. Steele, C. W. Kim, M. B. J. Roeffaers, J. Hofkens, *Acc. Chem. Res.* **2017**, *50*, 2353–2361.
[45] T. Yumura, M. Kumondai, Y. Kuroda, T. Wakasugi, H. Kobayashi, *RSC Adv.* **2017**, *7*, 4950–4959.
[46] P. Demontis, G. B. Suffritti, *Chem. Rev.* **1997**, *97*, 2845–2878.
[47] D. Bougeard, K. S. Smirnov, *Phys. Chem. Chem. Phys.* **2007**, *9*, 226–245.
[48] T. C. T. Pham, S. Docao, I. C. Hwang, M. K. Song, D. Y. Choi, D. Moon, P. Oleynikov, K. B. Yoon, *Energy Environ. Sci.* **2016**, *9*, 1050–1062.
[49] G. Schulz-Ekloff, D. Wöhrle, B. van Duffel, R. A. Schoonheydt, *Microporous Mesoporous Mater.* **2002**, *51*, 91–138.
[50] J. Caro, F. Marlow, M. Wübbenhorst, *Adv. Mater.* **1994**, *6*, 413–416.
[51] G. Calzaferri, K. Lutkouskaya, *Photochem. Photobiol. Sci.* **2008**, *7*, 879–910.
[52] K. V. Rao, A. Jain, S. J. George, *J. Mater. Chem. C* **2014**, *2*, 3055–3064.
[53] Y. Wang, H. Li, *CrystEngComm* **2014**, *16*, 9764–9778.
[54] A. Devaux, F. Cucinotta, S. Kehr, L. De Cola, in *Funct. Supramol. Archit.*, WILEY-VCH Verlag & Co. KGaA, Weinheim, Germany, **2014**, pp. 281–342.
[55] Y. P. Menshikov, *Zap. Vses. Miner. O-va,* **1984**, *113*, 607–612.
[56] G. Artioli, A. Kvick, *Eur. J. Mineral.* **1990**, *2*, 749–760.
[57] C. Baerlocher, L. B. McCusker, D. H. Olson, *Atlas of Zeolite Framework Types*, Published On Behalf Of The Structure Commission Of The International Zeolite Association By Elsevier, **2007**.
[58] R. M. Barrer, H. Villiger, *Zeitschrift für Krist. - Cryst. Mater.* **1969**, *128*, 352–370.
[59] C. Baerlocher, L. B. McCusker, "Database of Zeolite Structures http://www.iza-structure.org/databases/," **2017**.
[60] S. Huber, G. Calzaferri, *ChemPhysChem* **2004**, *5*, 239–242.
[61] J. Yu, Y. Cui, C. Wu, Y. Yang, Z. Wang, M. O'Keeffe, B. Chen, G. Qian, *Angew. Chemie - Int. Ed.* **2012**, *51*, 10542–10545.
[62] S. Inagaki, O. Ohtani, Y. Goto, K. Okamoto, M. Ikai, K. I. Yamanaka, T. Tani, T. Okada, *Angew. Chemie - Int. Ed.* **2009**, *48*, 4042–4046.
[63] L. Sun, H. Xing, Z. Liang, J. Yu, R. Xu, *Chem. Commun.* **2013**, *49*, 11155–11157.
[64] G. D. Gatta, Y. Lee, *Mineral. Mag.* **2014**, *78*, 267–291.
[65] D. Scelta, M. Ceppatelli, M. Santoro, R. Bini, F. A. Gorelli, A. Perucchi, M. Mezouar, A. Van Der Lee, J. Haines, *Chem. Mater.* **2014**, *26*, 2249–2255.
[66] R. Arletti, E. Fois, L. Gigli, G. Vezzalini, S. Quartieri, G. Tabacchi, *Angew. Chemie - Int. Ed.* **2017**, *56*, 2105–2109.
[67] H. E. Merwin, *Chemical Analysis of Pigments in Temple of the Warriors at Chichén-Itzá, Yucatán*, Carnegie Inst, Washington, **1931**.
[68] A. Doménech, M. T. Doménech-Carbõ, C. Vidal-Lorenzo, M. L. V. De Agredos-Pascual, *Angew. Chemie - Int. Ed.* **2012**, *51*, 700–703.
[69] H. Van Olphen, *Science (80-.).* **1966**, *154*, 645–646.
[70] H. Berke, *Chem. Soc. Rev.* **2007**, *36*, 15–30.
[71] A. Tilocca, E. Fois, *J. Phys. Chem. C* **2009**, *113*, 8683–8687.
[72] R. Giustetto, K. Seenivasan, F. Bonino, G. Ricchiardi, S. Bordiga, M. R. Chierotti, R. Gobetto, *J. Phys. Chem. C* **2011**, *115*, 16764–16776.
[73] M. M. Lezhnina, T. Grewe, H. Stoehr, U. Kynast, *Angew. Chemie - Int. Ed.* **2012**, *51*, 10652–10655.
[74] E. Fois, A. Gamba, A. Tilocca, *Microporous Mesoporous Mater.* **2003**, *57*, 263–272.
[75] N. Epelde-Elezcano, E. Duque-Redondo, V. Martínez-Martínez, H. Manzano, I. López-Arbeloa, *Langmuir* **2014**, *30*, 10112–10117.
[76] S. A. Hussain, R. A. Schoonheydt, *Langmuir* **2010**, *26*, 11870–11877.
[77] N. Epelde-Elezcano, V. Martínez-Martínez, E. Duque-Redondo, I. Temiño, H. Manzano, I. López-Arbeloa, *Phys. Chem. Chem. Phys.* **2016**, *18*, 8730–8738.
[78] D. A. Kunz, M. J. Leitl, L. Schade, J. Schmid, B. Bojer, U. T. Schwarz, G. A. Ozin, H. Yersin, J. Breu, *Small* **2015**, *11*, 792–796.
[79] E. D. Sloan, C. Koh, *Clathrate Hydrates of Natural Gases*, CRC Press, **2008**.
[80] C. A. Koh, *Chem. Soc. Rev.* **2002**, *31*, 157–167.
[81] K. C. Hester, P. G. Brewer, *Ann. Rev. Mar. Sci.* **2009**, *1*, 303–327.
[82] E. D. Sloan, *Nature* **2003**, *426*, 353–359.
[83] L. Mandelcorn, *Chem. Rev.* **1959**, *59*, 827–839.
[84] R. M. Barrer, *J. Chem. Soc.* **1948**, *0*, 2158.
[85] R. M. Barrer, J. L. Whiteman, *J. Chem. Soc. A* **1967**, 19–25.
[86] T. Bein, *Chem. Mater.* **1996**, *8*, 1636–1653.
[87] U. Simon, M. E. Franke, *Microporous Mesoporous Mater.* **2000**, *41*, 1–36.
[88] A. Corma, *Chem. Rev.* **1995**, *95*, 559–614.
[89] C. S. Cundy, P. A. Cox, *Chem. Rev.* **2003**, *103*, 663–701.
[90] M. E. Davis, C. Saldarriaga, C. Montes, J. Garces, C. Crowdert, *Nature* **1988**, *331*, 698–699.
[91] L. B. McCusker, C. Baerlocher, E. Jahn, M. Bülow, *Zeolites* **1991**, *11*, 308–313.
[92] M. W. Anderson, O. Terasaki, T. Ohsuna, A. Philippou, S. P. MacKay, A. Ferreira, J. Rocha, S. Lidin, *Nature* **1994**, *367*, 347–351.
[93] C. L. Bowes, G. A. Ozin, *Adv. Mater.* **1996**, *8*, 13–28.
[94] N. Zheng, X. Bu, B. Wang, P. Feng, *Science (80-.).* **2002**, *298*, 2366–2369.

[95] X. Bu, N. Zheng, P. Feng, *Chem. - A Eur. J.* **2004**, *10*, 3356–3362.

[96] P. Peng, B. U. Xianhui, N. Zheng, *Acc. Chem. Res.* **2005**, *38*, 293–303.

[97] M. Zeuner, S. Pagano, W. Schnick, *Angew. Chemie - Int. Ed.* **2011**, *50*, 7754–7775.

[98] F. Marlow, J. Caro, *J. Phys. Chem.* **1993**, *97*, 11286–11290.

[99] U. Vietze, O. Krauß, F. Laeri, G. Ihlein, F. Schüth, B. Limburg, M. Abraham, *Phys. Rev. Lett.* **1998**, *81*, 4628–4631.

[100] C. N. R. Rao, B. C. Satishkumar, A. Govindaraj, M. Nath, *ChemPhysChem* **2001**, *2*, 78–105.

[101] T. Yanagisawa, T. Shimizu, K. Kuroda, C. Kato, *Bull. Chem. Soc. Jpn.* **1990**, *63*, 988–992.

[102] C. T. Kresge, M. E. Leonowicz, W. J. Roth, J. C. Vartuli, J. S. Beck, *Nature* **1992**, *359*, 710–712.

[103] C. Yoshina-Ishii, T. Asefa, N. Coombs, M. J. MacLachlan, G. A. Ozin, *Chem. Commun.* **1999**, *0*, 2539–2540.

[104] A. K. Cheetham, G. Férey, T. Loiseau, *Angew. Chemie Int. Ed.* **1999**, *38*, 3268–3292.

[105] S. Kitagawa, R. Kitaura, S. Noro, *Angew. Chemie Int. Ed.* **2004**, *43*, 2334–2375.

[106] M. O'Keeffe, O. M. Yaghi, *Chem. Rev.* **2012**, *112*, 675–702.

[107] C. H. Hendon, A. J. Rieth, M. D. Korzyński, M. Dincă, *ACS Cent. Sci.* **2017**, *3*, 554–563.

[108] R. E. Morris, L. Brammer, *Chem. Soc. Rev.* **2017**, *46*, 5444–5462.

[109] B. Manna, A. K. Chaudhari, B. Joarder, A. Karmakar, S. K. Ghosh, *Angew. Chemie - Int. Ed.* **2013**, *52*, 998–1002.

[110] S. M. J. Rogge, A. Bavykina, J. Hajek, H. Garcia, A. I. Olivos-Suarez, A. Sepúlveda-Escribano, A. Vimont, G. Clet, P. Bazin, F. Kapteijn, et al., *Chem. Soc. Rev.* **2017**, *46*, 3134–3184.

[111] T. Iwamoto, *J. Incl. Phenom. Mol. Recognit. Chem.* **1996**, *24*, 61–132.

[112] T. Iwamoto, S. Nishikiori, T. Kitazawa, H. Yuge, *J. Chem. Soc. Dalt. Trans.* **1997**, *0*, 4127–4136.

[113] T. Iwamoto, T. Kitazawa, S. Nishikiori, R. Kuroda, in *Chem. Phys. Intercalation II (Proceedings Second NATO Adv. Study Inst. Chem. Phys. Intercalation, Chateau Bonas, June 29–July 9, 1992*, **1993**, pp. 325–332.

[114] T. Iwamoto, S. I. Nishikiori, T. Kitazawa, *Supramol. Chem.* **1995**, *6*, 179–186.

[115] N. A. Anurova, V. A. Blatov, G. D. Ilyushin, D. M. Proserpio, *J. Phys. Chem. C* **2010**, *114*, 10160–10170.

[116] E. M. Flanigen, *Pure Appl. Chem.* **1980**, *52*, 2191–2211.

[117] W. H. Baur, *Am. Mineral.* **1964**, *49*, 697–704.

[118] G. Vezzalini, S. Quartieri, E. Galli, A. Alberti, G. Cruciani, A. Kvick, *Zeolites* **1997**, *19*, 323–325.

[119] J. A. Ripmeester, J. S. Tse, C. I. Ratcliffe, B. M. Powell, *Nature* **1987**, *325*, 135–136.

[120] H. Lu, Y. T. Seo, J. W. Lee, I. Moudrakovski, J. A. Ripmeester, N. R. Chapman, R. B. Coffin, G. Gardner, J. Pohlman, *Nature* **2007**, *445*, 303–306.

[121] K. Momma, *J. Phys. Condens. Matter* **2014**, *26*, 103203.

[122] H. Gies, in *Handb. Porous Solids*, Wiley-VCH Verlag GmbH, Weinheim, Germany, **2008**, pp. 667–698.

[123] C. A. Geiger, E. Dachs, M. Nagashima, *Am. Mineral.* **2008**, *93*, 1179–1182.

[124] G. Gottardi, E. Galli, *Natural Zeolites*, Springer Berlin Heidelberg, **2012**.

[125] T. Armbruster, M. E. Gunter, *Rev. Mineral. Geochemistry* **2001**, *45*, 1–67.

[126] C. Dryzun, Y. Mastai, A. Shvalb, D. Avnir, *J. Mater. Chem.* **2009**, *19*, 2062–2069.

[127] R. C. Rouse, D. R. Peacor, *Am. Mineral.* **1986**, *71*, 1494–1501.

[128] S. V. Krivovichev, *Angew. Chemie - Int. Ed.* **2014**, *53*, 654–661.

[129] C. Lengauer, G. Giester, E. Tillmanns, *Mineral. Mag.* **1997**, *61*, 591–606.

[130] P. Guo, J. Shin, A. G. Greenaway, J. G. Min, J. Su, H. J. Choi, L. Liu, P. A. Cox, S. B. Hong, P. A. Wright, et al., *Nature* **2015**, *524*, 74–78.

[131] J. Shin, H. Xu, S. Seo, P. Guo, J. G. Min, J. Cho, P. A. Wright, X. Zou, S. B. Hong, *Angew. Chemie - Int. Ed.* **2016**, *55*, 4928–4932.

[132] G. Vezzalini, R. Arletti, S. Quartieri, *Acta Crystallogr. Sect. B Struct. Sci. Cryst. Eng. Mater.* **2014**, *70*, 444–451.

[133] B. Kamb, *Science (80-.).* **1965**, *148*.

[134] M. Tribaudino, A. Artoni, C. Mavris, D. Bersani, P. P. Lottici, D. Belletti, *Am. Mineral.* **2008**, *93*, 88–94.

[135] P. Macchi, *Crystallogr. Rev.* **2013**, *19*, 58–101.

[136] A. Cervellino, R. Frison, N. Masciocchi, A. Guagliardi, in *X-Ray Neutron Tech. Nanomater. Charact.*, Springer Berlin Heidelberg, Berlin, Heidelberg, **2016**, pp. 545–608.

[137] R. Gaillac, P. Pullumbi, K. A. Beyer, K. W. Chapman, D. A. Keen, T. D. Bennett, F.-X. Coudert, *Nat. Mater.* **2017**, *16*, 1149–1154.

[138] S. E. Ashbrook, D. M. Dawson, V. R. Seymour, *Phys. Chem. Chem. Phys.* **2014**, *16*, 8223–8242.

[139] S. Ramdas, J. M. Thomas, J. Klinowski, C. A. Fyfe, J. S. Hartman, *Nature* **1981**, *292*, 228–230.

[140] C. A. Fyfe, J. M. Thomas, J. Klinowski, G. C. Gobbi, *Angew. Chemie Int. Ed. English* **1983**, *22*, 259–275.

[141] C. A. Fyfe, G. C. Gobbi, G. J. Kennedy, *J. Phys. Chem.* **1984**, *88*, 3248–3253.

[142] T. Yokoi, H. Mochizuki, S. Namba, J. N. Kondo, T. Tatsumi, *J. Phys. Chem. C* **2015**, *119*, 15303–15315.

[143] I. I. Ivanova, Y. G. Kolyagin, I. A. Kasyanov, A. V. Yakimov, T. O. Bok, D. N. Zarubin, *Angew. Chemie - Int. Ed.* **2017**, *56*, 15344–15347.

[144] A. Zheng, S.-B. Liu, F. Deng, *Chem. Rev.* **2017**, acs.chemrev.7b00289.

[145] C. Martineau, *Solid State Nucl. Magn. Reson.* **2014**, *63*, 1–12.

[146] A. Marchetti, J. Chen, Z. Pang, S. Li, D. Ling, F. Deng, X. Kong, *Adv. Mater.* **2017**, *29*, 1605895.

[147] B. E. G. Lucier, Y. Zhang, Y. Huang, *Concepts Magn. Reson. Part A* **2017**, e21410.

[148] A. J. Rossini, A. Zagdoun, M. Lelli, J. Canivet, S. Aguado, O. Ouari, P. Tordo, M. Rosay, W. E. Maas, C. Copéret, et al., *Angew. Chemie Int. Ed.* **2012**, *51*, 123–127.

[149] J. A. Ripmeester, C. I. Ratcliffe, *J. Phys. Chem.* **1990**, *94*, 8773–8776.

[150] J. A. Ripmeester, C. I. Ratcliffe, *J. Phys. Chem.* **1990**, *94*, 7652–7656.

[151] S. Pawsey, I. Moudrakovski, J. Ripmeester, L.-Q. Wang, G. J. Exarhos, J. L. C. Rowsell, O. M. Yaghi, *J. Phys. Chem. C* **2007**, *111*, 6060–6067.

[152] P. Sozzani, A. Comotti, R. Simonutti, T. Meersmann, J. W. Logan, A. Pines, *Angew. Chemie Int. Ed.* **2000**, *39*, 2695–2699.

[153] a Nossov, E. Haddad, F. Guenneau, A. Galarneau, F. Di Renzo, F. Fajula, A. Gedeon, *J. Phys. Chem. B* **2003**, *107*, 12456–12460.

[154] V. V. Terskikh, I. L. Moudrakovski, S. R. Breeze, S. Lang, C. I. Ratcliffe, J. A. Ripmeester, A. Sayari, *Langmuir* **2002**, *18*, 5653–5656.

[155] F. Guenneau, K. Panesar, A. Nossov, M.-A. Springuel-Huet, T. Azaïs, F. Babonneau, C. Tourné-Péteilh, J.-M. Devoisselle, A. Gédéon, *Phys. Chem. Chem. Phys.* **2013**, *15*, 18805.

[156] D. I. Kolokolov, S. S. Arzumanov, D. Freude, J. Haase, A. G. Stepanov, *J. Phys. Chem. C* **2016**, *120*, 4993–5000.

[157] S. Bordiga, C. Lamberti, F. Bonino, A. Travert, F. Thibault-Starzyk, *Chem. Soc. Rev.* **2015**, *44*, 7262–7341.

[158] K. I. Hadjiivanov, G. N. Vayssilov, *Adv. Catal.* **2002**, *47*, 307–511.

[159] A. Zecchina, L. Marchese, S. Bordiga, C. Pazè, E. Gianotti, *J. Phys. Chem. B* **1997**, *101*, 10128–10135.

[160] A. Zecchina, C. Otero Areán, *Chem. Soc. Rev.* **1996**, *25*, 187–197.

[161] C. Otero Areán, A. A. Tsyganenko, E. Escalona Platero, E. Garrone, A. Zecchina, *Angew. Chemie - Int. Ed.* **1998**, *37*, 3161–3163.

[162] S. Coluccia, L. Marchese, G. Martra, *Microporous Mesoporous Mater.* **1999**, *30*, 43–56.

[163] J. Canivet, V. Lysenko, J. Lehtinen, A. Legrand, F. M. Wisser, E. A. Quadrelli, D. Farrusseng, *ChemPhysChem* **2017**, DOI 10.1002/cphc.201700663.

[164] K. F. Domke, J. P. R. Day, G. Rago, T. A. Riemer, M. H. F. Kox, B. M. Weckhuysen, M. Bonn, *Angew. Chemie - Int. Ed.* **2012**, *51*, 1343–1347.

[165] R. A. Schoonheydt, *Chem. Soc. Rev.* **2010**, *39*, 5051.

[166] A. Gasecka, L.-Q. Dieu, D. Brühwiler, S. Brasselet, *J. Phys. Chem. B* **2010**, *114*, 4192–4198.

[167] R. A. Schoonheydt, *Angew. Chemie - Int. Ed.* **2008**, *47*, 9188–9191.

[168] B. M. Weckhuysen, *Angew. Chemie - Int. Ed.* **2009**, *48*, 4910–4943.

[169] C. Blum, Y. Cesa, M. Escalante, V. Subramaniam, *J. R. Soc. Interface* **2009**, *6*, S35–S43.

[170] T. Bein, D. C. Lamb, J. Michaelis, *ChemPhysChem* **2012**, *13*, 881–1095.

[171] S. C. C. Wiedemann, Z. Ristanovic, G. T. Whiting, V. R. Reddy Marthala, J. Kärger, J. Weitkamp, B. Wels, P. C. A. Bruijnincx, B. M. Weckhuysen, *Chem. - A Eur. J.* **2016**, *22*, 199–210.

[172] V. Van Speybroeck, K. Hemelsoet, L. Joos, M. Waroquier, R. G. Bell, C. R. A. Catlow, *Chem. Soc. Rev.* **2015**, *44*, 7044–7111.

[173] R. A. van S. C.R.A. Catlow, Berend Smit, *Computer Modelling of Microporous Materials (Google eBook)*, Elsevier, **2004**.

[174] F. X. Coudert, A. H. Fuchs, *Coord. Chem. Rev.* **2015**, *307*, 211–236.

[175] M. Fischer, J. R. B. Gomes, M. Jorge, *Mol. Simul.* **2014**, *40*, 537–556.

[176] G. Fraux, F.-X. Coudert, *Chem. Commun.* **2017**, *53*, 7211–7221.

[177] L. Chen, P. S. Reiss, S. Y. Chong, D. Holden, K. E. Jelfs, T. Hasell, M. A. Little, A. Kewley, M. E. Briggs, A. Stephenson, et al., *Nat. Mater.* **2014**, *13*, 954–960.

[178] S. Jiang, Q. Song, A. Massey, S. Y. Chong, L. Chen, S. Sun, T. Hasell, R. Raval, E. Sivaniah, A. K. Cheetham, et al., *Angew. Chemie Int. Ed.* **2017**, *56*, 9391–9395.

[179] T. Ben, H. Ren, M. Shengqian, D. Cao, J. Lan, X. Jing, W. Wang, J. Xu, F. Deng, J. M. Simmons, et al., *Angew. Chemie - Int. Ed.* **2009**, *48*, 9457–9460.

[180] L. Vilà-Nadal, L. Cronin, *Nat. Rev. Mater.* **2017**, *2*, 17054.

[181] A. G. Slater, A. I. Cooper, *Science (80-.).* **2015**, *348*.

[182] B. Smit, T. L. M. Maesen, *Chem. Rev.* **2008**, *108*, 4125–4184.

[183] P. Demontis, J. Karger, G. B. Suffritti, A. Tilocca, *Phys. Chem. Chem. Phys.* **2000**, *2*, 1455–1463.

[184] A. Torres-Knoop, D. Dubbeldam, *ChemPhysChem* **2015**, *16*, 2046–2067.

[185] M. Pfenniger, G. Calzaferri, *ChemPhysChem* **2000**, *1*, 211–217.

[186] J. Rybka, J. Kärger, U. Tallarek, *ChemPhysChem* **2017**, *18*, 2094–2102.

[187] J. Kärger, *ChemPhysChem* **2015**, *16*, 24–51.

[188] F. Li, D. P. Josephson, A. Stein, *Angew. Chemie Int. Ed.* **2011**, *50*, 360–388.

[189] N. Vogel, M. Retsch, C. A. Fustin, A. Del Campo, U. Jonas, *Chem. Rev.* **2015**, *115*, 6265–6311.

[190] J. Čejka, A. Corma, S. Zones, *Zeolites and Catalysis: Synthesis, Reactions and Applications, Volume 2*, WILEY-VCH Verlag GmbH & Co. KGaA, Weinheim, Germany, **2010**.

[191] K. B. Yoon, *Acc. Chem. Res.* **2007**, *40*, 29–40.

[192] J. Cho, Y. Ishida, *Adv. Mater.* **2017**, *29*, 1605974.

[193] G. Tabacchi, E. Fois, G. Calzaferri, *Angew. Chemie Int. Ed.* **2015**, *54*, 11112–11116.

[194] W. Baur, R. X. Fischer, *Microporous and Other Framework Materials with Zeolite-Type Structures*, SPRINGER-VERLAG BERLIN AN, **2017**.

[195] R. Szostak, *Molecular Sieves - Springer*, Springer Netherlands, **1989**.

[196] D. S. Coombs, A. Alberti, T. Armbruster, G. Artioli, C. Colella, E. Galli, J. D. Grice, F. Liebau, E. H. Nickel, E. Passaglia, et al., *Can. Mineral.* **1997**, *35*, 1571–1606.

[197] M. M. J. Treacy, M. D. Foster, *Microporous Mesoporous Mater.* **2009**, *118*, 106–114.

[198] V. A. Blatov, O. Delgado-Friedrichs, M. O'Keeffe, D. M. Proserpio, *Acta Crystallogr. Sect. A Found. Crystallogr.* **2007**, *63*, 418–425.

[199] G. Sastre, A. Corma, *J. Phys. Chem. C* **2009**, *113*, 6398–6405.

[200] Y. Li, J. Yu, *Chem. Rev.* **2014**, *114*, 7268–7316.

[201] M. Moliner, C. Martínez, A. Corma, *Angew. Chemie - Int. Ed.* **2015**, *54*, 3560–3579.

[202] W. J. Roth, P. Nachtigall, R. E. Morris, J. Čejka, *Chem. Rev.* **2014**, *114*, 4807–4837.

[203] M. Choi, K. Na, J. Kim, Y. Sakamoto, O. Terasaki, R. Ryoo, *Nature* **2009**, *461*, 246–249.

[204] J. Choi, S. Ghosh, Z. Lai, M. Tsapatsis, *Angew. Chemie - Int. Ed.* **2006**, *45*, 1154–1158.

[205] J. A. Boscoboinik, X. Yu, B. Yang, F. D. Fischer, R. Wodarczyk, M. Sierka, S. Shaikhutdinov, J. Sauer, H. J. Freund, *Angew. Chemie - Int. Ed.* **2012**, *51*, 6005–6008.

[206] U. Díaz, A. Corma, *Dalt. Trans.* **2014**, *43*, 10292.

[207] S. Zanardi, A. Alberti, G. Cruciani, A. Corma, V. Fornés, M. Brunelli, *Angew. Chemie Int. Ed.* **2004**, *43*, 4933–4937.

[208] M. Hartmann, *Angew. Chemie - Int. Ed.* **2004**, *43*, 5880–5882.

[209] Y. Wei, T. E. Parmentier, K. P. de Jong, J. Zečević, *Chem. Soc. Rev.* **2015**, *44*, 7234–7261.

[210] M. A. Snyder, M. Tsapatsis, *Angew. Chemie Int. Ed.* **2007**, *46*, 7560–7573.

[211] G. A. Ozin, *http://www.artnanoinnovations.com/ozin/Nanochemistry Views.pdf* **2012**.

[212] F. C. Hendriks, J. E. Schmidt, J. A. Rombouts, K. Lammertsma, P. C. A. Bruijnincx, B. M. Weckhuysen, *Chem. - A Eur. J.* **2017**, *23*, 6305–6314.

[213] J. E. Schmidt, F. C. Hendriks, M. Lutz, L. C. Post, D. Fu, dr. B. M. Weckhuysen, *ChemPhysChem* **2017**, DOI 10.1002/cphc.201700583.

[214] C. Weidenthaler, R. X. Fischer, R. D. Shannon, O. Medenbach, *J. Phys. Chem.* **1994**, *98*, 12687–12694.

[215] S. Sklenak, J. Dědeček, C. Li, B. Wichterlová, V. Gábová, M. Sierka, J. Sauer, *Angew. Chemie - Int. Ed.* **2007**, *46*, 7286–7289.

[216] A. R. Ruiz-Salvador, R. Grau-Crespo, A. E. Gray, D. W. Lewis, *J. Solid State Chem.* **2013**, *198*, 330–336.

[217] L. Grajciar, C. O. Areán, A. Pulido, P. Nachtigall, *Phys. Chem. Chem. Phys.* **2010**, *12*, 1497–506.

[218] M. Fischer, *Phys. Chem. Chem. Phys.* **2016**, *18*, 15738–15750.

[219] C. Betti, E. Fois, E. Mazzucato, C. Medici, S. Quartieri, G. Tabacchi, G. Vezzalini, V. Dmitriev, *Microporous Mesoporous Mater.* **2007**, *103*, 190–209.

[220] E. Fois, A. Gamba, C. Medici, G. Tabacchi, S. Quartieri, E. Mazzucato, R. Arletti, G. Vezzalini, V. Dmitriev, *Microporous Mesoporous Mater.* **2008**, *115*, 267–280.

[221] E. Fois, G. Tabacchi, G. Calzaferri, *J. Phys. Chem. C* **2012**, *116*, 16784–16799.

[222] E. Fois, G. Tabacchi, A. Devaux, P. Belser, D. Brühwiler, G. Calzaferri, *Langmuir* **2013**, *29*, 9188–9198.

[223] D. W. Breck, *Zeolite Molecular Sieves: Structure, Chemistry, and Use*, Wiley, **1973**.

[224] H. G. (Hellmut G. . Karge, J. (Jens) Weitkamp, *Molecular Sieves - Science and Technology*, Springer, **2008**.

[225] A. Zecchina, F. Geobaldo, G. Spoto, S. Bordiga, G. Ricchiardi, R. Buzzoni, G. Petrini, *J. Phys. Chem.* **1996**, *100*, 16584–16599.

[226] M. Sierka, U. Eichler, J. Datka, J. Sauer, *J. Phys. Chem. B* **1998**, *102*, 10468–10468.

[227] T. Demuth, J. Hafner, L. Benco, H. Toulhoat, *J. Phys. Chem. B* **2000**, *104*, 4593–4607.

[228] L. Benco, *J. Catal.* **2002**, *205*, 147–156.

[229] E. Fois, A. Gamba, G. Tabacchi, *J. Phys. Chem. B* **1998**, *102*, 3974–3979.

[230] A. V. Larin, D. N. Trubnikov, D. P. Vercauteren, *Int. J. Quantum Chem.* **2005**, *102*, 971–979.

[231] R. Fricke, H. Kosslick, G. Lischke, M. Richter, *Chem. Rev.* **2000**, *100*, 2303–2405.

[232] R. M. Barrer, J. W. Baynham, F. W. Bultitude, W. M. Meier, *J. Chem. Soc.* **1959**, *36*, 195–208.

[233] C. Otero Areán, G. Turnes Palomino, F. Geobaldo, A. Zecchina, *J. Phys. Chem.* **1996**, *100*, 6678–6690.

[234] Z. Gabelica, J. B. Nagy, P. Bodart, G. Debras, *Chem. Lett.* **1984**, *13*, 1059–1062.

[235] G. Valerio, J. Ple´vert, A. Goursot, F. di Renzo, *Phys. Chem. Chem. Phys.* **2000**, *2*, 1091–1094.

[236] S. J. Hwang, C. Y. Chen, S. I. Zones, *J. Phys. Chem. B* **2004**, *108*, 18535–18546.

[237] F. Trudu, G. Tabacchi, A. Gamba, E. Fois, *J. Phys. Chem. C* **2008**, *112*, 15394–15401.

[238] E. Fois, A. Gamba, F. Trudu, G. Tabacchi, *Nuovo Cim. della Soc. Ital. di Fis. B* **2008**, *123*, 1567–1574.

[239] S. T. Wilson, B. M. Lok, C. A. Messina, T. R. Cannan, E. M. Flanigen, *J. Am. Chem. Soc* **1982**, *104*, 1146.

[240] H. O. Pastore, S. Coluccia, L. Marchese, *Annu. Rev. Mater. Res.* **2005**, *35*, 351–395.

[241] J. Yu, R. Xu, *Chem. Soc. Rev.* **2006**, *35*, 593.

[242] A. Corma, U. Diaz, M. E. Domine, V. Fornés, *Chem. Commun.* **2000**, *0*, 137–138.

[243] E. A. Eilertsen, F. Giordanino, C. Lamberti, S. Bordiga, A. Damin, F. Bonino, U. Olsbye, K. P. Lillerud, *Chem. Commun. (Camb).* **2011**, *47*, 11867–9.

[244] J. Jiang, J. Yu, A. Corma, *Angew. Chemie Int. Ed.* **2010**, *49*, 3120–3145.

[245] Z. Gabelica, J.-L. Guth, *Angew. Chemie Int. Ed. English* **1989**, *28*, 81–83.

[246] A. Corma, M. T. Navarro, F. Rey, J. Rius, S. Valencia, *Angew. Chemie* **2001**, *113*, 2337–2340.

[247] J. J. Gutiérrez-Sevillano, S. Calero, S. Hamad, R. Grau-Crespo, F. Rey, S. Valencia, M. Palomino, S. R. G. Balestra, A. R. Ruiz-Salvador, *Chem. - A Eur. J.* **2016**, *22*, 10036–10043.

[248] P. Eliášová, M. Opanasenko, P. S. Wheatley, M. Shamzhy, M. Mazur, P. Nachtigall, W. J. Roth, R. E. Morris, J. Čejka, *Chem. Soc. Rev.* **2015**, *44*, 7177–7206.

[249] R. L. Bedard, S. T. Wilson, L. D. Vail, J. M. Bennett, E. M. Flanigen, *Stud. Surf. Sci. Catal.* **1989**, *49*, 375–387.

[250] A. Corma, M. E. Davis, *ChemPhysChem* **2004**, *5*, 304–313.

[251] G. Bellussi, E. Montanari, E. Di Paola, R. Millini, A. Carati, C. Rizzo, W. O'Neil Parker, M. Gemmi, E. Mugnaioli, U. Kolb, et al., *Angew. Chemie - Int. Ed.* **2012**, *51*, 666–669.

[252] G. Bellussi, R. Millini, E. Montanari, A. Carati, C. Rizzo, W. O. Parker, G. Cruciani, A. de Angelis, L. Bonoldi, S. Zanardi, *Chem. Commun.* **2012**, *48*, 7356.

[253] E. Fois, A. Gamba, E. Spanò, *Phys. Chem. Chem. Phys.* **2001**, *3*, 1877–1882.

[254] A. Marchuk, W. Schnick, *Angew. Chemie Int. Ed.* **2015**, *54*, 2383–2387.

[255] M. W. Anderson, O. Terasaki, T. Ohsuna, P. J. Malley, A. Phiuppou, S. P. Mackay, A. Ferreira, J. Rocha, S. Lidin, *Philos. Mag. B* **1995**, *71*, 813–841.

[256] N. C. Jeong, M. H. Lee, K. B. Yoon, *Angew. Chemie - Int. Ed.* **2007**, *46*, 5868–5872.

[257] N. C. Jeong, H. Lim, H. Cheong, K. B. Yoon, *Angew. Chemie Int. Ed.* **2011**, *50*, 8697–8701.

[258] S. J. Datta, K. B. Yoon, *Catal. Today* **2013**, *204*, 60–65.

[259] S. Galioglu, M. Isler, Z. Demircioglu, M. Koc, F. Vocanson, N.

Destouches, R. Turan, B. Akata, *Microporous Mesoporous Mater.* **2014**, *196*, 136–144.

[260] J. Lin, Y. Dong, Q. Zhang, D. Hu, N. Li, L. Wang, Y. Liu, T. Wu, *Angew. Chemie - Int. Ed.* **2015**, *54*, 5103–5107.

[261] C. H. Hendon, K. T. Butler, A. M. Ganose, Y. Román-Leshkov, D. O. Scanlon, G. A. Ozin, A. Walsh, *Chem. Mater.* **2017**, *29*, 3663–3670.

[262] D. D. Hu, J. Lin, Q. Zhang, J. N. Lu, X. Y. Wang, Y. W. Wang, F. Bu, L. F. Ding, L. Wang, T. Wu, *Chem. Mater.* **2015**, *27*, 4099–4104.

[263] D.-D. Hu, L. Wang, J. Lin, F. Bu, T. Wu, *J. Mater. Chem. C* **2015**, *3*, 11747–11753.

[264] X. Chen, X. Bu, Q. Lin, C. Mao, Q.-G. Zhai, Y. Wang, P. Feng, *Chem. - A Eur. J.* **2017**, *23*, 11913–11919.

[265] M. Wiebcke, *J. Chem. Soc. Chem. Commun.* **1991**, 1507.

[266] K. E. Lazzeri, G. E. Bebout, C. A. Geiger, *Am. Mineral.* **2017**, *102*, 686–689.

[267] C. A. Fyfe, H. Gies, *J. Incl. Phenom. Mol. Recognit. Chem.* **1990**, *8*, 235–239.

[268] M. Tribaudino, G. D. Gatta, Y. Lee, *Microporous Mesoporous Mater.* **2010**, *129*, 267–273.

[269] B. A. Kolesov, C. A. Geiger, *Am. Mineral.* **2003**, *88*, 1364–1368.

[270] K. E. Lazzeri, G. E. Bebout, C. A. Geiger, *Am. Mineral.* **2017**, *102*, 686–689.

[271] A. Y. Likhacheva, S. V. Goryainov, Y. V. Seryotkin, K. D. Litasov, K. Momma, *Microporous Mesoporous Mater.* **2016**, *224*, 100–106.

[272] K. Momma, T. Ikeda, K. Nishikubo, N. Takahashi, C. Honma, M. Takada, Y. Furukawa, T. Nagase, Y. Kudoh, *Nat. Commun.* **2011**, *2*, 196.

[273] G. D. Gatta, F. Cámara, K. T. Tait, D. Belakovskiy, *Am. Mineral.* **2012**, *97*.

[274] V. V. Struzhkin, B. Militzer, W. L. Mao, H. K. Mao, R. J. Hemley, *Chem. Rev.* **2007**, *107*, 4133–4151.

[275] A. W. C. van den Berg, C. O. Areán, *Chem. Commun.* **2008**, *73*, 668–681.

[276] K. A. Udachin, C. I. Ratcliffe, J. A. Ripmeester, *J. Supramol. Chem.* **2002**, *2*, 405–408.

[277] A. Falenty, T. C. Hansen, W. F. Kuhs, *Nature* **2014**, *516*, 231–233.

[278] G. McLaurin, K. Shin, S. Alavi, J. A. Ripmeester, *Angew. Chemie Int. Ed.* **2014**, *53*, 10429–10433.

[279] K. S. Smirnov, *Phys. Chem. Chem. Phys.* **2017**, *19*, 23095–23105.

[280] K. A. Udachin, C. I. Ratcliffe, J. A. Ripmeester, *Angew. Chemie - Int. Ed.* **2001**, *40*, 1303–1305.

[281] J. S. Loveday, R. J. Nelmes, *Phys. Chem. Chem. Phys.* **2008**, *10*, 937–950.

[282] A. Y. Manakov, A. Y. Likhacheva, V. A. Potemkin, A. G. Ogienko, A. V. Kurnosov, A. I. Ancharov, *ChemPhysChem* **2011**, *12*, 2476–2484.

[283] Y. A. Dyadin, É. G. Larionov, E. Y. Aladko, A. Y. Manakov, F. V. Zhurko, T. V. Mikina, V. Y. Komarov, E. V. Grachev, *J. Struct. Chem.* **1999**, *40*, 790–795.

[284] R. M. Barrer, G. C. Bratt, *J. Phys. Chem. Solids* **1960**, *12*, 130–145.

[285] A. M. Guloy, R. Ramlau, Z. Tang, W. Schnelle, M. Baitinger, Y. Grin, *Nature* **2006**, *443*, 320–323.

[286] L. Senadheera, M. S. Conradi, *J. Phys. Chem. B* **2007**, *111*, 12097–12102.

[287] S. Alavi, J. A. Ripmeester, *Angew. Chemie - Int. Ed.* **2007**, *46*, 6102–6105.

[288] A. N. Salamatin, A. Falenty, T. C. Hansen, W. F. Kuhs, *Energy & Fuels* **2015**, *29*, 5681–5691.

[289] A. Falenty, A. N. Salamatin, W. F. Kuhs, *J. Phys. Chem. C* **2013**, *117*, 8443–8457.

[290] J. Zhu, S. Du, X. Yu, J. Zhang, H. Xu, S. C. Vogel, T. C. Germann, J. S. Francisco, F. Izumi, K. Momma, et al., *Nat. Commun.* **2014**, *5*, ncomms5128.

[291] M. Hiratsuka, R. Ohmura, A. K. Sum, S. Alavi, K. Yasuoka, *Phys. Chem. Chem. Phys.* **2015**, *17*, 12639–12647.

[292] K. Shin, I. L. Moudrakovski, C. I. Ratcliffe, J. A. Ripmeester, *Angew. Chemie Int. Ed.* **2017**, *56*, 6171–6175.

[293] J. A. Ripmeester, S. Alavi, *Curr. Opin. Solid State Mater. Sci.* **2016**, *20*, 344–351.

[294] U. Ranieri, M. M. Koza, W. F. Kuhs, S. Klotz, A. Falenty, P. Gillet, L. E. Bove, *Nat. Commun.* **2017**, *8*, 1076.

[295] G. Buscarino, A. Alessi, S. Agnello, B. Boizot, F. M. Gelardi, R. Boscaino, *Phys. Chem. Chem. Phys.* **2014**, *16*, 13360.

[296] F. Messina, M. Todaro, G. Buscarino, L. Vaccaro, M. Cannas, F. M. Gelardi, *Phys. Chem. Miner.* **2016**, *43*, 171–179.

[297] Y. A. Dmitriev, G. Buscarino, N. P. Benetis, *J. Phys. Chem. A* **2016**, *120*, 6155–6169.

[298] G. Flachenecker, V. A. Ermoshin, V. Engel, R. Neder, G. Wirnsberger, A. Materny, *Phys. Chem. Chem. Phys.* **2003**, *5*, 865–876.

[299] H. van Koningsveld, H. Gies, *Zeitschrift für Krist. - Cryst. Mater.* **2004**, *219*, 637–643.

[300] H. Gies, F. Liebau, H. Gerke, *Angew. Chemie* **1982**, *94*, 214–215.

[301] A. V. Shevelkov, K. Kovnir, *Struct. Bond.* **2011**, *139*, 97–142.

[302] N. A. Wagner, R. Raghavan, R. Zhao, Q. Wei, X. Peng, C. K. Chan, *ChemElectroChem* **2014**, *1*, 347–353.

[303] J. Pérez-Ramírez, S. Abelló, L. A. Villaescusa, A. Bonilla, *Angew. Chemie - Int. Ed.* **2008**, *47*, 7913–7917.

[304] J. Gryko, P. F. McMillan, R. F. Marzke, G. K. Ramachandran, D. Patton, S. K. Deb, O. F. Sankey, *Phys. Rev. B - Condens. Matter Mater. Phys.* **2000**, *62*, R7707–R7710.

[305] T. F. Fässler, *Angew. Chemie - Int. Ed.* **2007**, *46*, 2572–2575.

[306] G. S. Nolas, M. Beekman, J. Gryko, G. A. Lamberton, T. M. Tritt, P. F. McMillan, *Appl. Phys. Lett.* **2003**, *82*, 910–912.

[307] H. Zhang, W. Peng, G. Mu, T. Hu, F. Huang, X. Xie, *Chem. - A Eur. J.* **2017**, *23*, 9505–9516.

[308] Q. Fang, G. Zhu, M. Xue, J. Sun, Y. Wei, S. Qui, R. Xu, *Angew. Chemie - Int. Ed.* **2005**, *44*, 3845–3848.

[309] A. J. Karttunen, T. F. Fässler, *ChemPhysChem* **2013**, *14*, 1807–1817.

[310] L.-A. Jantke, A. J. Karttunen, T. F. Fässler, *ChemPhysChem* **2017**, *18*, 1992–2006.

[311] M. Beekman, G. S. Nolas, *J. Mater. Chem.* **2008**, *18*, 842–851.

[312] C. Gatti, L. Bertini, N. P. Blake, B. B. Iversen, *Chem. - A Eur. J.* **2003**, *9*, 4556–4568.

[313] R. Nesper, K. Vogel, P. E. Blöchl, *Angew. Chemie Int. Ed. English* **1993**, *32*, 701–703.

[314] I. A. Baburin, D. M. Proserpio, V. A. Saleev, A. V. Shipilova, *Phys. Chem. Chem. Phys.* **2015**, *17*, 1332–1338.

[315] R. Car, M. Parrinello, *Phys. Rev. Lett.* **1985**, *55*, 2471–2474.

[316] T. Zeng, R. Hoffmann, R. Nesper, N. W. Ashcroft, T. A. Strobel, D. M. Proserpio, *J. Am. Chem. Soc.* **2015**, *137*, 12639–12652.

[317] L. Zhu, H. Liu, R. E. Cohen, R. Hoffmann, T. A. Strobel, *http://arxiv.org/abs/1708.03483* **2017**.

[318] J. L. Schlenker, F. G. Dwyer, E. E. Jenkins, W. J. Rohrbaugh, G. T. Kokotailo, W. M. Meier, *Nature* **1981**, *294*, 340–342.

[319] G. Férey, C. Serre, C. Mellot-Draznieks, F. Millange, S. Surblé, J. Dutour, I. Margiolaki, *Angew. Chemie* **2004**, *116*, 6456–6461.

[320] Y. Wan, D. Zhao, *Chem. Rev.* **2007**, *107*, 2821–2860.

[321] U. Ciesla, F. Schüth, *Microporous Mesoporous Mater.* **1999**, *27*, 131–149.

[322] K. Ariga, A. Vinu, Y. Yamauchi, Q. Ji, J. P. Hill, *Bull. Chem. Soc. Jpn.* **2012**, *85*, 1–32.

[323] F. Hoffmann, M. Cornelius, J. Morell, M. Fröba, *Angew. Chemie - Int. Ed.* **2006**, *45*, 3216–3251.

[324] A. Thomas, *Angew. Chemie Int. Ed.* **2010**, *49*, 8328–8344.

[325] W. J. Hunks, G. A. Ozin, *J. Mater. Chem.* **2005**, *15*, 3716.

[326] W. Wang, J. E. Lofgreen, G. A. Ozin, *Small* **2010**, *6*, 2634–2642.

[327] F. Hoffmann, M. Fröba, *Chem. Soc. Rev.* **2011**, *40*, 608–620.

[328] H. H. P. Yiu, P. A. Wright, *J. Mater. Chem.* **2005**, *15*, 3690.

[329] A. Galarneau, G. Renard, M. Mureseanu, A. Tourrette, C. Biolley, M. Choi, R. Ryoo, F. Di Renzo, F. Fajula, *Microporous Mesoporous Mater.* **2007**, *104*, 103–114.

[330] F. Pitzalis, M. Monduzzi, A. Salis, *Microporous Mesoporous Mater.* **2017**, *241*, 145–154.

[331] D. I. Fried, F. J. Brieler, M. Fröba, *ChemCatChem* **2013**, *5*, 862–884.

[332] A. L. Doadrio, J. M. Sánchez-Montero, J. C. Doadrio, A. J. Salinas, M. Vallet-Regí, *Eur. J. Pharm. Sci.* **2017**, *97*, 1–8.

[333] A. Takai, Y. Doi, Y. Yamauchi, K. Kuroda, *J. Phys. Chem. C* **2010**, *114*, 7586–7593.

[334] P. Innocenzi, L. Malfatti, T. Kidchob, P. Falcaro, *Chem. Mater.* **2009**, *21*, 2555–2564.

[335] D. Zhao, J. Feng, Q. Huo, N. Melosh, G. Fredrickson, B. Chmelka, G. Stucky, *Science (80-.).* **1998**, *279*, 548–52.

[336] F. Di Renzo, A. Galarneau, P. Trens, F. Fajula, in *Handb. Porous Solids*, Wiley-VCH Verlag GmbH, Weinheim, Germany, **2008**, pp. 1311–1395.

[337] T. Maschmeyer, F. Rey, G. Sankar, J. M. Thomas, *Nature* **1995**, *378*, 159–162.

[338] D. Brunel, N. Bellocq, P. Sutra, A. Cauvel, M. Lasperas, P. Moreau, F. Di Renzo, A. Galarneau, F. Fajula, *Coord. Chem. Rev.* **1998**, *180*, 1085–1108.

[339] G. J. A. A. Soler-Illia, P. Innocenzi, *Chem. - A Eur. J.* **2006**, *12*, 4478–4494.

[340] G. Paul, G. E. Musso, E. Bottinelli, M. Cossi, L. Marchese, G. Berlier, *ChemPhysChem* **2017**, *18*, 839–849.

[341] G. E. Musso, E. Bottinelli, L. Celi, G. Magnacca, G. Berlier, *Phys. Chem. Chem. Phys.* **2015**, *17*, 13882–13894.

[342] N. Gartmann, D. Brühwiler, *Angew. Chemie Int. Ed.* **2009**, *48*, 6354–6356.

[343] D. Brühwiler, G. Calzaferri, T. Torres, J. H. Ramm, N. Gartmann, L.-Q. Dieu, I. López-Duarte, M. V. Martínez-Díaz, *J. Mater. Chem.* **2009**, *19*, 8040–8067.

[344] N. Zucchetto, D. Brühwiler, *Dalt. Trans.* **2016**, *45*, 14363–14369.

[345] Z. Li, J. C. Barnes, A. Bosoy, J. F. Stoddart, J. I. Zink, *Chem. Soc. Rev.* **2012**, *41*, 2590.

[346] C. Park, K. Oh, S. C. Lee, C. Kim, *Angew. Chemie Int. Ed.* **2007**, *46*, 1455–1457.

[347] C. Argyo, V. Weiss, C. Bräuchle, T. Bein, *Chem. Mater.* **2014**, *26*, 435–451.

[348] T. D. Nguyen, H.-R. Tseng, P. C. Celestre, A. H. Flood, Y. Liu, J. F. Stoddart, J. I. Zink, *Proc. Natl. Acad. Sci. U. S. A.* **2005**, *102*, 10029–34.

[349] C. Wang, Z. Li, D. Cao, Y. L. Zhao, J. W. Gaines, O. A. Bozdemir, M. W. Ambrogio, M. Frasconi, Y. Y. Botros, J. I. Zink, et al., *Angew. Chemie - Int. Ed.* **2012**, *51*, 5460–5465.

[350] T. Asefa, M. J. MacLachan, N. Coombs, G. A. Ozin, *Nature* **1999**, *402*, 867–871.

[351] S. Inagaki, S. Guan, Y. Fukushima, T. Ohsuna, O. Terasaki, *J. Am. Chem. Soc.* **1999**, *121*, 9611–9614.

[352] Brian J. Melde, Brian T. Holland, A. Christopher F. Blanford, A. Stein, *Chem. Mater* **1999**, *11*, 3302–3308.

[353] T. Asefa, M. J. MacLachlan, H. Grondey, N. Coombs, G. A. Ozin, *Angew. Chemie - Int. Ed.* **2000**, *39*, 1808–1811.

[354] L. Grösch, Y. J. Lee, F. Hoffmann, M. Fröba, *Chem. - A Eur. J.* **2015**, *21*, 331–346.

[355] T. Martin, A. Galarneau, F. Di Renzo, F. Fajula, D. Plee, *Angew. Chemie - Int. Ed.* **2002**, *41*, 2590–2592.

[356] A. Rimola, D. Costa, M. Sodupe, J.-F. Lambert, P. Ugliengo, *Chem. Rev.* **2013**, *113*, 4216–4313.

[357] B. Coasne, A. Galarneau, R. J. M. Pellenq, F. Di Renzo, *Chem. Soc. Rev.* **2013**, *42*, 4141–71.

[358] E. Fois, A. Gamba, G. Tabacchi, S. Coluccia, G. Martra, *J. Phys. Chem. B* **2003**, *107*, 10767–10772.

[359] E. Fois, A. Gamba, G. Tabacchi, S. Coluccia, G. Martra, *J. Porous Mater.* **2007**, *14*, 339–347.

[360] G. Tabacchi, E. Gianotti, E. Fois, G. Martra, L. Marchese, S. Coluccia, A. Gamba, *J. Phys. Chem. C* **2007**, *111*, 4946–4955.

[361] A. Rimola, P. Ugliengo, M. Sodupe, *Comput. Theor. Chem.* **2015**, *1074*, 168–177.

[362] S. Khanniche, D. Mathieu, F. Pereira, L. Hairault, *Microporous Mesoporous Mater.* **2017**, *250*, 158–169.

[363] M. Corno, M. Delle Piane, P. Choquet, P. Ugliengo, *Phys. Chem. Chem. Phys.* **2017**, *19*, 7793–7806.

[364] A. Gignone, M. Delle Piane, M. Corno, P. Ugliengo, B. Onida, *J. Phys. Chem. C* **2015**, *119*, 13068–13079.

[365] A. Rimola, M. Sodupe, P. Ugliengo, *J. Phys. Chem. C* **2009**, *113*, 5741–5750.

[366] M. Trachta, O. Bludský, M. Rubeš, *Comput. Theor. Chem.* **2017**, *1117*, 100–107.

[367] L. Giussani, G. Tabacchi, E. Gianotti, S. Coluccia, E. Fois, *Philos. Trans. A. Math. Phys. Eng. Sci.* **2012**, *370*, 1463–77.

[368] X. Y. Guo, T. Watermann, D. Sebastiani, *J. Phys. Chem. B* **2014**, *118*, 10207–10213.

[369] A. Kommu, J. K. Singh, *J. Phys. Chem. C* **2017**, *121*, 7867–7880.

[370] L. Giussani, E. Fois, E. Gianotti, G. Tabacchi, A. Gamba, S. Coluccia, *ChemPhysChem* **2010**, *11*, 1757–1762.

[371] L. Giussani, E. Fois, E. Gianotti, G. Tabacchi, A. Gamba, S. Coluccia, *Nuovo Cim. della Soc. Ital. di Fis. B* **2008**, *123*, 1477–1483.

[372] H. G. Manyar, E. Gianotti, Y. Sakamoto, O. Terasaki, S. Coluccia, S. Tumbiolo, *J. Phys. Chem. C* **2008**, *112*, 18110–18116.

[373] A. R. Abdel Hamid, R. Mhanna, P. Catrou, Y. Bulteau, R. Lefort, D. Morineau, *J. Phys. Chem. C* **2016**, *120*, 11049–11053.

[374] R. Mhanna, A. R. Abdel Hamid, S. Dutta, R. Lefort, L. Noirez, B. Frick, D. Morineau, *J. Chem. Phys.* **2017**, *146*, 24501.

[375] A. R. Abdel Hamid, R. Mhanna, R. Lefort, A. Ghoufi, C. Alba-Simionesco, B. Frick, D. Morineau, *J. Phys. Chem. C* **2016**, *120*, 9245–9252.

[376] T. Bui, A. Phan, D. R. Cole, A. Striolo, *J. Phys. Chem. C* **2017**, *121*, 15675–15686.

[377] M. Delle Piane, M. Corno, A. Pedone, R. Dovesi, P. Ugliengo, *J. Phys. Chem. C* **2014**, *118*, 26737–26749.

[378] P. Ugliengo, M. Sodupe, F. Musso, I. J. Bush, R. Orlando, R. Dovesi, *Adv. Mater.* **2008**, *20*, 4579–4583.

[379] B. Coasne, P. Ugliengo, *Langmuir* **2012**, *28*, 11131–11141.

[380] M. Delle Piane, M. Corno, P. Ugliengo, *Theor. Chem. Acc.* **2016**, *135*, 1–10.

[381] A. Pedone, J. Bloino, V. Barone, *J. Phys. Chem. C* **2012**, *116*, 17807–17818.

[382] A. Cauvel, D. Brunel, F. DiRenzo, E. Garrone, B. Fubini, *Langmuir* **1997**, *13*, 2773–2778.

[383] M. F. Ottaviani, A. Galarneau, D. Desplantier-Giscard, F. Di Renzo, F. Fajula, *Microporous Mesoporous Mater.* **2001**, *44–45*, 1–8.

[384] E. Fois, A. Gamba, G. Tabacchi, *Microporous Mesoporous Mater.* **2008**, *116*, 718–722.

[385] C. Allolio, F. Klameth, M. Vogel, D. Sebastiani, *ChemPhysChem* **2014**, *15*, 3955–3962.

[386] J. Geske, M. Vogel, *Mol. Simul.* **2017**, *43*, 13–18.

[387] M. Imperor-Clerc, P. Davidson, A. Davidson, *J. Am. Chem. Soc.* **2000**, *122*, 11925–11933.

[388] R. Ryoo, C. H. Ko, M. Kruk, V. Antochshuk, M. Jaroniec, *J. Phys. Chem. B* **2000**, *104*, 11465–11471.

[389] A. Galarneau, H. Cambon, F. Di Renzo, F. Fajula, *Langmuir* **2001**, *17*, 8328–8335.

[390] S. Naumov, R. Valiullin, J. Kärger, R. Pitchumani, M. O. Coppens, *Microporous Mesoporous Mater.* **2008**, *110*, 37–40.

[391] B. Rühle, M. Davies, T. Bein, C. Bräuchle, *Zeitschrift für Naturforsch. B* **2013**, *68*, 423–444.

[392] T. Lebold, L. A. Mühlstein, J. Blechinger, M. Riederer, H. Amentsch, R. Köhn, K. Peneva, K. Müllen, J. Michaelis, C. Bräuchte, et al., *Chem. - A Eur. J.* **2009**, *15*, 1661–1672.

[393] B. Rühle, M. Davies, T. Lebold, C. Bräuchle, T. Bein, *ACS Nano* **2012**, *6*, 1948–1960.

[394] M. Davies, B. Rühle, C. Li, K. Müllen, T. Bein, C. Bräuchle, *J. Phys. Chem. C* **2014**, *118*, 24013–24024.

[395] C. Janiak, *Angew. Chemie Int. Ed. English* **1997**, *36*, 1431–1434.

[396] J. Guo, Y. Xu, S. Jin, L. Chen, T. Kaji, Y. Honsho, M. A. Addicoat, J. Kim, A. Saeki, H. Ihee, et al., *Nat. Commun.* **2013**, *4*, 2736.

[397] X. Feng, X. Ding, D. Jiang, *Chem Soc Rev* **2012**, *41*, 6010–22.

[398] X.-C. Huang, Y.-Y. Lin, J.-P. Zhang, X.-M. Chen, *Angew. Chemie Int. Ed.* **2006**, *45*, 1557–1559.

[399] M. Fischer, R. G. Bell, *CrystEngComm* **2014**, *16*, 1934.

[400] F. X. Coudert, *ChemPhysChem* **2017**, DOI 10.1002/cphc.201700463.

[401] M. Eddaoudi, D. F. Sava, J. F. Eubank, K. Adil, V. Guillerm, *Chem. Soc. Rev.* **2015**, *44*, 228–249.

[402] D. Farrusseng, S. Aguado, C. Pinel, *Angew. Chemie - Int. Ed.* **2009**, *48*, 7502–7513.

[403] S. Bracco, F. Castiglioni, A. Comotti, S. Galli, M. Negroni, A. Maspero, P. Sozzani, *Chem. - A Eur. J.* **2016**, *23*, 11210–11215.

[404] S. J. Loeb, *Chem. Commun.* **2005**, *0*, 1511–1518.

[405] Q. Li, W. Zhang, O. Š. Miljanić, C. B. Knobler, J. F. Stoddart, O. M. Yaghi, *Chem. Commun.* **2010**, *46*, 380–382.

[406] Q. Li, C. H. Sue, S. Basu, A. K. Shveyd, W. Zhang, G. Barin, L. Fang, A. A. Sarjeant, J. F. Stoddart, O. M. Yaghi, *Angew. Chemie - Int. Ed.* **2010**, *49*, 6751–6755.

[407] M. Mauro, K. C. Schuermann, R. Pr??t??t, A. Hafner, P. Mercandelli, A. Sironi, L. De Cola, *Angew. Chemie - Int. Ed.* **2010**, *49*, 1222–1226.

[408] M. O'Keeffe, M. A. Peskov, S. J. Ramsden, O. M. Yaghi, *Acc. Chem. Res.* **2008**, *41*, 1782–1789.

[409] K. Rissanen, *Chem. Soc. Rev.* **2017**, *46*, 2638–2648.

[410] Y. Inokuma, S. Yoshioka, J. Ariyoshi, T. Arai, Y. Hitora, K. Takada, S. Matsunaga, K. Rissanen, M. Fujita, *Nature* **2013**, *495*, 461.

[411] G. Brunet, D. A. Safin, K. Robeyns, G. A. Facey, I. Korobkov, Y. Filinchuk, M. Murugesu, *Chem. Commun.* **2017**, *53*, 5645–5648.

[412] A. Gasparotto, D. Barreca, C. Maccato, E. Tondello, *Nanoscale* **2012**, *4*, 2813.

[413] A. Mayoral, T. Carey, P. A. Anderson, A. Lubk, I. Diaz, *Angew. Chemie - Int. Ed.* **2011**, *50*, 11230–11233.

[414] G. De Cremer, Y. Antoku, M. B. J. Roeffaers, M. Sliwa, J. Van Noyen, S. Smout, J. Hofkens, D. E. De Vos, B. F. Sels, T. Vosch, *Angew. Chemie Int. Ed.* **2008**, *47*, 2813–2816.

[415] A. Mayoral, T. Carey, P. A. Anderson, I. Diaz, *Microporous Mesoporous Mater.* **2013**, *166*, 117–122.

[416] G. De Cremer, B. F. Sels, J. I. Hotta, M. B. J. Roeffaers, E. Bartholomeeusen, E. Coutiño-Gonzalez, V. Valtchev, D. E. De Vos, T. Vosch, J. Hofkens, *Adv. Mater.* **2010**, *22*, 957–960.

[417] K. Kennes, E. Coutino-Gonzalez, C. Martin, W. Baekelant, M. B. J. Roeffaers, M. Van der Auweraer, *Adv. Funct. Mater.* **2017**, *27*, 1606411.

[418] T. Yumura, A. Oda, H. Torigoe, A. Itadani, Y. Kuroda, T. Wakasugi, H. Kobayashi, *J. Phys. Chem. C* **2014**, *118*, 23874–23887.

[419] C. E. Martinez-Nunez, M. Cortez-Valadez, Y. Delgado-Beleno, N. S. Flores-Lòpez, J. F. Romàn-Zamorano, J. Flores-Valenzuela, M. Flores-Acosta, *J. Nanoparticle Res.* **2017**, *19*, 31.

[420] N. C. Jeong, H. S. Kim, K. B. Yoon, *J. Phys. Chem. C* **2007**, *111*, 10298–10312.

[421] Herron N, *Inorg. Chem.* **1986**, *25*, 4714–4717.

[422] A. Corma, H. Garcia, *Eur. J. Inorg. Chem.* **2004**, *2004*, 1143–1164.

[423] L. Liu, U. Díaz, R. Arenal, G. Agostini, P. Concepción, A. Corma, *Nat. Mater.* **2016**, *16*, 132–138.

[424] T. Hirai, H. Okubo, I. Komasawa, *J. Phys. Chem. B* **1999**, *103*, 4228–4230.

[425] L. Pauling, *Zeitschrift für Krist.* **1930**, 213–225.

[426] R. X. Fischer, W. H. Baur, *Zeitschrift für Krist.* **2009**, *224*, 185–197.

[427] I. Hassan, R. C. Peterson, H. D. Grundy, *Acta Cryst.* **1985**, *C41*, 827–832.

[428] M. Ganio, E. S. Pouyet, S. M. Webb, C. M. Schmidt Patterson, M. S. Walton, *Pure Appl. Chem.* **2017**, *0*, DOI 10.1515/pac-2017-0502.

[429] E. V. Sokolova, V. B. Rybakov, L. A. Pautov, *Sov. Phys. Dokl. Vol. 36, p.267* **1991**, *36*, 267.

[430] B. L. Sherriff, E. V Sokolova, J. Cramer, G. Kunath-Fandrei, C. J. Ger, L. A. Pautov, *Am. Mineral.* **1997**, *82*, 405–415.

[431] F. X. Llabrés i Xamena, A. Abad, A. Corma, H. Garcia, *J. Catal.* **2007**, *250*, 294–298.

[432] F. J. Ma, S. X. Liu, C. Y. Sun, D. D. Liang, G. J. Ren, F. Wei, Y. G. Chen, Z. M. Su, *J. Am. Chem. Soc.* **2011**, *133*, 4178–4181.

[433] M. Brandle, G. Calzaferri, *Res. Chem. Intermed.* **1994**, *20*, 783–806.

[434] A. Trave, F. Buda, A. Selloni, *J. Phys. Chem. B* **1998**, *102*, 1522–1527.

[435] F. Buda, A. Fasolino, *Phys. Rev. B* **1999**, *60*, 6131–6136.

[436] L. Grajciar, *J. Phys. Chem. C* **2016**, *120*, 27050–27065.

[437] J. Antúnez-García, A. Posada-Amarillas, D. H. Galván, E. Smolentseva, V. Petranovskii, S. F. Moyado, *RSC Adv.* **2016**, *6*, 79160–79165.

[438] S. G. Chiodo, T. Mineva, *J. Phys. Chem. C* **2016**, *120*, 4471–4480.

[439] D. Brühwiler, R. Seifert, G. Calzaferri, *J. Phys. Chem. B* **1999**, *103*, 6397–6399.

[440] A. Baldansuren, R.-A. Eichel, E. Roduner, *Phys. Chem. Chem. Phys.* **2009**, *11*, 6664.

[441] E. Coutino-Gonzalez, W. Baekelant, D. Grandjean, M. B. J. Roeffaers, E. Fron, M. S. Aghakhani, N. Bovet, M. Van der Auweraer, P. Lievens, T. Vosch, et al., *J. Mater. Chem. C* **2015**, *3*, 11857–11867.

[442] I. Tkach, A. Baldansuren, E. Kalabukhova, S. Lukin, A. Sitnikov, A. Tsvir, M. Ischenko, Y. Rosentzweig, E. Roduner, *Appl. Magn. Reson.* **2008**, *35*, 95–112.

[443] A. Baldansuren, E. Roduner, *Chem. Phys. Lett.* **2009**, *473*, 135–137.

[444] A. Baldansuren, H. Dilger, R.-A. Eichel, J. A. van Bokhoven, E. Roduner, *J. Phys. Chem. C* **2009**, *113*, 19623–19632.

[445] E. Coutino-Gonzalez, M. B. J. Roeffaers, B. Dieu, G. De Cremer, S. Leyre, P. Hanselaer, W. Fyen, B. Sels, J. Hofkens, *J. Phys. Chem. C* **2013**, *117*, 6998–7004.

[446] O. Fenwick, E. Coutiño-Gonzalez, D. Grandjean, W. Baekelant, F. Richard, S. Bonacchi, D. De Vos, P. Lievens, M. Roeffaers, J. Hofkens, et al., *Nat. Mater.* **2016**, *15*, 1017–1022.

[447] G. De Cremer, E. Coutiño-Gonzalez, M. B. J. Roeffaers, D. E. De Vos, J. Hofkens, T. Vosch, B. F. Sels, *ChemPhysChem* **2010**, *11*, 1627–1631.

[448] A. Mayoral, T. Carey, P. A. Anderson, A. Lubk, I. Diaz, *Angew. Chemie Int. Ed.* **2011**, *50*, 11230–11233.

[449] T. Yumura, T. Nanba, H. Torigoe, Y. Kuroda, H. Kobayashi, *Inorg. Chem.* **2011**, *50*, 6533–6542.

[450] M. Meyer, A. Currao, G. Calzaferri, *ChemPhysChem* **2005**, *6*, 2167–2178.

[451] M. Meyer, C. Leiggener, G. Calzaferri, *ChemPhysChem* **2005**, *6*, 1071–1080.

[452] G. Calzaferri, *Phys. Chem. Chem. Phys.* **2017**, *19*, 10611–10621.

[453] E. Roduner, C. Jensen, J. Vanslageren, R. A. Rakoczy, O. Larlus, M. Hunger, *Angew. Chemie - Int. Ed.* **2014**, *53*, 4318–4321.

[454] X. Liu, M. Bauer, H. Bertagnolli, E. Roduner, J. van Slageren, F. Phillipp, *Phys. Rev. Lett.* **2006**, *97*, 253401.

[455] T. Schmauke, R.-A. Eichel, A. Schweiger, E. Roduner, *Phys. Chem. Chem. Phys.* **2003**, *5*, 3076.

[456] O. Terekhina, E. Roduner, *J. Phys. Chem. C* **2012**, *116*, 6973–6979.

[457] M. Zaarour, B. Dong, I. Naydenova, R. Retoux, S. Mintova, *Microporous Mesoporous Mater.* **2014**, *189*, 11–21.

[458] H. S. Kim, N. C. Jeong, K. B. Yoon, *J. Am. Chem. Soc.* **2011**, *133*, 1642–1645.

[459] D. J. Moon, W. T. Lim, K. Seff, *J. Phys. Chem. C* **2016**, *120*, 16722–16731.

[460] H. S. Kim, N. C. Jeong, K. B. Yoon, *Langmuir* **2011**, *27*, 14678–14688.

[461] D. Hu, Y. Zhang, J. Lin, Y. Hou, D. Li, T. Wu, *Dalt. Trans.* **2017**, *46*, 3929–3933.

[462] F. J. Brieler, P. Grundmann, M. Fröba, L. Chen, P. J. Klar, W. Heimbrodt, H. A. K. Von Nidda, T. Kurz, A. Loidl, *J. Am. Chem. Soc.* **2004**, *126*, 797–807.

[463] S. Alam, C. Anand, K. Ariga, T. Mori, A. Vinu, *Angew. Chemie - Int. Ed.* **2009**, *48*, 7358–7361.

[464] J. Burschka, N. Pellet, S.-J. Moon, R. Humphry-Baker, P. Gao, M. K. Nazeeruddin, M. Grätzel, *Nature* **2013**, *499*, 316–319.

[465] F. Bertolotti, L. Protesescu, M. V. Kovalenko, S. Yakunin, A. Cervellino, S. J. L. Billinge, M. W. Terban, J. S. Pedersen, N. Masciocchi, A. Guagliardi, *ACS Nano* **2017**, *11*, 3819–3831.

[466] D. N. Dirin, L. Protesescu, D. Trummer, I. V. Kochetygov, S. Yakunin, F. Krumeich, N. P. Stadie, M. V. Kovalenko, *Nano Lett.* **2016**, *16*, 5866–5874.

[467] J. Aguilera-Sigalat, D. Bradshaw, *Coord. Chem. Rev.* **2015**, *307*, 267–291.

[468] C. R. Kim, T. Uemura, S. Kitagawa, *Chem. Soc. Rev.* **2016**, *45*, 3828–3845.

[469] G. Lu, S. Li, Z. Guo, O. K. Farha, B. G. Hauser, X. Qi, Y. Wang, X. Wang, S. Han, X. Liu, et al., *Nat. Chem.* **2012**, *4*, 310–316.

[470] J. R. Avila, A. W. Peters, Z. Li, M. A. Ortuño, A. B. F. Martinson, C. J. Cramer, J. T. Hupp, O. K. Farha, *Dalt. Trans.* **2017**, *46*, 5790–5795.

[471] T. Islamoglu, S. Goswami, Z. Li, A. J. Howarth, O. K. Farha, J. T. Hupp, *Acc. Chem. Res.* **2017**, *50*, 805–813.

[472] J.-J. Liu, Y.-F. Guan, L. Li, Y. Chen, W.-X. Dai, C.-C. Huang, M.-J. Lin, *Chem. Commun.* **2017**, *53*, 4481–4484.

[473] E. Meneghinello, A. Martucci, A. Alberti, F. Di Renzo, *Microporous Mesoporous Mater.* **1999**, *30*, 89–94.

[474] A. Godelitsas, T. Armbruster, *Microporous Mesoporous Mater.* **2003**, *61*, 3–24.

[475] A. Godelitsas, D. Charistos, A. Tsipis, C. Tsipis, A. Filippidis, C. Triantafyllidis, G. Manos, D. Siapkas, *Chemistry* **2001**, *7*, 3705–21.

[476] G. D. Gatta, P. Lotti, F. Nestola, D. Pasqual, *Microporous Mesoporous Mater.* **2012**, *163*, 259–269.

[477] L. Campana, A. Selloni, J. Weber, A. Goursot, *J. Phys. Chem. B* **1997**, *101*, 9932–9939.

[478] L. Bernasconi, E. Fois, A. Selloni, *J. Chem. Phys.* **1999**, *24*, 9048–9055.

[479] F. Trudu, G. Tabacchi, A. Gamba, E. Fois, *J. Phys. Chem. A* **2007**, *111*, 11626–37.

[480] A. R. Ruiz-Salvador, N. Almora-Barrios, A. Gomez, D. W. Lewis, A. Gomez, D. W. Lewis, *Phys. Chem. Chem. Phys.* **2007**, *9*, 521–532.

[481] S. R. G. Balestra, S. Hamad, A. R. Ruiz-Salvador, V. Domínguez−García, P. J. Merkling, D. Dubbeldam, S. Calero, *Chem. Mater.* **2015**, *27*, 5657–5667.

[482] A. A. Rybakov, A. V. Larin, G. M. Zhidomirov, *Inorg. Chem.* **2012**, *51*, 12165–12175.

[483] I. A. Bryukhanov, A. A. Rybakov, A. V Larin, D. N. Trubnikov, D. P. Vercauteren, *J. Mol. Model.* **2017**, *23*, DOI 10.1007/s00894-017-3237-8.

[484] X.-J. Hou, H. Li, P. He, S. Li, *Mol. Simul.* **2017**, *43*, 926–934.

[485] T. Frising, P. Leflaive, *Microporous Mesoporous Mater.* **2008**, *114*, 27–63.

[486] E. Passaglia, R. A. Sheppard, *Rev. Mineral. Geochemistry* **2001**, *45*.

[487] P. Demontis, J. Gulín-Gonzalez, G. B. Suffritti, *J. Phys. Chem. B* **2006**, *110*, 7513–8.

[488] K. S. Smirnov, D. Bougeard, *J. Phys. Condens. Matter* **2010**, *22*, 284115.

[489] P. Demontis, J. Gulín-González, M. Masia, G. B. Suffritti, *J. Phys. Condens. Matter* **2010**, *22*, 284106.

[490] P. Demontis, J. Gulín-González, H. Jobic, G. B. Suffritti, *J. Phys. Chem. C* **2010**, *114*, 18612–18621.

[491] P. Demontis, H. Jobic, M. A. Gonzalez, G. B. Suffritti, *J. Phys. Chem. C* **2009**, *113*, 12373–12379.

[492] E. Fois, A. Gamba, G. Tabacchi, F. Trudu, *Stud. Surf. Sci. Catal.* **2008**, *174*, 751–754.

[493] M. Fischer, *Zeitschrift für Krist. - Cryst. Mater.* **2015**, *230*, 325–336.

[494] M. Fischer, *Phys. Chem. Chem. Phys.* **2015**, *17*, 25260–25271.

[495] P. Gómez-Álvarez, S. Calero, *CrystEngComm* **2015**, *17*, 412–421.

[496] E. Fois, A. Gamba, A. Tilocca, *J. Phys. Chem. B* **2002**, *106*, 4806–4812.

[497] J. Hunger, I. A. Beta, H. Böhlig, C. Ling, H. Jobic, B. Hunger, *J. Phys. Chem. B* **2006**, *110*, 342–353.

[498] A. Di Lella, N. Desbiens, A. Boutin, I. Demachy, P. Ungerer, J.-P. Bellat, A. H. Fuchs, *Phys. Chem. Chem. Phys.* **2006**, *8*, 5396.

[499] P. Demontis, G. Stara, G. B. Suffritti, *J. Phys. Chem. B* **2003**, *107*, 4426–4436.

[500] T. Zhou, P. Bai, J. I. Siepmann, A. E. Clark, *J. Phys. Chem. C* **2017**, acs.jpcc.7b04991.

[501] P. Demontis, J. Gulìn-Gonzàlez, H. Jobic, M. Masia, R. Sale, G. B. Suffritti, *ACS Nano* **2008**, *2*, 1603–1614.

[502] N. Floquet, J. P. Coulomb, N. Dufau, G. Andre, C. R. M. C. Cnrs, C. De Luminy, M. Cedex, *J. Phys. Chem. B* **2004**, *108*, 13107–13115.

[503] F.-X. Coudert, R. Vuilleumier, A. Boutin, *ChemPhysChem* **2006**, *7*, 2464–2467.

[504] F.-X. Coudert, F. Cailliez, R. Vuilleumier, A. H. Fuchs, A. Boutin, *Faraday Discuss.* **2009**, *141*, 377–398.

[505] E. Fois, A. Gamba, G. Tabacchi, R. Arletti, S. Quartieri, G. Vezzalini, *Am. Mineral.* **2005**, *90*, 28–35.

[506] R. C. Boggs, D. G. Howard, J. V. Smith, G. L. Klein, *Am. Mineral.* **1993**, *78*.

[507] A. Alberti, G. Cruciani, E. Galli, S. Merlino, R. Millini, S. Quartieri, G. Vezzalini, S. Zanardi, *J. Phys. Chem. B* **2002**, *106*, 10277–10284.

[508] A. Martucci, A. Alberti, M. de Lourdes Guzman-Castillo, F. Di Renzo, F. Fajula, *Microporous Mesoporous Mater.* **2003**, *63*, 33–42.

[509] H. Effenberger, G. Giester, W. Krause, H.-J. Bernhardt, *Am. Mineral.* **1998**, *83*, 607–617.

[510] E. Galli, S. Quartieri, G. Vezalini, A. Alberti, *Eur. J. Mineral.* **1995**, *7*, 1029–1032.

[511] G. D. Gatta, P. Lotti, G. Tabacchi, *Phys. Chem. Miner.* **2017**, 1–24.

[512] G. D. Gatta, *Zeitschrift fur Krist.* **2008**, *223*, 160–170.

[513] R. Arletti, O. Ferro, S. Quartieri, A. Sani, G. Tabacchi, G. Vezzalini, *Am. Mineral.* **2003**, *88*, 1416–1422.

[514] G. D. Gatta, *Eur. J. Mineral.* **2005**, *17*, 411–422.

[515] A. Sartbaeva, S. A. Wells, M. M. J. Treacy, M. F. Thorpe, *Nat. Mater.* **2006**, *5*, 962–965.

[516] P. Ballone, S. Quartieri, A. Sani, G. Vezzalini, *Am. Mineral.* **2002**, *87*, 1194–1206.

[517] E. Fois, A. Gamba, G. Tabacchi, S. Quartieri, R. Arletti, G. Vezzalini, *Stud. Surf. Sci. Catal.* **2005**, *155*, 271–280.

[518] J. S. Tse, D. D. Klug, J. A. Ripmeester, S. Desgreniers, K. Lagarec, *Nature* **1994**, *369*, 724–727.

[519] K. Ståhl, Å. Kvick, S. Ghose, *Zeolites* **1989**, *9*, 303–311.

[520] S. Quartieri, A. Sani, G. Vezzalini, E. Galli, E. Fois, A. Gamba, G. Tabacchi, *Microporous Mesoporous Mater.* **1999**, *30*, 77–87.

[521] P. Norby, A. N. Christensen, I. G. K. Andersen, **1986**, *40A*, 500–506.

[522] E. Fois, G. Tabacchi, S. Quartieri, G. Vezzalini, *J. Chem. Phys.* **1999**, *111*, 355–359.

[523] C. Ceriani, E. Fois, A. Gamba, G. Tabacchi, O. Ferro, S. Quartieri, G. Vezzalini, *Am. Mineral.* **2004**, *89*, 102–109.

[524] O. Ferro, S. Quartieri, G. Vezzalini, E. Fois, A. Gamba, G. Tabacchi, *Am. Mineral.* **2002**, *87*, 1415–1425.

[525] P. Comodi, G. D. Gatta, P. F. Zanazzi, *Eur. J. Mineral.* **2003**, *15*, 247–255.

[526] E. Fois, A. Gamba, G. Tabacchi, O. Ferro, S. Quartieri, G. Vezzalini, *Stud. Surf. Sci. Catal.* **2002**, *142 B*, 1877–1884.

[527] Y. V. Seryotkin, *Microporous Mesoporous Mater.* **2016**, *226*, 415–423.

[528] P. Demontis, G. Stara, G. B. Suffritti, *J. Chem. Phys.* **2004**, *120*, 9233–9244.

[529] A. V. Larin, D. N. Trubnikov, D. P. Vercauteren, *Int. J. Quantum Chem.* **2003**, *92*, 71–84.

[530] B. A. Kolesov, *J. Struct. Chem.* **2006**, *47*, 21–34.

[531] K. At, *Am. Mineral.* **2002**, *87*, 1426–1431.

[532] K. Larsson, J. Tegenfeldt, Å. Kvick, *J. Phys. Chem. Solids* **1989**, *50*, 107–110.

[533] K. Larsson, J. Tegenfeldt, K. Hermansson, *J. CHEM. SOC. FARADAY TRANS* **1991**, *87*, 1193–1200.

[534] E. Fois, A. Gamba, G. Tabacchi, S. Quartieri, G. Vezzalini, *J. Phys. Chem. B* **2001**, *105*, 3012–3016.

[535] E. Fois, A. Gamba, G. Tabacchi, S. Quartieri, G. Vezzalini, *Phys. Chem. Chem. Phys.* **2001**, *3*, 4158–4163.

[536] P. Demontis, G. Stara, G. B. Suffritti, *Microporous Mesoporous Mater.* **2005**, *86*, 166–175.

[537] T. Wen, W. Zhang, X. Hu, L. He, H. Li, *Chempluschem* **2013**, *78*, 438–442.

[538] R. Q. Albuquerque, Z. Popović, L. De Cola, G. Calzaferri, *ChemPhysChem* **2006**, *7*, 1050–1053.

[539] G. Calzaferri, H. Li, D. Brühwiler, *Chem. - A Eur. J.* **2008**, *14*, 7442–7449.

[540] A. Devaux, G. Calzaferri, *Int. J. Photoenergy* **2009**, *2009*, 1–9.

[541] S. Hashimoto, *J. Phys. Chem. Lett.* **2011**, *2*, 509–519.

[542] L. Gartzia-Rivero, J. Bañuelos, I. López-Arbeloa, *Int. Rev. Phys. Chem.* **2015**, *34*, 515–556.

[543] F. Y. Jiang, R. C. Liu, *J. Phys. Chem. Solids* **2007**, *68*, 1552–1555.

[544] J. T. Ye, Z. K. Tang, G. G. Siu, *Appl. Phys. Lett.* **2006**, *88*, 73114.

[545] T. Hertzsch, F. Budde, E. Weber, J. Hulliger, *Angew. Chemie - Int. Ed.* **2002**, *41*, 2281–2284.

[546] W. Guo, D. Wang, J. Hu, Z. K. Tang, S. Du, *Appl. Phys. Lett.* **2011**, *98*, 43105.

[547] N. Ozaki, H. Sakamoto, T. Nishihara, T. Fujimori, Y. Hijikata, R. Kimura, S. Irle, K. Itami, *Angew. Chemie - Int. Ed.* **2017**, *56*, 11196–11202.

[548] G. Flachenecker, A. Materny, *J. Chem. Phys.* **2004**, *120*, 5674–5690.

[549] S. Chen, M. Yao, Y. Yuan, F. Ma, Z. Liu, R. Liu, W. Cui, X. Yang, B. Liu, B. Zou, et al., *Phys. Chem. Chem. Phys.* **2014**, *16*, 8301–9.

[550] Y. Yuan, M. Yao, S. Chen, S. Liu, X. Yang, W. Zhang, Z. Yao, R. Liu, B. Liu, B. Liu, *Nanoscale* **2016**, *8*, 1456–1461.

[551] Y. Q. Hu, M. Q. Li, Y. Wang, T. Zhang, P. Q. Liao, Z. Zheng, X. M. Chen, Y. Z. Zheng, *Chem. - A Eur. J.* **2017**, *23*, 8409–8413.

[552] G. Brunet, D. A. Safin, M. Z. Aghaji, K. Robeyns, I. Korobkov, T. K. Woo, M. Murugesu, *Chem. Sci.* **2017**, *8*, 3171–3177.

[553] J. M. Hu, J. P. Zhai, F. M. Wu, Z. K. Tang, *J. Phys. Chem. B* **2010**, *114*, 16481–16486.

[554] J. Hu, D. Wang, W. Guo, S. Du, Z. K. Tang, *J. Phys. Chem. C* **2012**, *116*, 4423–4430.

[555] S. Chen, M. Yao, Y. Yuan, F. Ma, Z. Liu, B. Li, R. Liu, Q. Li, B. Zou, T. Cui, et al., *J. Raman Spectrosc.* **2015**, *46*, 400–405.

[556] E. Fois, A. Gamba, E. Spano, G. Tabacchi, *J. Mol. Struct.* **2003**, *644*, 55–66.

[557] J. P. Zhai, I. L. Li, S. C. Ruan, H. F. Lee, Z. K. Tang, *Appl. Phys. Lett.* **2008**, *92*, 43117.

[558] Z. Liu, M. Yao, Y. Yuan, S. Chen, R. Liu, S. Lu, B. Zou, T. Cui, B. Liu, *J. Raman Spectrosc.* **2015**, *46*, 413–417.

[559] W. Guo, D. Wang, J. Hu, Z. K. Tang, S. Du, *Appl. Phys. Lett.* **2011**, *98*, 43105.

[560] Z. Liu, Z. Yao, M. Yao, J. Lv, S. Chen, Q. Li, H. Lv, T. Wang, S. Lu, R. Liu, et al., *J. Chem. Phys.* **2016**, *145*, 124319.

[561] S. Megelski, A. Lieb, M. Pauchard, A. Drechsler, S. Glaus, C. Debus, A. J. Meixner, G. Calzaferri, *J. Phys. Chem. B* **2001**, *105*, 25–35.

[562] S. Huber, A. Z. Ruiz, H. Li, G. Patrinoiu, C. Botta, G. Calzaferri, *Inorganica Chim. Acta* **2007**, *360*, 869–875.

[563] G. Herzberg, *Molecular Spectra and Molecular Structure - Vol I.*, Read Books Ltd, **2013**.

[564] V. E. Bondybey, C. Fletcher, *J. Chem. Phys.* **1976**, *64*, 3615–3620.

[565] E. Fois, A. Gamba, C. Medici, G. Tabacchi, *ChemPhysChem* **2005**, *6*, 1917–1922.

[566] I. Frank, J. Hutter, D. Marx, M. Parrinello, *J. Chem. Phys.* **1998**, *108*, 4060.

[567] D. L. Dexter, *J. Chem. Phys.* **1953**, *21*, 836–850.

[568] S. Minakata, R. Tsuruoka, M. Komatsu, *J. AM. CHEM. SOC* **2008**, *130*, 1536–1537.

[569] B. Ye, M. L. Trudeau, D. M. Antonelli, *Adv. Mater.* **2001**, *13*, 561–565.

[570] T. Itoh, K. Yano, T. Kajino, S. Itoh, Y. Shibata, H. Mino, R. Miyamoto, Y. Inada, S. Iwai, Y. Fukushima, *J. Phys. Chem. B* **2004**, *108*, 13683–13687.

[571] I. Oda, K. Hirata, S. Watanabe, Y. Shibata, T. Kajino, Y. Fukushima, S. Iwai, S. Itoh, *J. Phys. Chem. B* **2006**, *110*, 1114–1120.

[572] H. Ikemoto, S. Tubasum, T. Pullerits, J. Ulstrup, Q. Chi, *J. Phys. Chem. C* **2013**, *117*, 2868–2878.

[573] H. M. El-Kaderi, J. R. Hunt, J. L. Mendoza-Cortes, A. P. Cote, R. E. Taylor, M. O'Keeffe, O. M. Yaghi, *Science (80-.).* **2007**, *316*, 268–272.

[574] M. B. Majewski, A. J. Howarth, P. Li, M. R. Wasielewski, J. T. Hupp, O. K. Farha, *CrystEngComm* **2017**, *19*, 4082–4091.

[575] G. Tabacchi, G. Calzaferri, E. Fois, *Chem. Commun.* **2016**, *52*, 11195–11198.

[576] R. M. Barrer, E. A. D. White, *J. Chem. Soc.* **1951**, *0*, 1267.

[577] G. Tabacchi, S. Silvi, M. Venturi, A. Credi, E. Fois, *ChemPhysChem* **2016**, 1913–1919.

[578] S. A. Moggach, T. D. Bennett, A. K. Cheetham, *Angew. Chemie - Int. Ed.* **2009**, *48*, 7087–7089.

[579] E. Haldoupis, T. Watanabe, S. Nair, D. S. Sholl, *ChemPhysChem* **2012**, *13*, 3449–3452.

[580] G. Calzaferri, N. Gfeller, *J. Phys. Chem.* **1992**, *96*, 3428–3435.

[581] F. Binder, G. Calzaferri, N. Gfeller, *Sol. Energy Mater. Sol. Cells* **1995**, *38*, 175–186.

[582] M. Pauchard, S. Huber, R. Méallet-Renault, H. Maas, R. Pansu, G. Calzaferri, *Angew. Chemie Int. Ed.* **2001**, *40*, 2839–2842.

[583] G. Calzaferri, M. Pauchard, H. Maas, S. Huber, A. Khatyr, T. Schaafsma, *J. Mater. Chem.* **2002**, *12*, 1–13.

[584] D. Brühwiler, G. Calzaferri, *Comptes Rendus Chim.* **2005**, *8*, 391–398.

[585] C. Minkowski, G. Calzaferri, *Angew. Chemie Int. Ed.* **2005**, *44*, 5325–5329.

[586] A. Devaux, G. Calzaferri, P. Belser, P. Cao, D. Brühwiler, A. Kunzmann, *Chem. Mater.* **2014**, *26*, 6878–6885.

[587] J. El-Gindi, K. Benson, L. De Cola, H. J. Galla, N. Seda Kehr, *Angew. Chemie - Int. Ed.* **2012**, *51*, 3716–3720.

[588] E. A. Prasetyanto, P. Manini, A. Napolitano, O. Crescenzi, M. d'Ischia, L. De Cola, *Chem. - A Eur. J.* **2014**, *20*, 1597–1601.

[589] A. Bertucci, H. Lülf, D. Septiadi, A. Manicardi, R. Corradini, L. De Cola, *Adv. Healthc. Mater.* **2014**, *3*, 1812–1817.

[590] B. Ergün, L. De Cola, H.-J. Galla, N. S. Kehr, *Adv. Healthc. Mater.* **2016**, *5*, 1588–1592.

[591] A. Greco, L. Maggini, L. De Cola, R. De Marco, L. Gentilucci, *Bioconjug. Chem.* **2015**, *26*, 1873–1878.

[592] M. Becker, L. De Cola, A. Studer, *Chem. Commun.* **2011**, *47*, 3392.

[593] D. Kim, H. S. Kim, *Microporous Mesoporous Mater.* **2017**, *243*, 69–75.

[594] V. Martínez-Martínez, R. García, L. Gómez-Hortigüela, J. Pérez-Pariente, I. López-Arbeloa, *Chem. - A Eur. J.* **2013**, *19*, 9859–9865.

[595] R. Sola-Llano, V. Martínez-Martínez, Y. Fujita, L. Gómez-Hortigüela, A. Alfayate, H. Uji-i, E. Fron, J. Pérez-Pariente, I. López-Arbeloa, *Chem. - A Eur. J.* **2016**, *22*, 15700–15711.

[596] V. Martínez-Martínez, R. García, L. Gómez-Hortigüela, R. Sola Llano, J. Pérez-Pariente, I. López-Arbeloa, *ACS Photonics* **2014**, *1*, 205–211.

[597] D. Lencione, M. H. Gehlen, L. N. Trujillo, R. C. F. Leitao, R. Q. Albuquerque, *Photochem. Photobiol. Sci.* **2016**, *15*, 398–404.

[598] M. Łukarska, A. Jankowska, J. Gapiński, S. Valable, C. Anfray, B. Menard, S. Mintova, S. Kowalak, *New J. Chem.* **2017**, DOI 10.1039/C7NJ01427A.

[599] H. Awala, E. Leite, L. Saint-Marcel, G. Clet, R. Retoux, I. Naydenova, S. Mintova, *New J. Chem.* **2016**, *40*, 4277–4284.

[600] B. Onida, B. Bonelli, M. Lucco-Borlera, L. Flora, C. Otero Areán, E. Garrone, *Stud. Surf. Sci. Catal.* **2001**, *135*, 364.

[601] F. Cucinotta, F. Carniato, A. Devaux, L. De Cola, L. Marchese, *Chem. - A Eur. J.* **2012**, *18*, 15310–15315.

[602] B. Onida, B. Bonelli, L. Flora, F. Geobaldo, C. O. Arean, E. Garrone, *Chem. Commun. (Camb).* **2001**, *0*, 2216–2217.

[603] P. Kittikhunnatham, B. Som, V. Rassolov, M. Stolte, F. Würthner, L. S. Shimizu, A. B. Greytak, *J. Phys. Chem. C* **2017**, *121*, 18102–18109.

[604] W. P. Lustig, S. Mukherjee, N. D. Rudd, A. V. Desai, J. Li, S. K. Ghosh, *Chem. Soc. Rev.* **2017**, *46*, 3242–3285.

[605] M. C. So, G. P. Wiederrecht, J. E. Mondloch, J. T. Hupp, O. K. Farha, *Chem. Commun.* **2015**, *51*, 3501–3510.

[606] R. Medishetty, J. K. Zaręba, D. Mayer, M. Samoć, R. A. Fischer, *Chem. Soc. Rev.* **2017**, *46*, 4976–5004.

[607] M. Handke, T. Adachi, C. Hu, M. D. Ward, *Angew. Chemie Int. Ed.* **2017**, DOI 10.1002/anie.201707097.

[608] T. H. Noh, J. Jang, W. Hong, H. Lee, O.-S. Jung, *Chem. Commun.* **2014**, *50*, 7451–7454.

[609] T. H. Noh, H. Lee, J. Jang, O. S. Jung, *Angew. Chemie - Int. Ed.* **2015**, *54*, 9284–9288.

[610] H. He, E. Ma, Y. Cui, J. Yu, Y. Yang, T. Song, C.-D. Wu, X. Chen, B. Chen, G. Qian, *Nat. Commun.* **2016**, *7*, 11087.

[611] J. Yu, Y. Cui, H. Xu, Y. Yang, Z. Wang, B. Chen, G. Qian, *Nat. Commun.* **2013**, *4*, ncomms3719.

[612] H. Dong, C. Zhang, Y. S. Zhao, *J. Mater. Chem. C* **2017**, *5*, 5600–5609.

[613] S. Megelski, G. Calzaferri, *Adv. Funtional Mater.* **2001**, *11*, 277–286.

[614] L. Gartzia-Rivero, J. Bañuelos, U. Izquierdo, V. L. Barrio, K. Bizkarra, J. F. Cambra, I. López-Arbeloa, *Part. Part. Syst. Charact.* **2014**, *31*, 110–120.

[615] H. S. Cho, A. R. Hill, M. Cho, K. Miyasaka, K. Jeong, M. W. Anderson, J. K. Kang, O. Terasaki, *Cryst. Growth Des.* **2017**, *17*, 4516–4521.

[616] Z. Popović, M. Busby, S. Huber, G. Calzaferri, L. De Cola, *Angew. Chemie - Int. Ed.* **2007**, *46*, 8898–8902.

[617] S. Hashimoto, K. Samata, T. Shoji, N. Taira, T. Tomita, S. Matsuo, *Microporous Mesoporous Mater.* **2009**, *117*, 220–227.

[618] Z. Popović, M. Otter, G. Calzaferri, L. De Cola, *Angew. Chemie Int. Ed.* **2007**, *46*, 6188–6191.

[619] C. A. Strassert, M. Otter, R. Q. Albuquerque, A. Hone, Y. Vida, B. Maier, L. De Cola, *Angew. Chemie - Int. Ed.* **2009**, *48*, 7928–7931.

[620] H. van Koningsveld, J. H. Koegler, *Microporous Mater.* **1997**, *9*, 71–81.

[621] B. Hennessy, S. Megelski, C. Marcolli, V. Shklover, C. Ba, *J. Phys. Chem. B* **1999**, 3340–3351.

[622] R. Hoppe, G. Schulz-Ekloff, D. Wöhrle, C. Kirschhock, H. Fuess, L. Uytterhoeven, R. Schoonheydt, *Adv. Mater.* **1995**, *7*, 61–64.

[623] P. Simoncic, T. Armbruster, P. Pattison, *J. Phys. Chem. B* **2004**, *108*, 17352–17360.

[624] L. Gigli, R. Arletti, G. Tabacchi, E. Fois, J. G. Vitillo, G. Martra, G. Agostini, S. Quartieri, G. Vezzalini, *J. Phys. Chem. C* **2014**, *118*, 15732–15743.

[625] L. Gigli, R. Arletti, J. G. Vitillo, G. Alberto, G. Martra, A. Devaux, G. Vezzalini, *J. Phys. Chem. C* **2015**, *119*, 16156–16165.

[626] P. Simoncic, T. Armbruster, *Microporous Mesoporous Mater.* **2005**, *81*, 87–95.

[627] C. Dejoie, P. Martinetto, N. Tamura, M. Kunz, F. Porcher, P. Bordat, R. Brown, E. Dooryhée, M. Anne, L. B. McCusker, *J. Phys. Chem. C* **2014**, *118*, 28032–28042.

[628] P. Cao, O. Khorev, A. Devaux, L. Sägesser, A. Kunzmann, A. Ecker, R. Häner, D. Brühwiler, G. Calzaferri, P. Belser, *Chem. - A Eur. J.* **2016**, *22*, 4046–4060.

[629] H. Maas, G. Calzaferri, *Angew. Chemie - Int. Ed.* **2002**, *41*, 2284–2288.

[630] S. Huber, G. Calzaferri, *Angew. Chemie - Int. Ed.* **2004**, *43*, 6738–6742.

[631] Y. Wang, H. Li, Y. Feng, H. Zhang, G. Calzaferri, T. Ren, *Angew. Chemie - Int. Ed.* **2010**, *49*, 1434–1438.

[632] A. Z. Ruiz, H. Li, G. Calzaferri, *Angew. Chemie - Int. Ed.* **2006**, *45*, 5282–5287.

[633] N. S. Kehr, B. Ergün, H. Lülf, L. De Cola, *Adv. Mater.* **2014**, *26*, 3248–3252.

[634] S. Fibikar, G. Luppi, V. Martínez-Junza, M. Clemente-León, L. De Cola, *Chempluschem* **2015**, *80*, 62–67.

[635] L.-Q. Dieu, A. Devaux, I. López-Duarte, M. Victoria Martínez-Díaz, D. Brühwiler, G. Calzaferri, T. Torres, *Chem. Commun.* **2008**, *0*, 1187–1189.

[636] I. Lõpez-Duarte, Le-Quyenha Dieu, I. Dolamic, M. V. Martínez-Díaz, T. Torres, G. Calzaferri, D. Brühwiler, *Chem. - A Eur. J.* **2011**, *17*, 1855–1862.

[637] G. Bottari, G. de la Torre, D. M. Guldi, T. Torres, *Chem. Rev.* **2010**, *110*, 6768–6816.

[638] F. Cucinotta, A. Guenet, C. Bizzarri, W. Mroz, C. Botta, B. Milian-Medina, J. Gierschner, L. De Cola, *Chempluschem* **2014**, *79*, 45–57.

[639] J. M. Beierle, R. Roswanda, P. M. Erne, A. C. Coleman, W. R. Browne, B. L. Feringa, *Part. Part. Syst. Charact.* **2013**, *30*, 273–279.

[640] F. Würthner, *Chem. Commun.* **2004**, *0*, 1564–1579.

[641] F. Würthner, C. R. Saha-Möller, B. Fimmel, S. Ogi, P. Leowanawat, D. Schmidt, *Chem. Rev.* **2015**, DOI 10.1021/acs.chemrev.5b00188.

[642] G. Calzaferri, R. Méallet-Renault, D. Brühwiler, R. Pansu, I. Dolamic, T. Dienel, P. Adler, H. Li, A. Kunzmann, *ChemPhysChem* **2011**, *12*, 580–594.

[643] A. Devaux, C. Minkowski, G. Calzaferri, *Chem. - A Eur. J.* **2004**, *10*, 2391–2408.

[644] B. Bussemer, D. Munsel, H. Wünscher, G. J. Mohr, U. W. Grummt, *J. Phys. Chem. B* **2007**, *111*, 8–15.

[645] S. Hashimoto, M. Hagiri, N. Matsubara, S. Tobita, *Phys. Chem. Chem. Phys.* **2001**, *3*, 5043–5051.

[646] W. Insuwan, K. Rangsriwatananon, *J. Porous Mater.* **2014**, *21*, 345–354.

[647] C. Minkowski, R. Pansu, M. Takano, G. Calzaferri, *Adv. Funct. Mater.* **2006**, *16*, 273–285.

[648] Y. Huang, J. Wang, Z. Wei, E. Yashima, K. Maeda, H. Iida, Y. Furusho, K. Nagai, Y. Wang, J. Xu, et al., *Chem. Commun.* **2014**, *50*, 8343.

[649] S. Herbst, B. Soberats, P. Leowanawat, M. Lehmann, F. Würthner, *Angew. Chemie Int. Ed.* **2017**, *56*, 2162–2165.

[650] M. Busby, A. Devaux, C. Blum, V. Subramaniam, G. Calzaferri, L. De Cola, *J. Phys. Chem. C* **2011**, *115*, 5974–5988.

[651] A. Devaux, G. Calzaferri, I. Miletto, P. Cao, P. Belser, D. Brühwiler, O. Khorev, R. Häner, A. Kunzmann, *J. Phys. Chem. C* **2013**, *117*, 23034–23047.

[652] C. Jia, A. Migliore, N. Xin, S. Huang, J. Wang, Q. Yang, S. Wang, H. Chen, D. Wang, B. Feng, et al., *Science (80-.).* **2016**, *352*, 13153–13161.

[653] E. Fois, G. Tabacchi, G. Calzaferri, *J. Phys. Chem. C* **2010**, *114*, 10572–10579.

[654] X. Zhou, T. A. Wesolowski, G. Tabacchi, E. Fois, G. Calzaferri, A. Devaux, *Phys. Chem. Chem. Phys.* **2013**, *15*, 159–167.

[655] S. Deore, P. Simoncic, A. Navrotsky, *Microporous Mesoporous Mater.* **2008**, *109*, 342–349.

[656] J. Tsuwi, R. Berger, G. Labat, G. Couderc, N. R. Behrnd, P. Ottiger, F. Cucinotta, K. Schürmann, M. Bertoni, L. Viani, et al., *J. Phys. Chem. A* **2010**, *114*, 6956–6963.

[657] L. Viani, A. Minoia, J. Cornil, D. Beljonne, H. J. Egelhaaf, J. Gierschner, *J. Phys. Chem. C* **2016**, *120*, 27192–27199.

[658] L. Gartzia-Rivero, J. Bañuelos-Prieto, V. Martínez-Martínez, I. López Arbeloa, *Chempluschem* **2012**, *77*, 61–70.

[659] W. Insuwan, S. Jungsuttiwong, K. Rangsriwatananon, *J. Lumin.* **2015**, *161*, 31–36.

[660] W. Insuwan, K. Rangsriwatananon, J. Meeprasert, S. Namuangruk, Y. Surakhot, N. Kungwan, S. Jungsuttiwong, *Microporous Mesoporous Mater.* **2017**, *241*, 372–382.

[661] H. Manzano, L. Gartzia-Rivero, J. Bañuelos, I. López-Arbeloa, *J. Phys. Chem. C* **2013**, *117*, 13331–13336.

[662] E. Fois, A. Gamba, G. Tabacchi, *ChemPhysChem* **2008**, *9*, 538–543.

[663] V. Ramamurthy, D. R. Sanderson, D. F. Eaton, *J. Am. Chem. Soc.* **1993**, *115*, 10438–10439.

[664] R. Arletti, L. Ronchi, S. Quartieri, G. Vezzalini, A. Ryzhikov, H. Nouali, T. J. Daou, J. Patarin, *Microporous Mesoporous Mater.* **2016**, *235*, 253–260.

[665] G. Ihlein, F. Schüth, O. Krauß, U. Vietze, F. Laeri, *Adv. Mater.* **1998**, *10*, 1117–1119.

[666] V. Martínez-Martínez, R. García, L. Gómez-Hortigüela, R. Sola Llano, J. Pérez-Pariente, I. López-Arbeloa, *ACS Photonics* **2014**, *1*, 205–211.

[667] R. García, V. Martínez-Martínez, R. Sola Llano, I. López-Arbeloa, J. Pérez-Pariente, *J. Phys. Chem. C* **2013**, *117*, 24063–24070.

[668] R. Sola-Llano, Y. Fujita, L. Gómez-Hortigüela, A. Alfayate, H. Ujii, E. Fron, S. Toyouchi, J. Perez-Pariente, I. Lopez-Arbeloa, V. Martinez-Martinez, *ACS Photonics* **2017**, acsphotonics.7b00553.

[669] W. Grochala, R. Hoffmann, J. Feng, N. W. Ashcroft, *Angew. Chemie - Int. Ed.* **2007**, *46*, 3620–3642.

[670] L. Merrill, W. A. Bassett, *Rev. Sci. Instrum.* **1974**, *45*, 290–294.

[671] R. Miletich, D. R. Allan, W. F. Kuhs, *Rev. Mineral. Geochemistry* **2000**, *41*, 445–519.

[672] R. J. Angel, M. Bujak, J. Zhao, G. D. Gatta, S. D. Jacobsen, *J. Appl. Crystallogr.* **2007**, *40*, 26–32.

[673] G. D. Gatta, G. Tabacchi, E. Fois, Y. Lee, *Phys. Chem. Miner.* **2016**, *43*, 209–216.

[674] P. Lotti, R. Arletti, G. D. Gatta, S. Quartieri, G. Vezzalini, M. Merlini, V. Dmitriev, M. Hanfland, *Microporous Mesoporous Mater.* **2015**, *218*, 42–54.

[675] R. M. Hazen, L. W. Finger, *J. Appl. Phys.* **1984**, *56*, 1838–1840.

[676] Y. Lee, T. Vogt, J. A. Hriljac, J. B. Parise, J. C. Hanson, S. J. Kim, *Nature* **2002**, *420*, 485–489.

[677] Y. Lee, T. Vogt, J. A. Hriljac, J. B. Parise, G. Artioli, *J. Am. Chem. Soc.* **2002**, *124*, 5466–5475.

[678] Y. Lee, C. C. Kao, S. J. Kim, H. H. Lee, D. R. Lee, T. J. Shin, J. Y. Choi, *Chem. Mater.* **2007**, *19*, 6252–6257.

[679] F. Cailliez, M. Trzpit, M. Soulard, I. Demachy, A. Boutin, J. Patarin, A. H. Fuchs, *Phys. Chem. Chem. Phys.* **2008**, *10*, 4817.

[680] T. Martin, B. Lefevre, D. Brunel, A. Galarneau, F. Di Renzo, F. Fajula, P. F. Gobin, J. F. Quinson, G. Vigier, *Chem. Commun.* **2002**, *0*, 24–5.

[681] G. D. Gatta, K. S. Scheidl, T. Pippinger, R. Skála, Y. Lee, R. Miletich, *Microporous Mesoporous Mater.* **2015**, *206*, 34–41.

[682] C. L. I. M. White, A. R. Ruiz-Salvador, D. W. Lewis, *Angew. Chemie* **2004**, *116*, 475–478.

[683] G. D. Gatta, Y. Lee, *Phys. Chem. Miner.* **2006**, *32*, 726–732.

[684] D. Seoung, Y. Lee, C.-C. Kao, T. Vogt, Y. Lee, *Chem. Mater.* **2015**, *27*, 3874–3880.

[685] G. Fraux, F.-X. Coudert, A. Boutin, A. H. Fuchs, *Chem. Soc. Rev.* **2017**, *46*, 7421–7437.

[686] L. Ronchi, A. Ryzhikov, H. Nouali, T. J. Daou, J. Patarin, *New J. Chem.* **2017**, *41*, 2586–2592.

[687] N. Desbiens, I. Demachy, A. H. Fuchs, H. Kirsch-Rodeschini, M. Soulard, J. Patarin, *Angew. Chemie - Int. Ed.* **2005**, *44*, 5310–5313.

[688] Y. Lee, T. Vogt, Y. Lee, *Microporous Mesoporous Mater.* **2017**, *244*, 109–118.

[689] A. Y. Likhacheva, Y. V. Seryotkin, A. Y. Manakov, S. V. Goryainov, A. I. Ancharov, M. A. Sheromov, *Am. Mineral.* **2007**, *92*.

[690] Y. Lee, Y. Lee, D. Seoung, *Am. Mineral.* **2010**, *95*, 1636–1641.

[691] Y. Lee, Y. Lee, D. Seoung, J. H. Im, H. J. Hwang, T. H. Kim, D. Liu, Z. Liu, S. Y. Lee, C. C. Kao, et al., *Angew. Chemie - Int. Ed.* **2012**, *51*, 4848–4851.

[692] J. N. Grima, R. Gatt, V. Zammit, J. J. Williams, K. E. Evans, A. Alderson, R. I. Walton, *J. Appl. Phys.* **2007**, *101*, 86102.

[693] A. Kremleva, T. Vogt, N. Rösch, *J. Phys. Chem. C* **2013**, *117*,

19020–19030.
[694] A. Kremleva, T. Vogt, N. Rösch, *J. Phys. Chem. C* **2014**, *118*, 22030–22039.
[695] V. Schettino, R. Bini, *Chem. Soc. Rev.* **2007**, *36*, 869–880.
[696] M. Citroni, M. Ceppatelli, R. Bini, V. Schettino, *High Press. Res.* **2002**, *22*, 507–510.
[697] P. Enzel, J. J. Zoller, T. Bein, A. G. MacDiarmid, A. J. Heeger, *J. Chem. Soc. Chem. Commun.* **1992**, *0*, 633–635.
[698] M. Santoro, F. A. Gorelli, R. Bini, J. Haines, A. van der Lee, *Nat. Commun.* **2013**, *4*, 1557.
[699] M. Santoro, D. Scelta, K. Dziubek, M. Ceppatelli, F. A. Gorelli, R. Bini, G. Garbarino, J. M. Thibaud, F. Di Renzo, O. Cambon, et al., *Chem. Mater.* **2016**, *28*, 4065–4071.
[700] M. Santoro, K. Dziubek, D. Scelta, M. Ceppatelli, F. A. Gorelli, R. Bini, J. M. Thibaud, F. Di Renzo, O. Cambon, J. Rouquette, et al., *Chem. Mater.* **2015**, *27*, 6486–6489.
[701] M. Yao, T. Wang, Z. Yao, D. Duan, S. Chen, Z. Liu, R. Liu, S. Lu, Y. Yuan, B. Zou, et al., *J. Phys. Chem. C* **2013**, *117*, 25052–25058.
[702] J. Im, Y. Lee, D. A. Blom, T. Vogt, Y. Lee, *Dalt. Trans.* **2016**, *45*, 1622–1630.
[703] D. Santamaría-Pérez, T. Marqueño, S. MacLeod, J. Ruiz-Fuertes, D. Daisenberger, R. Chuliá-Jordan, D. Errandonea, J. L. Jordá, F. Rey, C. McGuire, et al., *Chem. Mater.* **2017**, *29*, 4502–4510.
[704] P. Lotti, G. D. Gatta, M. Merlini, H.-P. Liermann, *Zeitschrift für Krist. - Cryst. Mater.* **2015**, *230*, 201–211.
[705] R. Arletti, L. Leardini, G. Vezzalini, S. Quartieri, L. Gigli, M. Santoro, J. Haines, J. Rouquette, L. Konczewicz, *Phys. Chem. Chem. Phys.* **2015**, *17*, 24262–24274.
[706] J. Richard, S. L. Cid, J. Rouquette, A. Van Der Lee, S. Bernard, J. Haines, *J. Phys. Chem. C* **2016**, *120*, 9334–9340.
[707] A. Corma, F. Rey, J. Rius, M. J. Sabater, S. Valencia, *Nature* **2004**, *431*, 287–290.
[708] P. A. Vaughan, *Acta Crystallogr.* **1966**, *21*, 983–990.
[709] A. Alberti, C. Sabelli, *Zeitschrift fur Krist. - New Cryst. Struct.* **1987**, *178*, 249–256.
[710] R. Arletti, G. Vezzalini, S. Quartieri, F. Di Renzo, V. Dmitriev, *Microporous Mesoporous Mater.* **2014**, *191*, 27–37.
[711] C. Wang, P. Bai, J. I. Siepmann, A. E. Clark, **2014**.
[712] P. Bai, M. Y. Jeon, L. Ren, C. Knight, M. W. Deem, M. Tsapatsis, J. I. Siepmann, *Nat. Commun.* **2015**, *6*, 5912.
[713] R. F. DeJaco, P. Bai, M. Tsapatsis, J. I. Siepmann, *Langmuir* **2016**, *32*, 2093–2101.
[714] N. Mittal, P. Bai, J. I. Siepmann, P. Daoutidis, M. Tsapatsis, *J. Memb. Sci.* **2017**, *540*, 464–476.
[715] R. Arletti, E. Fois, G. Tabacchi, S. Quartieri, G. Vezzalini, *Adv. Sci. Lett.* **2017**, *23*, 5966–5969.
[716] C. H. Wang, P. Bai, J. I. Siepmann, A. E. Clark, *J. Phys. Chem. C* **2014**, *118*, 19723–19732.
[717] S. C. McKellar, S. A. Moggach, IUCr, *Acta Crystallogr. Sect. B Struct. Sci. Cryst. Eng. Mater.* **2015**, *71*, 587–607.
[718] E. A. Kapustin, S. Lee, A. S. Alshammari, O. M. Yaghi, *ACS Cent. Sci.* **2017**, *3*, 662–667.
[719] W. Li, M. R. Probert, M. Kosa, T. D. Bennett, A. Thirumurugan, R. P. Burwood, M. Parinello, J. A. K. Howard, A. K. Cheetham, *J. Am. Chem. Soc.* **2012**, *134*, 11940–11943.
[720] T. D. Bennett, P. Simoncic, S. A. Moggach, F. Gozzo, P. Macchi, D. A. Keen, J.-C. Tan, A. K. Cheetham, *Chem. Commun.* **2011**, *47*, 7983–7985.
[721] J. Im, D. Seoung, G. C. Hwang, J. W. Jun, S. H. Jhung, C.-C. Kao, T. Vogt, Y. Lee, *Chem. Mater.* **2016**, *28*, 5336–5341.
[722] A. U. Ortiz, A. Boutin, A. H. Fuchs, F.-X. Coudert, *J. Chem. Phys.* **2013**, *138*, 174703.
[723] J. Sotelo, C. H. Woodall, D. R. Allan, E. Gregoryanz, R. T. Howie, K. V. Kamenev, M. R. Probert, P. A. Wright, S. A. Moggach, *Angew. Chemie Int. Ed.* **2015**, *54*, 13332–13336.
[724] C. L. Hobday, R. J. Marshall, C. F. Murphie, J. Sotelo, T. Richards, D. R. Allan, T. Düren, F. X. Coudert, R. S. Forgan, C. A. Morrison, et al., *Angew. Chemie - Int. Ed.* **2016**, *55*, 2401–2405.
[725] M. R. Ryder, B. Civalleri, J.-C. Tan, *Phys. Chem. Chem. Phys.* **2016**, *18*, 9079–9087.
[726] W. F. Perger, J. Criswell, B. Civalleri, R. Dovesi, *Comput. Phys. Commun.* **2009**, *180*, 1753–1759.
[727] A. Erba, D. Caglioti, C. M. Zicovich-Wilson, R. Dovesi, *J. Comput. Chem.* **2017**, *38*, 257–264.
[728] J.-C. Tan, B. Civalleri, A. Erba, E. Albanese, *CrystEngComm* **2015**, *17*, 375–382.
[729] L. Öhrström, *ACS Cent. Sci.* **2017**, *3*, 528–530.
[730] J. L. Jordá, F. Rey, G. Sastre, S. Valencia, M. Palomino, A. Corma, A. Segura, D. Errandonea, R. Lacomba, F. J. Manjón, et al., *Angew. Chemie - Int. Ed.* **2013**, *52*, 10458–10462.
[731] L. Bertrand, C. Gervais, A. Masic, L. Robbiola, *Angew. Chemie Int. Ed.* **2017**, DOI 10.1002/anie.201709303.
[732] J. Bujdák, *Clay Miner.* **2015**, *50*, 549–571.
[733] M. Ogawa, R. Takee, Y. Okabe, Y. Seki, *Dye. Pigment.* **2017**, *139*, 561–565.
[734] M. Matejdes, D. Himeno, Y. Suzuki, J. Kawamata, *Appl. Clay Sci.* **2017**, *140*, 119–123.
[735] F. Olivero, F. Carniato, C. Bisio, L. Marchese, *Chem. - An Asian J.* **2014**, *9*, 158–165.
[736] U. Costantino, F. Costantino, F. Elisei, L. Latterini, M. Nocchetti, *Phys. Chem. Chem. Phys.* **2013**, *15*, 13254–69.
[737] E. Duque-Redondo, H. Manzano, N. Epelde-Elezcano, V. Martínez-Martínez, I. López-Arbeloa, *Chem. Mater.* **2014**, *26*, 4338–4345.
[738] P. Woodtli, S. Giger, P. Müller, L. Sägesser, N. Zucchetto, M. J. Reber, A. Ecker, D. Brühwiler, *Dye. Pigment.* **2017**, DOI 10.1016/j.dyepig.2017.10.029.
[739] X. Y. Li, Y. Jiang, X. Q. Liu, L. Y. Shi, D. Y. Zhang, L. B. Sun, *ACS Sustain. Chem. Eng.* **2017**, *5*, 6124–6130.
[740] B. Dong, R. Retoux, V. de Waele, S. G. Chiodo, T. Mineva, J. Cardin, S. Mintova, *Microporous Mesoporous Mater.* **2017**, *244*, 74–82.
[741] S. Gul, D. Cody, A. Kharchenko, S. Martin, S. Mintova, J. Cassidy, I. Naydenova, *Microporous Mesoporous Mater.* **2018**, *261*, 268–274.

Author version of: ChemPhysChem 2018, doi:10.1002/cphc.201701090

Entry for the Table of Contents (Please choose one layout)

Layout 1:

REVIEW

Under tight confinement in nanosized cavities, molecules may self-assemble creating beautiful patterns and technologically useful materials. The complexity and potential of nanospace-confined supramolecular organization is illustrated by natural and artificial examples, highlighting, beside diversity, their common molecular bases and interconnections.

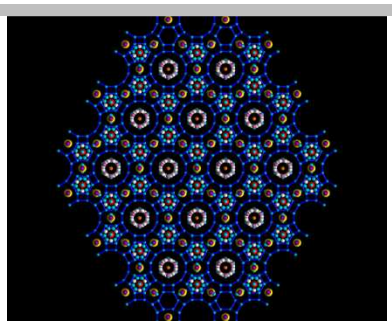

*Gloria Tabacchi**

Supramolecular organization and confined nanospaces